INSTITUTO SUPERIOR TÉCNICO
Universidade Técnica de Lisboa

Modelling of Building Height Interference Dependence in UMTS

Armando Jorge Alexandre Marques

Dissertation submitted for obtaining the degree of
Master in Electrical and Computer Engineering

Jury

Supervisor: Prof. Luis M. Correia

Co-Supervisor: Mr. Sérgio Pires

President: Prof. António Topa

Members: Prof. António Rodrigues

September 2008

To my parents and sisters

"The mediocre teacher tells. The good teacher explains. The superior teacher straights. The great teacher inspires."

(**William Arthur Ward)**

"Thinking is the hardest work there is, which is probably the reason so few engage in it."

(Henry Ford)

"Without hard work, nothing grows but weeds."

(Gordon B. Hinckley)

Acknowledgements

To all that believed in me.

In the first place, I would like to thank Professor Luis Correia for choosing me and giving me the opportunity to perform this thesis, and for the constant knowledge and experience sharing. His orientation, discipline, availability, constant support, and guidelines, were a key factor to finish this work with the demanded and desired quality. I am thankful for all his help and advising that were very useful in the present, and which will also be useful in the future of my professional life.

To Celfinet, in particular to Sérgio Pires, for all his constructive critics, technical support, suggestions, advice, and his precious time to answer all my questions. His knowledge and experience were very helpful throughout this journey. I also would like to thank to Nuno Silva for the help given to perform the measurements, which gave me a better inside view of the technology, and allowed me to improve my technical knowledge.

To all GROW members for the support, clarifications and the contact with their several areas. The possibility to participate in the GROW meetings allowed me to contact with several other areas of wireless and mobile communications, as well as to practice my critical thought and presentations.

To all my teachers, who provided me with tools and technical knowledge and support in my academic life. In particular to Alexandre Bernardino, António Topa, António Rodrigues, Carlos Fernandes, Isabel Lourtie, João Lemos, Maria Rosário and Paulo Oliveira.

I also want to thank all RF2 lab team, Telmo Batista, Filipe Leonardo, Ricardo Preguiça, Sara Duarte and Vikash Mukesh, for their constructive critics, useful suggestions, different points of view, knowledge and availability, as well as their friendship, good company and support.

I also want to thank to all my friends for all their support, patience and encouragement. In particular to Gonçalo Santos, João Pinto, David Fernandes, Paulo Braz and Pedro Lopes for their enormous encouragement and help, without which the completion of this work would have been a much more difficult task.

Finally I would like to thank my family, especially my parents, Artur and Jaquelina, my sisters, Sandra and Clara, and my aunt, Otília. I am very grateful for their unconditional love, care, understanding, and support, which kept me going in the hardest times.

Abstract

The main purpose of this thesis was to study the interference dependence in UMTS-FDD with the buildings height. For this, an interference model was developed and implemented in a simulator. This model calculates intra- and inter-cell interferences independently in DL and UL. Some simulations results are compared with measurements performed in a live network in order to assess the simulator. With the purpose of knowing how interference behaves, several simulations were performed, changing some parameters, such as the distance between MT and BS, centre building height, street widths, antennas tilts and number of BSs. The simulations results show that the interference has its higher value in the case of rooms directly facing the outside, and it also shows an increase trend of 2.5dB per floor, and a difference of 2.8dB between each penetrated wall situation. This result is different when the analysis is performed in terms of NLoS and LoS. In the case of NLoS, the interference has a rise of 1.3dB per floor, and 3.3dB in the case of LoS, i.e., when the MT is in LoS the slope increases almost two times faster than when it is in NLoS. The principal conclusion was: the higher the MT is in the building, and the less penetrated wall it has, the higher the interference will be.

Keywords

UMTS, Interference, Height dependence, Measurements, Modelling.

Resumo

O principal objectivo da presente tese foi o estudo da dependência da interferência com a altura dos edifícios no sistema UMTS-FDD. Para tal, foram desenvolvidos alguns modelos de interferência e implementados num simulador. Este simulador foi criado de raiz. O modelo desenvolvido calcula separadamente a interferência intra- e inter-celular para DL e UL. Foram efectuadas medições, e comparadas com os resultados de simulação, de forma a certificar o correcto funcionamento do simulador. Para compreender como a interferência se comporta, foram efectuas varias simulações, variando alguns parâmetros, um a um, dos quais a distância entre o terminal móvel e a estação base, a altura do edifício do centro, largura das ruas, a inclinação das antenas e o número de estações base. Os resultados de simulação mostraram que a interferência é mais acentuada nos casos em que as divisórias se encontram perto do exterior. À medida que o terminal móvel vai subindo no edifício, a interferência sobe a 2.5dB por piso e tem uma diferença entre cada situação de atenuação de 2.8dB. Estes são resultados de um ponto de vista geral, mas quando a análise foi divida em linha de vista e sem linha de vista, entre o terminal móvel e a estação base, revelou-se que quando o terminal móvel se encontra em linha de vista a interferência cresce a 1.28dB por andar, e 3.27dB para o outro caso. Concluindo-se então, que quando o terminal móvel se encontra em linha de vista com a estação base, a interferência cresce quase duas vezes. No final, a principal conclusão a que se chegou foi que, a interferência cresce com a subida do terminal móvel no edifício, isto é, quanto mais alto e mais próximo da janela o terminal móvel estiver maior irá ser a interferência.

Palavras-chave

Dependência com Altura, UMTS, Interferência, Medições, Modelação.

Table of Contents

List of Figures

List of Tables

List of Acronyms

1SM	One-Slope Model
2G	Second Generation
3G	Third Generation
3GPP	3rd Generation Partnership Project
AMC	Adaptive Modulation and Coding
BERs	Maximal Bit Error Rates
BS	Base Station
CDMA	Code Division Multiple Access
ChN	Channel Number
CI	Cell Identification
CN	Core Network
DL	Downlink
EIRP	Equivalent Isotropic Radiated Power
FDD	Frequency Division Duplex
GSM	Global System for Mobile Communication
HARQ	Hybrid Automatic Repeat-Request
HSDPA	High-Speed Downlink Packet Access
HSPA	High-Speed Packet Access
HSUPA	High-Speed Uplink Packet Access
IMT	International Mobile Telecommunications
LAC	Location Area Code
LAM	Linear Attenuation Model
LoS	Line-of-Sight
LTE	Long-Term Evolution
MAI	Multiple Access Interference
ME	Mobile Equipment
MSS	Mobile Satellite Service
MT	Mobile Terminal
MWM	Multi-Wall Model
NLoS	Non Line-of-Sight
OVSF	Orthogonal Variable Spreading Factor
QoS	Quality of Service
RNC	Radio Network Controller
RSCP	Received Signal Code Power

RSSI	Received Signal Strength Indication
SC	Scrambling Code
SF	Spreading Factor
SIR	Signal-to-Interference Ratio
SNR	Signal-to-Noise Ratio
TDD	Time Division Duplex
UE	User Equipment
UICC	Universal Integrated Circuit Card
UL	Uplink
UMTS	Universal Mobile Telecommunications System
USIM	UMTS Subscriber Identify Module
UTRAN	Terrestrial Radio Access Network
WARC	World Administrative Radio Conference
WCDMA	Wideband Code Division Multiple Access

List of Symbols

α	DL Orthogonality Factor
α_j	DL channel orthogonality factor of user *j*
ΔP	Power control variation
η	Load Factor
σ	Standard deviation
Θ	Angle between MT and Roof-Top corner
ν_j	Activity factor of user *j*
μ	Average
E_b	Energy per user bit
f	Frequency
F	Receiver's noise figure
F_N	Floor Number
G_{div}	Diversity gain
G_p	Processing gain
G_r	Gain of the receiving antenna
G_{SHO}	Soft handover gain
G_t	Gain of the transmitting antenna
h_{Roof}	Buildings height
i	Ratio of inter-cell to intra-cell interferences
i_j	Ratio of inter-cell to intra-cell interferences for user *j*
k	Propagation constant
k_d	Dependence of the multi-screen diffraction loss versus distance
k_f	Number of penetrated floors
k_f	Dependence of the multi-screen diffraction loss versus frequency
k_{wi}	Number of penetrated walls of type *i*
L_0	Free space loss
L_{bsh}	Losses due to the fact that BS antennas are above or below the roof-top level
L_{cable}	Cable losses between emitter and antenna
L_f	Floor attenuation loss
l_{glass}	Glass loss attenuation
L_{msd}	Multiple screen diffraction loss
L_{ori}	Street orientation loss
L_p	Path loss attenuation

$L_{p\ extra}$	Extra attenuation
$L_{p\ ind}$	Path loss attenuation gives by indoor model
$L_{p\ outd}$	Path loss attenuation gives by outdoor model
$L_{p\ \mathrm{Total}}$	Total path loss attenuation
L_{rts}	Roof-top-to-street diffraction and scatter loss
L_u	Body losses
L_{wi}	Loss attenuation of wall type *i*
M_{FF}	Fast fading margin
M_I	Interference Margin
M_{SF}	Slow fading margin
N	Total noise power
N_0	Noise power density
N_{BS}	Number of interfering BSs
N_{serv}	Total number of services
$N_{j,g}$	Number of MTs using the service *g* within the cell of BS *j*
$N_{k,g}$	Number of users using service *g* in interfering cell *k*
N_u	Number of users
N_u	Number of users within the cell
$P_{BS\rightarrow MTi}$	Transmitted power from BS to MTs *i*
$P_{MT\rightarrow BSi}$	Transmitted power from MT to BS *j*
$P_{MTk\rightarrow BSj}$	MT *k* power transmitted to BS *j* in an adjacent cell
P_r	Power available at the receiving antenna
P_{Rx}	Received power at receiver input
P_t	Power fed to the transmitting antenna
$P_{Total,BS}$	Total transmitted power of BS to MTs within the cell
$P_{Total,BSj}$	Total transmitted power of BS *j*
P_{Tx}	Transmitted power
r	Distance between roof-top and the MT
R_c	Chip Rate
$r_{j,n}$	Distance from MT *n* using service *g* to BSs *j*
$r_{k,n}$	Distance from MT *n* using service *g* to BSs *k*
w_b	Building separation
w_s	Street width
x	Horizontal distance between the MT and diffracting edges

List of Software

Borland Builder C++

Google Earth

Matlab

Microsoft Excel

Microsoft Visio

Microsoft Word

NEMO Outdoor

Chapter 1

Introduction

This chapter presents a brief overview of the work. Before establishing work targets and original contributions, the scope and motivations are presented. A brief state of the art on mobile communications systems is also presented. At the end of the chapter, the work structure is provided.

1.1 Overview

Nowadays, mobile communications systems have become an important infrastructure in our society. Over the last decade, it has undergone significant changes and experienced gigantic growth, from analogue to digital technology, from a simple voice call to the data service with higher data rates. The evolution of mobile systems is shown in Figure 1.1.

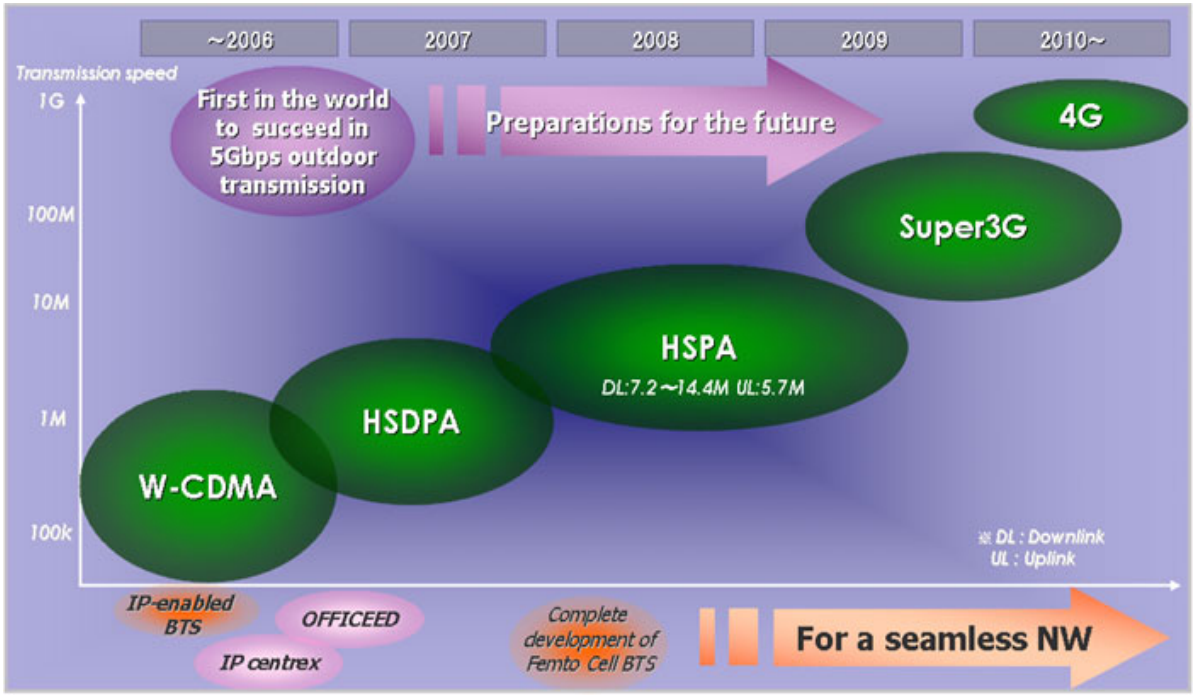

Figure 1.1. Evolution of mobile systems (extracted from [NTTD08]).

The massive success of 2G technologies is pushing mobile networks to grow extremely fast as ever-growing mobile traffic puts a lot of pressure on network capacity. In addition, the current strong drive towards new applications, such as wireless Internet access and video telephony, has generated a need for a universal standard at higher user bitrates: third-generation (3G). In 1999, the 3rd Generation Partnership Project (3GPP) launched Universal Mobile Telecommunications System (UMTS), a Third Generation (3G) first release. UMTS uses Wideband Code Division Multiple Access (WCDMA) as access technique, and was designed from the beginning to offer multi-service applications [HoTo04]. In UMTS, there are two different modes of operation possible: Time Division Duplex (TDD) and Frequency Division Duplex (FDD). The former never came into commercial deployment.

Mobile communications evolution does not stop. New studies have been leading to news technologies, improving the system. In March 2002, High Speed Downlink Packet Access (HSDPA) was set as a standard in 3GPP Release 5. In 2005, networks with HSDPA became available providing 1.8 Mbps, increasing to 3.6 Mbps in 2006, and achieving 7.2 Mbps during 2007, with the maximum peak data rate of 14.4 Mbps in a near future, starting the mobile IP revolution, [HoTo06]. In December 2004, High Speed Uplink Packet Access (HSUPA) was launched by 3GPP in Release 6 with the

Enhanced Dedicated Channel (E-DCH). HSDPA and HSUPA are commonly known as High Speed Packet Access (HSPA). Further HSPA evolution is specified in 3GPP Release 7, and its commercial deployment is expected by 2009. HSPA evolution is also known as HSPA+. 3GPP is also working to specify a new radio system called Long-Term Evolution (LTE) [NTTD08]. Release 7 and 8, solutions for HSPA evolution, will be worked in parallel with LTE development, and some aspects of LTE work are also expected to reflect on HSPA evolution. Now the challenge is UMTS deployment on the lower frequency band, UMTS 900. In UMTS 900, for the same service as HSDPA, results shows a better coverage, both in terms of extended coverage in rural areas and improved indoor coverage, at much lower cost.

When working in the world of radio waves, which has no arbitrary boundaries and no geographic licensing, interference issues always will pop up. Interference is a physical phenomenon which exists and will always exist in different ways on mobile communications. Since the last decade, studies on interference have been growing because the capacity of a Base Station (BS) in UMTS is limited by interference. Thus, its evaluation is one of the fundamental procedures for analysing UMTS. On the Uplink (UL), the multiple access interference (MAI) at a BS is caused by all Mobile Terminals (MTs) whether they belong to this BS or not. On the Downlink (DL), the capacity is limited by the transmit power of the BS or by the interference it causes, respectively. The power control mechanisms in both links provide that the signals are transmitted with such powers that for each service they are received with nearly equal strength. A detailed examination of the interference on UL is no simple task. Due to the universal frequency reuse in UMTS, all users both in the considered cell and in the neighbouring ones contribute to the total interference, thus, influencing the link quality in terms of received bit-energy-to-noise ratio (E_b/N_0) [MäSt03].

The planning of UMTS networks consists of two aspects: coverage and capacity planning, and a trade off between the two exist. The more users are active at a BS, the larger is the MAI at the BS, and the higher are the transmit powers required by the MTs to fulfil their E_b/N_0 requirements. Additionally, due to the restriction of the MTs transmit power, the coverage area shrinks with an increasing number of users. Attaining a certain coverage area for a BS demands a limitation of the MAI, which is done by admission control. The MAI level used as threshold for the acceptance of new calls determines not only the coverage area but also the capacity of the BS. Capacity here means the maximum possible offered load for a BS with a particular service mix, while meeting predetermined blocking probabilities.

In UMTS operating in FDD, interference happens only between MT and BS and between BS and MT, due to its nature. The total interference experienced by an MT is composed of two parts: intra- and inter-cells, Figure 1.2. The intra-cell is created within one cell, caused by MTs or BS of the cell. The inter-cell is caused by MTs or BSs that are out of the cell under consideration.

Interference, among other factors, changes with the MTs locations. Mobile phones are used everywhere, not only outdoor, but also more and more indoor. In these environments, customers demand a good coverage and quality of service. Nevertheless, these systems were not deployed to satisfy specifically these requirements. Operator deployment requirements typically guarantee coverage, with certain quality requirements, of a minimum percent of the geographical area and

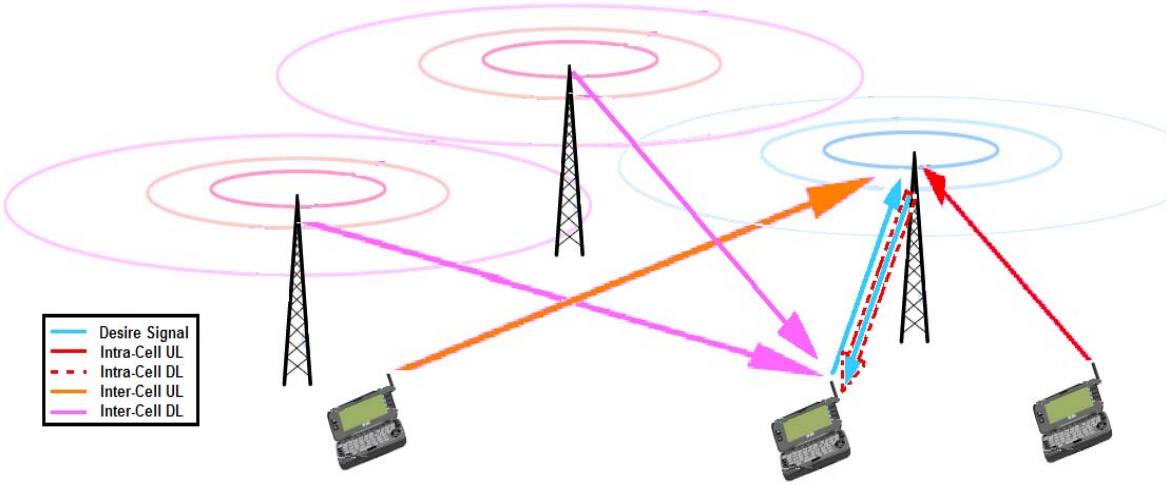

Figure 1.2. Interference representation.

population. Planning tools, key elements for the efficient dimensioning of a network, usually provide only outdoor coverage predictions. They estimate the path loss from the BS to the centre of the street where MTs are assumed to be. Therefore, an extra signal attenuation associated to building penetration is required in the planning of the network. A specific attenuation value for building penetration can improve the indoor coverage for a certain percentage of indoor environments.

The estimation of an extra signal attenuation associated to building penetration can be obtained via propagation models, or to predictions extracted from measurement campaigns. Nevertheless, building construction characteristics and city morphology have a strong impact on propagation characteristics, which makes the correct adaptation of these models and predictions a difficult task. Some concern must be taken when the median level outside is determined. If a Line of Sight (LoS) exists between the BS antenna and one or several external walls a considerable variation, tens of dB, of the path loss around the perimeter of the building may occur. Thus, the corresponding penetration loss will vary considerably depending on which reference level is used [FKRC06].

The penetration loss can be divided into four major categories: wall loss, room loss, floor loss and building loss, each one relative the median path loss level outside the building. The wall loss, which is angle dependent, is the penetration loss through the wall. The penetration loss of the external wall can be different at Non Line of Sight (NLoS) conditions compared to a perpendicular LoS situation. Thus, one single external wall can have considerable different penetration losses, depending on the environmental conditions. The room loss is the median loss determined from measurements taken in the whole room about 1-2 m above the floor. The floor loss is the median loss in all of the rooms on the same floor in a building. In some cases, the penetration loss decreases with increasing floor level, which is called floor height gain. Since, the heights of the storeys vary between different buildings, it is sometimes better to describe the dependence as a function of the physical height. The height gain effect ceases to be applicable at floor levels that are considerable above the average height of the neighbouring buildings. The sum of the outside reference loss and the height gain loss, which is negative, must not be less than the free space propagation loss [DaCo99].

1.2 Motivation and Organisation of the Thesis

Despite UMTS being well known, and already employed throughout the world, there are not enough studies and conclusions about interference on it, so it is important to have a more detailed study. The main scope of this thesis is to study the interference dependence in UMTS with the buildings height. These objectives will be accomplished through the development of a model and its implementation in a simulator. The interference is obtained by intra- and inter-cell interferences combination, in each link, DL and UL.

This thesis was made in collaboration with Celfinet, a Portuguese consulting company. Several technical details were discussed with the company, and one used the suggested values for several parameters throughout this thesis. All measurements were performed with Celfinet support, and all the equipment was supplied by them.

The main contribution of this thesis is the analysis of the UMTS interference dependence with the buildings height, and a model that calculates the interference in DL and UL. A new simulator is created, that enables the interference analysis, being capable to produce results according to several parameters defined by the user.

This work is composed by 5 Chapters, including the present one, followed by a set of annexes.

Chapter 2 mainly introduces UMTS, propagation models and interference. UMTS basic concepts are explained, the services and the architecture are shown, and then the radio interface. Afterwards, a brief overview of propagations models is given, for outdoor models and indoors. Later on, the interference basic aspects are shown, following by the interference models.

Chapter 3 presents all issues related to the implementation of the models in the simulator. At the beginning, all models used and decisions made are presented. Then, a simulator overview is given, concerning architecture and functionality. Afterwards, detailed descriptions of the interference and propagation models algorithms are performed, and output files are detailed. At the end of the chapter, the simulator assessment is presented.

Chapter 4 begins with the description of the default scenario. Then, a measurements overview is highlighted, following by its results. After that, a comparison between measurements and simulations is presented. This chapter finishes with the presentation of the results obtain for each case in study and its analysis.

Chapter 5 summarises the work in this thesis, draws the conclusions, and also discusses future work.

A set of annexes with auxiliary information and results is also included. In Annex A, the extrapolation of the Gaussian Approach model is shown. In Annex B, the detailed link budget used throughout this thesis is presented. In Annex C, one presents the flowcharts of some used algorithms. In Annex D, one presents the antennas properties. In Annex E, one presents the simulator and auxiliary programs user's manual. In Annex F, one presents auxiliary results regarding the simulator assessment. In Annex G and H, one shows additional results of measurements and simulations, respectively.

Chapter 2

Basic Aspects

This chapter outlines the basic concepts of UMTS and presents the required background information necessary for a clear understanding of this system. Afterwards, the models that characterise the propagation phenomena and the interference in mobile radio environments are described.

2.1 Services and Architecture

UMTS came from the inevitable evolution of GSM, therefore, this technology has the same services and much more. Moreover, it has bearer services that give the subscriber the capacity required to transmit appropriate signals between certain access points [UMTS07]. Among those services it offers Point-to-Point and Point-to-Multipoint communications.

Bearer services offer a maximal data rate and highest user velocity according to each hierarchy cell [UMTS07], [Moli05]. Consequently the data rate offers are: 144 kbps for rural outdoor, macro-cell, at speeds up to 500 km/h; 384 kbps urban outdoor, micro-cell, at maximal speeds 120 km/h; and 2048 kbps indoor and low range outdoor, pico-cell, for a maximal user speed up to 10 km/h. However, these data rates became obsolete when HSDPA began to be used [HoTo06]. With this breakthrough, DL speeds may reach 1.8, 3.6, 7.2 or even 14.4 Mbps. Nevertheless the biggest difference between the HSDPA and the conventional UMTS is the lack of two basic features of the channels: variable spreading factor and fast power control. Furthermore, there are other differences such as: improved DL performance, for instance using Adaptive Modulation and Coding (AMC), fast packet scheduling at the BS, and fast retransmissions from the BS, known as Hybrid Automatic Repeat-request (HARQ).

UMTS services have different Quality of Service (QoS) out of four kinds of traffic. Each class shows a maximal Bit Error Ratio (BER) and a transmission delay characteristic of the target user choice. Therefore, the user may choose among the Conversational, Streaming, Interactive or Background classes. The Conversational class is mainly chosen for services like voice, video telephone and video game. It is rather similar to GSM, so the delay should be within the rate of 100 ms or less, and BERs around 10^{-4} or less, because the user does not allow any interruption. The Streaming class is used for multimedia, video on demand, webcast, thus, a large delay can be tolerated, as the receiver typically buffers several seconds of streaming material. BERs are usually smaller, since the noise in the audio signal (music) is more irritating than voice conversation. Interactive class contemplates all applications where the user requests data from a remote appliance, such as web browsing, network gaming, and database access. The delay should never exceed a few seconds and BERs have to be lower, within 10^{-6} or less. The last group, the so-called Background class, figures the email service, SMS, downloading, where transmission delays are not critical.

As it can be seen in Figure 2.1, the UMTS network is composed by three main groups: Core Network (CN), UMTS Terrestrial Radio Access Network (UTRAN) and User Equipment (UE). In this scheme, the CN is rather similar to the GSM one with GPRS, but all equipment has to be modified [UMTS07], [Bodi03].

The CN includes the databases and the management functions, so the main task is to provide switching, routing and transit for user traffic, therefore, CN is mainly divided in circuit and packet switched domains. Figure 2.1 shows MSC, VLR and GMSC which constitute the circuit switched elements, while SGSN and GGSN represent the packet switched ones. However, there are some elements that share both domains, such as the HLR and VLR.

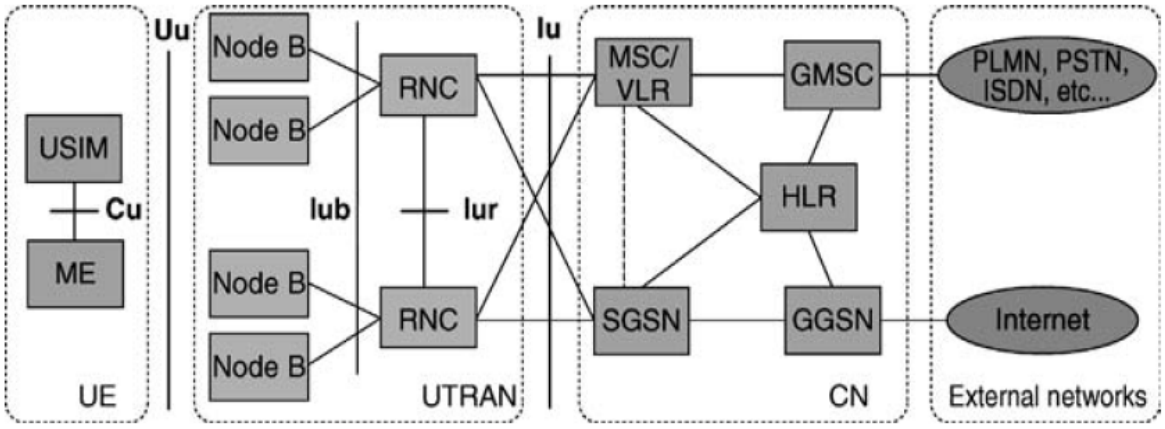

Figure 2.1. UMTS architecture (extracted from [HoTo04]).

UTRAN is the key element in the UMTS network. Composed by Nodes B (the BS) and Radio Network Controllers (RNCs), it makes the bridge between UEs and CN. This transmission is established via the air interface. The Node B interconnects with the RNC via the Iub interface. The RNC controls the resources in the system and interfaces with the CN.

UE is normally known as MT. This terminal usually appears as a form of a handset and it is composed of a Mobile Equipment (ME) and an UMTS Subscriber Identify Module (USIM). The radio transceiver, the display and the digital signal processors are also part of the ME. The USIM is a 3G application running in a Universal Integrated Circuit Card (UICC), i.e., a mere logical entity on the physical card, which contains the subscriber identity, authentication information and also provides storage space for text messages and phone book contacts.

The UE is able to communicate with the legacy system, such as GSM and GPRS. Furthermore, 3GPP developed the multi-mode that UEs support, which can be divided into four different categories [UMTS07]:

- Type 1: user equipment operates in one single mode at a time, GSM or UTRA. While operating in a given mode, the user equipment does not scan for or monitor any other mode. Switching from one mode to another is done manually by the subscriber.
- Type 2: user equipment can scan for and monitor another mode of operation. The user equipment reports to the subscriber on the status of another mode by using the current mode of operation. In this type the user equipment does not support simultaneous reception or transmission through different modes. Switching from one mode to another is performed automatically.
- Type 3: it is fairly similar to type 2. However, in this one the UE can receive in more than one mode at a time. But, type 3 cannot transmit simultaneously in more than one mode. As in type 2, switching from one mode to another is performed automatically.
- Type 4: user equipment can receive and transmit simultaneously in more than one mode. As in the previous two types, switching from one mode to another is performed automatically.

2.2 Radio Interface

According to the World Administrative Radio Conference - 92 (WARC-92) frequencies resolution for International Mobile Telecommunications-2000 (IMT-2000), the bands 1885-2025 MHz and 2110-2200 MHz are intended for using on a worldwide basis, by administrations wishing to implement IMT-2000. Such use does not preclude the use of these bands by other services to which they are allocated [UMTS07]. Nonetheless, WARC-2000 made some arrangements in the frequencies spectrum. Therefore, in Europe UMTS works in the range from 1900 MHz to 2025 MHz and from 2110 MHz to 2200MHz. The main bands are 1920-1980MHz and 2110-2170MHz used for UMTS UL and DL, respectively [Moli05].

Figure 2.2 illustrates some of the UTRA features. Using a variable spreading factor and multi-code links, it supports bit rates up to 2 Mbps. It has a chip rate of 3.84 Mcps within 5 MHz carrier spacing, although the actual carrier spacing can be selected on a 200 kHz grid between approximately 4.4 and 5 MHz, depending on the interference situation between the carriers **Erro! A origem da referência não foi encontrada.**.

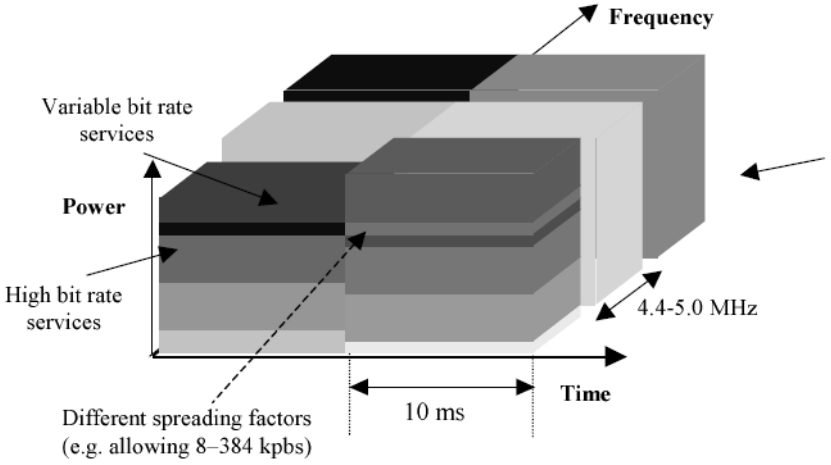

Figure 2.2. FDD mode characteristics (extracted from **Erro! A origem da referência não foi encontrada.**).

Spreading operation in UMTS, also known as channelisation, is the multiplication of each user data bit by a sequence of code bits called chips, resulting in a spread data with the same random appearance as the spreading code. The channelisation codes increase the transmission bandwidth and use the Orthogonal Variable Spreading Factor (OVSF) technique, which allows the Spreading Factor (SF) to be changed, while maintaining orthogonality among codes with different lengths. The scrambling operation is used over spreading, but it does not modify the signal bandwidth. In DL, it differentiates the sectors of the cell, and in UL, it separates MTs from each other. The scrambling code (SC) can be either a short or a long one, the latter being a 10 ms code based on the Gold family, and the former being based on the extended S(2) family. UL scrambling uses both short and long codes, while DL employs only long codes. Codes characteristics are summarised in Table 2.1.

The signal resulting from the multiplication of the user's data by the channelisation code is again

multiplied by the scrambling code, which gives the final chip rate that will be transmitted, Figure 2.3.

Table 2.1. Functionality of the channelisation and scrambling codes, [Corr07].

	Channelisation	Scrambling
Use	DL: MT separation UL: Channel separation	DL: Sector separation UL: MT separation
Duration	DL: 4 – 512 chip UL: 4 – 256 chip	38 400 chip
Number	Spreading Factor	DL: 512 UL: several millions
Family	OVSF	Gold or S(2)
Spreading	Yes	No

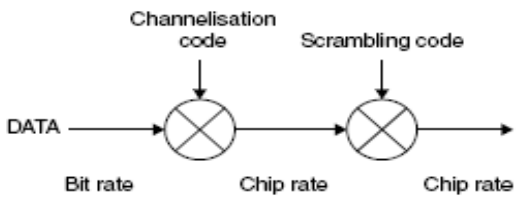

Figure 2.3. Relationship between spreading and chip rate (extracted from [HoTo04]).

UMTS has a self timing point of reference through the operation of asynchronous BSs. It uses coherent detection in the UL and DL, based on the use of pilot reference symbols. Its architecture allows the introduction of advanced capacity and coverage enhancing CDMA receiver techniques. It may seamlessly co-exist with GSM networks through its inter-system handover functions UMTS.

In UMTS, the capacity of each cell is essentiality given by the number of users and the services they use [HoTo04]. The maximum number of users per cell depends on noise and interference levels, which results in an admissible QoS, for a different date rate. The interference results from the existence and proximity of users in the cell, therefore, to get a good management and to assure a minimum admissible QoS, it is necessary to measure the load factor in order to limit the maximum noise. The noise rise is defined as the interference margin:

$$M_{I[\mathrm{dB}]} = -10\log(1-\eta) \tag{2.1}$$

where:

- η: load factor.

The higher the system load is, the higher the interference margin will be. When η approaches 1, the system reach its pole capacity and the noise rises to infinity.

The global load factor of the cell is shown in (2.2) and (2.3), in order to get a good estimation of BS

coverage, for UL and DL.

$$\eta_{UL} = (1+i)\sum_{j=1}^{N_u} \frac{1}{1+\frac{R_c}{\left(\frac{E_b}{N_0}\right)_j \cdot R_j \cdot \nu_j}} \tag{2.2}$$

$$\eta_{DL} = \sum_{j=1}^{N_u} \nu_j \cdot \frac{\left(\frac{E_b}{N_o}\right)_j}{\frac{R_c}{R_j}} \cdot \left[\left(1-\alpha_j\right)+i_j\right] \tag{2.3}$$

where:

- i: ratio of inter-cell to intra-cell interferences;
- N_u: number of users per cell;
- R_c: WCDMA chip rate (always 3.84 Mcps).
- E_b: energy per user bit;
- N_0: noise power density;
- R_b: bit rate of user j;
- ν_j: activity factor of user j (typically 0.5 for speech and 1.0 for data);
- α_j: DL channel orthogonality factor of user j (between 0.4 and 0.9 in multipath channels);
- i_j: ratio of inter-cell to intra-cell interferences for user j.

Coverage in DL is more dependent on the load than in UL, since the BS has a maximum transmission power, despite the number of users in the cell. Table 2.2 shows the maximum transmission power.

Table 2.2. Typical values of the transmitter output power (extract from [Corr07]).

BS [dBm]			MT [dBm]
Macro	Micro	Pico	
[40, 43]	[30, 33]	[20, 23]	[10, 33]

A very important key feature of WCDMA is power control, since without it an MT could block a whole cell, giving rise to the so-called near-far problem of CDMA. In UMTS, MTs adaptively adjust their power level so as not to swamp all the others in the network. The power control mechanisms in both links provide that the signals are transmitted with such powers that for each service they are received with nearly equal strength, i.e., the transmitted power for an MT at different locations is adjusted according to the power control law; with knowledge on the locations of MTs, it is possible to minimise

the total transmitted power by transmitting high power level for far-end users and low power level for near-in users. There are different types of power control, the two main are: Open loop and Fast closed loop power control.

Open loop power control is only used to provide a coarse initial power setting of the MT at the beginning of a connection. In closed loop power control in the UL, the BS performs frequent estimates of the received Signal-to-Interference Ratio (SIR) and compares it to a target. If the measured SIR is higher than the target, the BS will command the MT to lower the power; if it is too low it will command the MT to increase its power. Thus, closed loop power control will prevent any power imbalance among all the UL signals received at the BS. The same technique is also used on the DL, though here the motivation is different: on the DL there is no near–far problem due to the one-to-many scenario. All the signals within one cell originate from one BS to all MTs. It is, however, desirable to provide a marginal amount of additional power to MTs at the cell edge, as they suffer from increased inter-cell interference [HoTo04].

WCDMA employs orthogonal codes in the DL, $\alpha_{j,}$ to separate users. Moreover, without any multipath propagation the orthogonality remains the same when the BS signal is received by the MT. However, if there is enough delay spread in the radio channel, the MT will handle part of the BS signal as multiple access interference. The orthogonality of 1 corresponds to perfectly orthogonal codes. The coverage in rural areas depends on the UL load factor and on the limited MT transmission power. Otherwise in urban ones, micro- or pico-cells, intended for high data rates, are used, whose capacity is limited by the DL load factor.

The number of available codes in a certain cell depends on the number of users and on the bit rate required by the type of service each user is accessing. The number of channelisation codes is given by the Spreading Factor (SF). The higher the bit rate is, the smaller the SF will be. So, when the number of users increases, the bit rate of the bearer service will also increase, leading to a decrease of the available SF, and hence of the number of codes. The number of available scrambling codes may be a limitative factor only in DL, as there are only 512 available codes, Table 2.1. Although this is the least important factor of the three that are listed, it must be taken into account.

2.3 Propagation Models

2.3.1 Basic Aspects

In mobile communications, the transmission medium depends a lot on the surrounding environment. In fact, it can be affected by an “infinite” number of parameters describing the environment. Anyway, the phenomena that influence radio waves propagation may generally be described by four basic mechanisms: reflection, penetration, diffraction and scattering [DaCo99].

Scattering can be caused by multiple reflections, resulting in an increase of the multipath. Multipath depends on the objects because multipath can change the time delay, and the delay may spread the

propagated signal. So, multipath is one point to take into account for signal degradation. However, the main cause of a lower performance in a mobile radio system is fading [Yaco93].

Fading can be split in to slow and fast. This is done according to the rate at which the magnitude and phase change. Due to the randomness of these phenomena, the mobile radio signal is normally treated on a statistical basis, using some probability distributions. The best distribution that fits slow fading is the Log-Normal distribution with standard deviation in the range 4-10 dB. On the other hand, fast fading is not so simple, i.e., for a good approximation it is required to know if MT and BS are in LoS or in NLoS. Therefore, fast fading is due to multipath propagation and it has a Rayleigh distribution for NLoS. Within buildings, where both multipath and LoS waves may be found, fast fading follows a Ricean distribution. For a good design of a communication network, it is necessary to keep the fading boundaries near average values.

In a mobile radio system, wave propagation models are extremely important to determine propagation characteristics in order to get a good coverage and capacity planning. The propagation models can be divided into two main groups: theoretical and empirical ones. The theoretical models provide an approximation of the reality based on assumptions that simplify the problem and allow for an easy change in parameters. However, these models have low versatility when the scenario change and do not take into account the environment that influences directly the signal. The empirical models are based on measurements, leading to best fit equations, taking into account many parameters. Consequently, the models are usually very complex. The disadvantage of these models is their limitation of boundaries, since any kind of extrapolation needs to be checked in environments different from those in which they were measured. Sometimes the combination of these groups of models gives rise to a simplified prediction model with excellent results where high accuracy is not required [Yaco93], [Corr07].

The model usage requires an environment classification, which takes into account some parameters like terrain undulation, vegetation density, building density and height, open areas density and water areas density. Consequently, the environments are usually divided into three types: rural, suburban and urban. In order to distinguish these categories, some authors proposed calculations and others only made some assumptions respecting this matter. Thus, the rural environment is the one with the largest open area, which normally consists of a flat terrain without any obstacles. Suburban type is characterised by the existence of a few obstacles, as for instance small cities and residential areas. The last one, the urban type, is a highly dense environment, consisting of buildings higher than 4 floors, such as large cities, commercial and industrial areas.

It is also important to point out the classification of the service type. Therefore, the cells used in these environments are usually classified according to their radius range and to the relative position of the BS antennas. So, the cell type can be divided into four different types [DaCo99]: large macro-cell, small macro-cell, micro-cell and pico-cell. Small macro-cells are built above the medium roof-top level, and therefore the heights of some surrounding buildings are above BS antenna height. They are used for outdoor and its coverage radius range is between 0.5 and 3km (urban scenarios).

Indoor models are very important as a means of predicting the propagation characteristics of the

indoor environment. This is because measuring radio propagation in every building in order to reduce the interference would be unthinkable, since the cost would be very high.

In the indoor environment, the characteristics that degrade the performance of communication systems are quite different from the outdoor. The variation of building size, shape, and structure, the rooms layouts and, above all, the construction materials, make the electromagnetic-wave propagation inside a building a highly complex multipath structure, much more than the one of terrestrial mobile radio channels. The variation of materials used in internal partitions, outside walls, ceilings and floors, the size and percentage of windows, age of building, people density and activity are factors that make indoor electromagnetic-wave propagation fairly complex [TaTr95].

Consequently propagation models have been developed as a suitable low-cost alternative. The existing indoor models can be classified into two classes: statistical models and semi-deterministic models. In statistical models the additional attenuation is taken as a function of the percentage of indoor locations to be covered, accounting for the general characteristics of the building, that is to say, it relies on measurement data. In site-specific propagation models, since they are based on the electromagnetic-wave propagation theory, it is required to take into account a considerable detail of the indoor environment.

After viewing the basic knowledge of the aspects taken into account for a correct choice of propagation models, a detailed description follows. Since there are many models in this field, it is necessary to select models that work in UMTS frequencies, such as small macro-cells and urban sceneries (outdoor and indoor). So, the chosen models are COST231 – Walfish-Ikegami [DaCo99] and 3GPP [3GPP98], COST231 – Multi-Wall [DaCo99] and a Gaussian Approach [Corr07], for outdoor and indoor, respectively.

Before a description of the models, it is necessary to characterise the maximum loss which propagation tolerates in order to get a good dimensioning of a cell, and to take into account the coverage, capacity and optimisation. In Annex B, this characterisation is shown in further detail. Nevertheless, generically the path loss can be given by [Corr07]:

$$L_{p[\mathrm{dB}]} = P_{t[\mathrm{dBm}]} + G_{t[\mathrm{dBi}]} - \mathrm{P}_{\mathrm{r}[\mathrm{dBm}]} + G_{r[\mathrm{dBi}]} \tag{2.4}$$

where:

- L_p: path loss attenuation;
- P_t: power fed to the transmitting antenna;
- G_t: gain of the transmitting antenna;
- P_r: power available at the receiving antenna;
- G_r: gain of the receiving antenna.

With the combination of the outdoor and indoor losses the total path loss can be achieved:

$$L_{pTotal[\mathrm{dB}]} = L_{p\ outd[\mathrm{dB}]} + L_{p\ ind[\mathrm{dB}]} \tag{2.5}$$

where:

- $L_{p\ \mathrm{Total}}$: total path loss attenuation;
- $L_{p\ outd}$: path loss attenuation gives by outdoor model;
- $L_{p\ ind}$: path loss attenuation gives by indoor model.

2.3.2 Outdoor Models

For outdoors [Corr07] two models are suggested, COST 231 – Okumura-Hata and COST 231 – Walfish-Ikegami. The Okumura-Hata is based on Hata [Hata80] and Okumura [OkOh68] models, and Walfish-Ikegami is the result of the combination of Walfish-Bertoni [WaBe88] with Ikegami [IkYo84]. They were developed for urban, suburban and rural environments. Okumura-Hata is for large distances, usually more than 5 km. Walfish-Ikegami is used for cases where the distances are less than 5 km in both urban and suburban environments. The parameters for this model for path loss prediction are: buildings height (h_{Roof}), roads width (w_s), building separation (w_b) and road orientation with respect to the direct radio path (φ), as shown in Figures 2.4 and 2.5.

This model has one particularity, it distinguishes LoS from NLoS. For LoS propagation ($\varphi = 0$) the loss is calculated by (2.6). For NLoS propagation the loss is composed by three terms: free space loss (L_0), multiple screen diffraction loss (L_{msd}), and roof-top-to-street diffraction and scatter loss (L_{rts}). So, in the NLoS the prediction is calculated by (2.7).

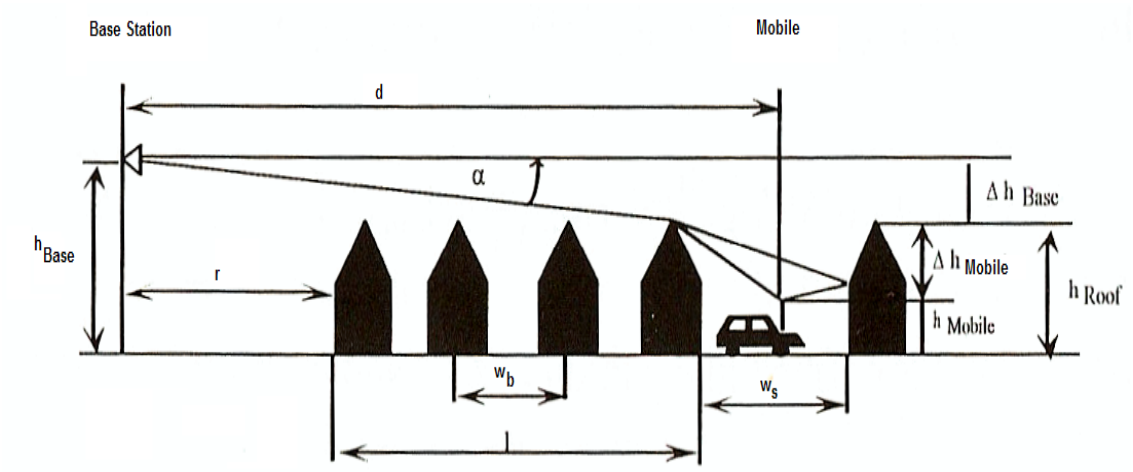

Figure 2.4. Definition of the parameters used in the COST 231 WI model (extracted from [DaCo99]).

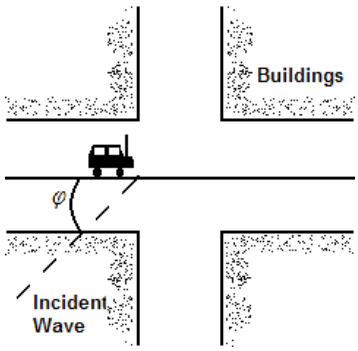

Figure 2.5. Definition of the street orientation angle φ (extracted from [DaCo99]).

$$L_{p[\mathrm{dB}]} = 42.6 + 26\log(d_{[km]}) + 20\log(f_{[\mathrm{MHz}]}) \text{ for } d \geq 0.02 \text{ km} \tag{2.6}$$

$$L_{p[\mathrm{dB}]} = \begin{cases} L_{0[\mathrm{dB}]} + L_{rts[\mathrm{dB}]} + L_{mts[\mathrm{dB}]} & \text{for} \quad L_{rts} + L_{mts} > 0 \\ L_{0[\mathrm{dB}]} & \text{for} \quad L_{rts} + L_{mts} \leq 0 \end{cases} \tag{2.7}$$

The free-space loss is given by

$$L_{0[\mathrm{dB}]} = 32.4 + 20\log(d_{[\mathrm{Km}]}) + 20\log(f_{[\mathrm{MHz}]}) \tag{2.8}$$

The term L_{rts} basically describes the loss between last roof-top and MT. This parameter is mainly based on Ikegami's model (accounting street orientation and its width). However, rather than Ikegami, COST 231 applies a different street-orientation function.

$$L_{rts[\mathrm{dB}]} = -16.9 - 10\log(w_{s[\mathrm{m}]}) + 10\log(f_{[\mathrm{MHz}]}) + 20\log(\Delta h_{Mobile[\mathrm{m}]}) + L_{Ori[\mathrm{dB}]} \tag{2.9}$$

where:

- Δh_{Mobile}: difference between the roof height and the mobile height (2.10);

$$\Delta h_{Mobile[\mathrm{m}]} = h_{Roof[\mathrm{m}]} - h_{Mobile[\mathrm{m}]} \tag{2.10}$$

- L_{ori}: street orientation loss (2.11).

$$L_{Ori[dB]} = \begin{cases} -10 + 0.354\varphi_{[\mathrm{deg}]} & \text{for} \quad 0^\circ \leq \varphi < 35^\circ \\ 2.5 + 0.075(\varphi_{[\mathrm{deg}]} - 35) & \text{for} \quad 35^\circ \leq \varphi < 55^\circ \\ 4.0 - 0.114(\varphi_{[\mathrm{deg}]} - 55) & \text{for} \quad 55^\circ \leq \varphi < 90^\circ \end{cases} \tag{2.11}$$

The L_{msd} parameter basically describes the loss between BS antennas and the last roof-top and MT. It appears as an extension of the Walfish and Bertoni original model by COST 231 for BS antennas height bellow the roof-top levels, using an empirical function based on measurements.

$$L_{msd[\mathrm{dB}]} = L_{bsh[\mathrm{dB}]} + k_a + k_d \log(d_{[\mathrm{Km}]}) + k_f \log(f_{[\mathrm{MHz}]}) - 9\log(w_{b[\mathrm{m}]}) \tag{2.12}$$

where:

- L_{bsh}: losses due to the fact that BS antennas are above or below the roof-top level (2.13);

$$L_{bsh[\mathrm{dB}]} = \begin{cases} -18\log(1+\Delta h_{base[\mathrm{m}]}) & \text{for} \quad h_{base} > h_{Roof} \\ 0 & \text{for} \quad h_{base} \le h_{Roof} \end{cases} \tag{2.13}$$

with

- Δh_{Base}: difference between the BS antenna height and the roof-top height (2.14).

$$\Delta h_{Base[\mathrm{m}]} = h_{Base[\mathrm{m}]} - h_{Roof[\mathrm{m}]} \tag{2.14}$$

- k_a: represents the increase of the path loss for BS antennas below the roof tops of the adjacent buildings;

$$k_a = \begin{cases} 54 & \text{for} \quad h_{base} > h_{Roof} \\ 54 - 0.8\Delta h_{Base} & \text{for} \quad d \ge 0.5Km \ \text{ and } \ h_{base} \le h_{Roof} \\ 54 - 1.6\Delta h_{Base} d_{[\mathrm{Km}]} & \text{for} \quad d < 0.5Km \ \text{ and } \ h_{base} \le h_{Roof} \end{cases} \tag{2.15}$$

- k_d: control the dependence of the multi-screen diffraction loss versus distance;

$$k_d = \begin{cases} 18 & \textit{for} \quad h_{Base} > h_{Roof} \\ 18 - 15\dfrac{\Delta h_{Base}}{\Delta h_{Roof}} & \textit{for} \quad h_{Base} \le h_{Roof} \end{cases} \tag{2.16}$$

- k_f: control the dependence of the multi-screen diffraction loss versus frequency;

$$k_f = \begin{cases} -4 + 0.7\left(\dfrac{f_{[\mathrm{MHz}]}}{925} - 1\right) & \textit{for} \quad \text{medium sized city and suburban centres with medium tree density} \\ -4 + 1.5\left(\dfrac{f_{[\mathrm{MHz}]}}{925} - 1\right) & \textit{for} \quad \text{metropolitan centres (dense urban)} \end{cases} \tag{2.17}$$

If the structure environment data is unknown the following values are recommended:

$$h_{Roof[m]} = 3 \times \{number\ \ of\ \ floors\} + roof\text{-}height_{[m]}$$

$$roof\text{-}height_{[m]} = \begin{cases} 3 & for \quad pitched \\ 0 & for \quad flat \end{cases}$$

$$w_{b[m]} = 20...50$$

$$w_{s[m]} = \frac{w_{b[m]}}{2}$$

$$\varphi = 90^{\circ}$$

As Table 2.3 shows, the COST – WI model has restrictions. One of them, already mentioned, is the short distance of estimation. Other is the limitation for UMTS frequencies, that is to say, the system frequency spectrum does not cover it thoroughly.

In this model, the standard deviation takes values around [4, 7] dB and the error increases when h_{Base} decreases relatively to the h_{Roof} [Corr07].

Table 2.3. Restrictions of the COST 231 - WI (extracted from [DaCo99]).

Parameters	Interval Values
Frequency	[800, 2000] MHz
BS Height	[4, 50] m
MT Height	[1, 3] m
Distance between BS and MT	[0.02, 5] Km

Sometimes when the BS is on the building top and the building is adjacent to the MT, the path loss calculation can be done according to (2.18). The extra attenuation is based on [WaAC03] and represents the attenuation due to diffraction from the roof to the MT. This can be calculated using (2.19).

$$L_{p[\mathrm{dB}]} = L_{0[\mathrm{dB}]} + L_{p_{extra}[dB]} \tag{2.18}$$

where:

- $L_{p\ extra}$: extra attenuation given by:

$$L_{p_{extra}[\mathrm{dB}]} = -20\log\left[\frac{1}{\sqrt{\pi k r_{[\mathrm{m}]}}}\left(\frac{1}{\theta_{[\mathrm{rad}]}} - \frac{1}{2\pi - \theta_{[\mathrm{rad}]}}\right)\right] \tag{2.19}$$

with

- Θ : angle between MT and Roof-Top corner defined by (2.20) and as shown in Figure 2.6;

$$\theta_{[rad]} = \tan^{-1}\left(\frac{|\Delta h_{Mobile[m]}|}{x_{[m]}}\right) \tag{2.20}$$

- k: propagation constant that is given by (2.21);
- r: distance between roof-top and the MT as shown Figure 2.6 and given by (2.22).

$$k = \frac{2\pi f_{[\mathrm{MHZ}]}}{300} \tag{2.21}$$

$$r_{[m]} = \sqrt{\left(\Delta h_{Mobile[m]}\right)^2 + x_{[m]}^{\ 2}} \tag{2.22}$$

with

- Δh_{Mobile}: difference between the roof height and the MT height, (2.10);
- x: horizontal distance between the MT and diffracting edges.

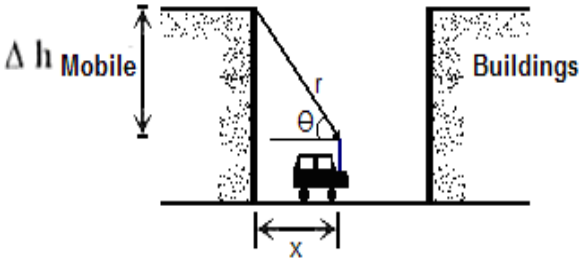

Figure 2.6. Illustration of the extra attenuation parameters (extract from [Corr07]).

For outdoors, there is another model proposed by 3GPP, [3GPP98]. This model is based on [WaBe88] with some measures adjustments in urban environments [XiBe94]. So the loss predicted for this model is given by:

$$L_{p[\mathrm{dB}]} = -10\log\left[\left(\frac{\lambda_{[\mathrm{m}]}}{4\pi d_{[\mathrm{m}]}}\right)^2\right] - 10\log\left[\frac{\lambda_{[\mathrm{m}]}}{2\pi^2 r_{[\mathrm{m}]}}\left(\frac{1}{\theta_{[\mathrm{rad}]}} - \frac{1}{2\pi + \theta_{[\mathrm{rad}]}}\right)^2\right] - 10\log\left[\frac{2.35^2}{d_{[\mathrm{m}]}^{2\left(1-0.04\,\Delta h_{Base[\mathrm{m}]}\right)}}\left(\Delta h_{Base[\mathrm{m}]}\sqrt{\frac{w_{b[\mathrm{m}]}}{\lambda_{[\mathrm{m}]}}}\right)^{1.8}\right] \tag{2.23}$$

where:

- λ: wavelength;

This model, as in COST 231 – WI can be divided into three parts. The first part of (2.23) represents L_0, the second represents L_{rts} and the last part represents the L_{msd}.

This model has limitations. It considers the BS antenna height above roof-top level, L_p shall not be less than L_0 in any circumstances, the Δh_{Base} has to be between 0 and 50 m, and applicable for the test scenarios in urban and suburban areas outside the high rise core where the buildings are of nearly uniform height [3GPP98].

2.3.3 Indoor Models

For indoor models [Corr07], it is suggested a statistic model that was developed by IST based on measurements made in Lisbon. This model, Gaussian Approach, gives the penetration attenuation, L_{pind}, for a given overall indoor coverage probability and follows a Log-Normal distribution with an average of 11.6 dB and a standard deviation of 13.8 dB. These values are an extrapolation of the GSM1800 Band and all the calculations are shown in Annex A. This approximation can be done because the frequency band of UMTS is very close to the GSM1800 one.

This model is a good approach, because it gives the average loss of urban scenarios for indoors environments. Another positive point is the city where the measurements were made, since this work has the same city as scenario.

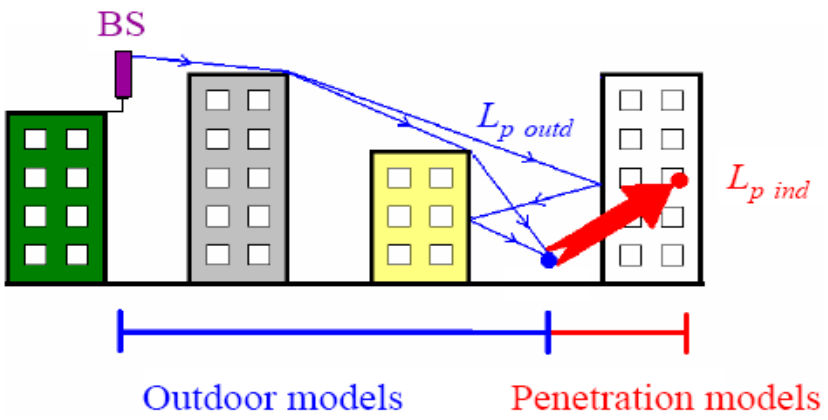

Figure 2.7. Interpretation of the Gaussian Approach.

Another model that can be considered is one of the three models investigated by COST 231 [DaCo99]. The first one, One-Slope model (1SM) assumes a linear dependence between the path loss and the logarithmic distance. The second, Multi-Wall model (MWM) takes into account the free space loss plus other losses, as well as the walls and floors penetration loss by the direct path between the transmitter and the receiver. The particularity of MWM is the empirical factor *b* [TöBe93], which makes the total floor loss a non-linear function of the number of penetrated floors. The last model, Linear Attenuation model (LAM) gives the path loss as a linearly dependence with the distance plus free space loss.

The MWM can be given by:

$$L_{p\ ind[dB]} = L_{0[dB]} + l_{glass} + k_i L_{wi} + k_f L_{f[dB]} \tag{2.24}$$

where:

- k_{wi}: number of penetrated walls of type *i*;
- k_f: number of penetrated floors;
- L_{wi}: loss attenuation of wall type *i*, Table 2.4;
- L_f: floor loss attenuation;
- l_{glass}: glass loss attenuation.

Table 2.4. Wall types for the multi-wall model and weighted average loss (based on [OlCa02]).

Loss category	Description	Factor [dB]
L_f	Typical floor structures (i.e. offices) - hollow pot tiles - reinforced concrete - thickness type. < 30 cm	2
L_{w1}	Light internal walls (<10cm) - plasterboard - walls with large numbers of holes (e.g. windows)	10
l_{glass}	Typical glass	1

2.4 Interference

2.4.1 Basic Aspects

Interference is a phenomenon that operators do not like and its levels have increased by the fast growth of communications system. Tall antennas with a higher transmitted power to provide coverage were changed to smaller size cells as a way to combat the overcapacity. This way, providers can reuse the channels or frequencies repeatedly and consequently operate with less power. However, the overcapacity problem was more or less solved, but the interference was increased.

Interference can be expressed in many different ways, as Figure 2.8 suggests. Intermodulation interference is generated in any nonlinear circuit when the products of two or more signals result into another signal, having a frequency that is equal or almost equal to the wanted signal. Intersymbol interference is intrinsic to digital networks and it is usually caused by echoes or non-linear frequency response of the channel. Ways to fight against intersymbol interference include adaptive equalisation or error correcting codes. These two types of interference are well-known phenomena that have already been extensively explored in the literature. So the main interference in mobile radio systems is adjacent-channel and co-channel interference [Yaco93].

Adjacent channel interference occurs as a collateral effect by keeping the channels very close to each other in the frequency spectrum for obtaining maximum spectrum efficiency. Co-channel interference is basically caused by another signal operating on the same channel. In UMTS, the channels have 5 MHz of separation and 4.4 MHz of bandwidth. In spite of this, adjacent channel interference can happen, but this kind of interference has more relevance on GSM because the frequency channel of separation and bandwidth are the same. This work is about UMTS, so co-channel is the interference that really matters.

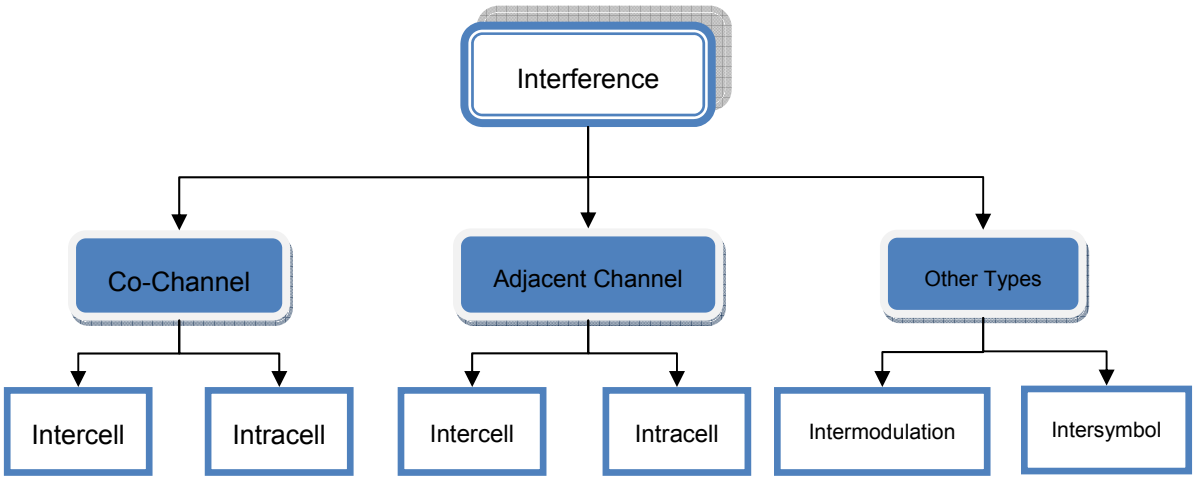

Figure 2.8. Interference Type

Co-channel interference is divided into two parts: intra- and inter-cells, and it happens in two ways: UL (caused by MTs on BSs) and DL (caused by BSs on MTs).

In UL, the intra-cell interference is caused by MTs within the cell and inter-cell interference is composed of all the signals received from the MTs in adjacent cells, as shown in Figure 2.9 (a). So, in UL, the interference is related to the load distribution within the network, but not related to the MTs own location [Chen03].

In DL, as shown in Figure 2.9 (b), the intra-cell interference occurs when one BS causes interference into the MT that it serves, which can be caused by the partial loss of orthogonality between the different codes used for all users in the same cell. The inter-cell interference is the power received by the MT from the adjacent BSs. Since BSs are not synchronised, the inter-cell interference does not get benefits from the orthogonality as happens with the intra-cell interference [Chen03]. So, in DL, the main factor is the loss of orthogonality factor between user codes due to the multipath.

Other kinds of interference scenarios do not exist in FDD, i.e., interference among BSs or MTs. Interference among BSs cannot exist because in UMTS-FDD the UL and DL use different frequency bands. Interference among MTs cannot exist because in the commutation to the BS each MT has a unique identifying code and the UL and DL use different frequency bands.

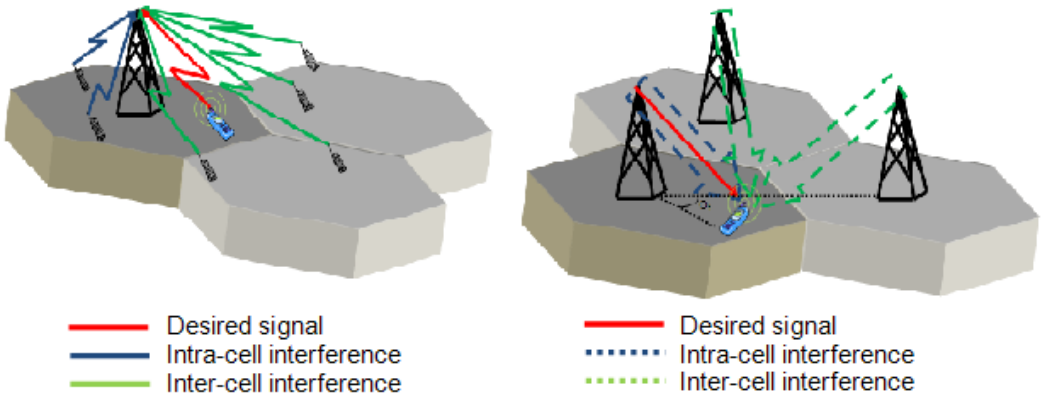

(a) UL. (b) DL.

Figure 2.9. Different cases of interference (based on [Chen03]).

Handover is the essential component for dealing with the mobility of users, since it guarantees the continuity of the communication when the MT moves across cellular boundaries. But, DL interference is affected by soft/softer handover, as shown in Figure 2.10 (a) e (b). Soft handover occurs when the MT goes from one cell to another and simultaneously communicates with both cells. Softer handover does not occur when the MT goes from one cell to another, but when the MT moves from one sector to another within the cell, as shown in Figure 2.10 (c). In Figure 2.10, if MT1 is in soft handover, it communicates with BS1 and BS2 simultaneously. Two DL dedicated channels are set up to support the soft handover, Figure 2.10 (b). Let P1 and P2 represent the power allocated to channels from BS1 and BS2 separately. P1 acts as intra-cell interference to MT2 and inter-cell interference to MT3 and P2 acts as inter-cell interference to MT2 and intra-cell interference to MT 3.

Comparing the two cases, when the MT is not in soft handover, MT1 contributes power P to the total DL interference and when it is in soft handover, the total contribution is the sum of P1 and P2. The increment of the interference due to MT 1 has influence on all other active MTs within the network, therefore, all these MTs need to adjust their channel power to meet the change in the interference.

This, in return, changes the total interference received by MT 1, resulting the alteration of P or P1 and P2. This circulation repeats until the system reaches a new balance. In the case of softer handover, the problems are the same as in soft handover, the only difference is the situation that occurs. The big problem is when the MT is in soft and softer handover, but this is unusual.

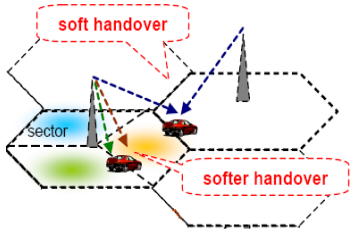

(a) Situation without handover (b) Soft handover effects on the DL interference (c) Soft/Softer handover

Figure 2.10. Handover interpretation (extracted from [Chen03])

established. So, the interference problems motivated by this mechanism do not have an important impact in the system.

2.4.2 Interference Models

In the last years, interference has gained importance in the mobile telecommunication world since it has become a limitation for the cellular networks. So, many works have been, and are being, developed in this area, studying ways to avoid or minimise interference. Therefore, in this section different points of view are shown, starting with intra-cell interference and then inter-cell one.

In [ZhLi00], the model is for the intra-cell interference UL case, using the service and the number of users using that service. This model obtains the maximum number of users in each service within the system. However, perfect power control is assumed (the signals power arrived at BS are equal) and it does not take slow fading effects into account.

In [MäSt03], the power of MTs and number of users are used to calculate the intra-cell interference in UL. Perfect power control is assumed, and inter-cell interference is taken as known a priori. This model depends on the inter-cell interference, the number of users, the service used, and the target equivalent Signal-to-Noise Ratio (SNR), E_b/N_0 ratio. In [MäSt04], UL intra-cell interference is calculated by another algorithm but with the same idea, i.e., the intra-cell interference depends on the inter-cell one. The difference is in the calculation of the mutual generated load among all cells in the network as a way to obtain the inter-cell interference, and then the intra-cell one.

In [NaSh03], UL intra-cell interference is calculated by taking the user load factor into account, and number of users in soft handover. However, for the calculation it is necessary to know the total interference a priori, i.e., the sum of the intra- and inter-cell interferences and noise received by the user. This model was studied for UMTS multi-services.

In [Nguy05], the model is for the intra-cell interference UL case, using the power received by BS, activity factor of the service and number of users using that service. Perfect power control is assumed

as well as uniform distribution by users.

In [SKYM03], a model for the case of intra-cell interference in DL is shown. For hard handover this model takes into account: orthogonality factor, path loss, total power transmitted of BS to MTs within the cell and log-normal distribution for the slow fading. For soft handover the model is the same, but with one additional parameter, i.e., number of users of adjacent cells in handover situation.

In [NaSh03], UL intra-cell interference is not the only model described, presenting one way to calculate the DL intra-cell interference too. DL intra-cell uses the following parameters: total average received power of MT, path loss, orthogonality loss between codes, power of the synchronise channel. However, this model does not take slow fading into account.

In [Chen03], DL inter-cell interference is explored, so for its calculation the following are taken into account: the total transmitted power of BS, the path loss, slow fading with a uniform distribution, distance from the MT to BS and the angle that MT does with BS, as shown Figure 2.9. However, this model does not allow multi-service. So [EPCC06], as a way to allow the multi-service, they add the orthogonality factor parameter in this model.

In [ZhLi00], UL inter-cell interference is calculated taking into account the following parameters of adjacent cells: the service, number of users using that service, path loss. Perfect power control is assumed but slow fading is not.

In [WaAC03], the model is for the case of inter-cell interference in UL, with the parameters: received power by BS, distances of MTs to BSs, path loss, slow fading with log-normal distribution and the multi-path fading with Rayleigh distribution. Multi-service is assumed, where each user has a use probability and they are uniformly distributed.

In [YYZM03], a model for the case of inter-cell interference in UL is shown, taking into account the transmitted power of MT, distance of MTs to BSs, slow fading with log-normal distribution. The signals are mutually independent among each others and users are uniformly distributed in the cell.

In [Nguy05], a model for UL inter-cell interference is also presented. It takes power received by BS, service, number of users using that service, activity factor and the distribution of users into account. Perfect power control is assumed and multi-services are supported. However, this model gives the inter-cell interference average per cell in all its area. In [EPCC06], the previously described model is the same with a difference, they do not consider a non-uniform user distribution statistical function in the cell area, i.e., instead of integrating the user distribution function in the cell area, a sum of all users' distance to their serving BSs is taken into account.

In [AkPN06], they calculate the actual per-user interference and analyse the effect of user-distribution on the capacity of a CDMA network. The authors calculate the inter-cell interference taking into account the distance of MTs to BSs, number of users in adjacent cells, path loss, slow fading with log-normal distribution. However, the total relative average inter-cell interference experienced by one cell i is simply the sum of the product of number of users in other cell j and their respective per-user interference factor f_{ji}.

Chapter 3

Model Development and Implementation

In this chapter, a functional description of the simulator platform is provided on which the models used and developed within the scope of this thesis were implemented. After giving an overview of the simulator, the description of the interference and path loss algorithms are presented. The last section shows the simulator assessment.

3.1 Models

Some theoretical assumptions are required to understand what is done, such as the study cases, models and algorithm used and the description of some decisions that were made.

The scenario in study is a neighbourhood with *N* x *M* buildings. To simplify, a Cartesian coordinates system is considered: *N* buildings are distributed on *x*-axis and *M* buildings on *y*-axis. All buildings have the same characteristics, i.e., width, length, height and 3m of height floor. However, the centre building has one exception, i.e., its height can be different from the others. All streets in each axis, *x* and *y*, have the same width.

Although the system has two frequencies bands, DL and UL, for the purpose of this work the only frequency considered is 2000 MHz.

The interference is calculated using (3.1), (3.3), (3.4), (3.5). After the analysis in Section 2.4.2, it has been concluded that all models are very similar. So, the models chosen are the same as [EPCC06]. This choice was made because the work developed in [EPCC06] has the same purpose as the present work, and they have got good results. Thus, the interference model for DL intra-cell interference, in MT *i*, is calculated by (3.1), [SKYM03]. It depends the total BS transmitted power for other MT within the cell, the orthogonality factor and path loss.

$$I_{Intra,i}^{DL} = \left(P_{Total,BS} - P_{BS \to MT_i}\right) \times \alpha \times L_p \quad \text{[W]} \tag{3.1}$$

where

- $P_{Total,BS}$: total transmitted power from BS to MTs within the cell;
- $P_{BS \to MTi}$: transmitted power from BS to MTs *i* (MT where is calculated the interference);
- α: DL Orthogonality Factor.

$$P_{Total,BS} - P_{BS \to MT_i} = \sum_{j=1, j \neq i}^{N_u} P_{BS \to MT_j} \tag{3.2}$$

with

- $P_{BS \to MTj}$: Transmitted power from BS to other MT *j* within the cell;
- N_u: Number of users within the cell.

For intra-cell interference in UL on cell *j* the calculation is done according to (3.3), [Nguy05]. This model takes into account the MT transmitted power, the service activity factor, the number of users using the same service as MT in study, and the path loss.

$$I_{Intra,j[\mathrm{W}]}^{UL} = \sum_{g=1}^{N_{serv}} P_{MT \to BS_j} \times L_p \times \eta_g \times N_{j,g} \tag{3.3}$$

where

- $P_{MT \rightarrow BSi}$: transmitted power from MT to BS *j;*
- η_g: activity factor of the used service *g*;
- $N_{j,g}$: number of MTs using the service *g* within the cell of BS *j*;
- N_{serv}: total number of services.

For inter-cell interference in DL, the interference in one MT *i* using the service *g* is calculated according to (3.4), [EPCC06]. It takes into account the total transmitter power of BSs that are causing interference, orthogonality factor and the path loss.

$$I_{Inter,i[\mathrm{W}]}^{DL} = \sum_{j=2}^{N_{BS}} P_{Total,BS_j} \times \alpha \times L_p \tag{3.4}$$

where

- $P_{Total,BSj}$: total transmitted power of BS *j* (including antennas gain);
- N_{BS}: number of interfering BSs.

In case of inter-cell interference calculation in UL, on BS *j* is given by (3.5), [EPCC06]. This depends on the transmitter power of the MTs outside the cell, the path loss, service activity factor and one distance relation between to the cell that MT is causing interference and the cell that is serving it.

$$I_{Inter,j[W]}^{UL} = \sum_{k=1,k\neq j}^{N_{BS}} \sum_{g=1}^{N_{serv}} \sum_{k=1}^{N_k} P_{MT_k \rightarrow BS_j} \times L_p \times \eta_g \times A \tag{3.5}$$

where

- $P_{MTk \rightarrow BSj}$: MT *k* power transmitted to BS *j* in an adjacent cell;
- $N_{k,g}$: number of users using service *g* in interfering cell *k*.

$$A = \sum_{n=1}^{N_{k,g}} \frac{r_{j,n}{}^{a}}{r_{k,n}{}^{a}} \tag{3.6}$$

with

- $r_{k,n}$: distance from MT *n* using service g to BSs *k*;
- $r_{j,n}$: distance from MT *n* using service g to BSs *j*.

For path loss calculation, the propagation models outdoors and indoor were combined. All models used were previously described in Sections 2.3.2 and 2.3.3. The algorithm behind is explained further in Section 3.3. In the meanwhile, the different situations of path loss are presented.

In the case of outdoor models, Okumura-Hata can not be used in this thesis because the cells used are small macro-cells, and the distance between MT and BS is less than 5 Km. Walfish-Ikegami is used for cases where the distances are less than 5 Km in both urban and suburban environments. Thus, the better choice is the COST 231 - Walfish-Ikegami because it allows better path-loss

prediction since it considers more parameters to describe the environment, namely buildings height, roads width, building separation and road orientation with respect to the direct radio path.

In Section 2.3.3, four indoor models are described, however, only MWM indoor model is used. This choice was made not because the Gaussian approach is a “bad” model, but because this model explores the problem from a statistical point of view, i.e., this model gives attenuation according to a percentage of building penetration independently from the MT location. Concerning COST 231, the better choice when small cells are used it is the second model, the MWM, because it gives the path loss as the free space loss added with losses introduced by the walls and floors penetrated by the direct path between the transmitter and the receiver.

The MWM model given by (2.24) is the general case. But two variations of this model were used. The first is when the MT is served by one BS on the building top, Figure 3.1, case 1. The calculation is done according to (3.7). In this particular case, the attenuation does not depend on the MT position on the floor, i.e., the loss only depends on the floor numbers between MT and BS, plus the free space. The other one is the most common case, when the BS is not in the same building as the MT, Figure 3.1, other cases, and the calculation is done according to (3.8). Notice this k_f is equal to 0 when BS is in LoS with the MT.

$$L_{p\ ind[\mathrm{dB}]} = L_{0[\mathrm{dB}]} + k_f \times L_{f[\mathrm{dB}]} \tag{3.7}$$

$$L_{p\ ind[\mathrm{dB}]} = \begin{cases} k_i \times L_{w1[\mathrm{dB}]} - k_f \times L_{f[\mathrm{dB}]} + \mathrm{l}_{glass[\mathrm{dB}]} & \text{for NLoS} \\ k_i \times L_{w1[\mathrm{dB}]} + \mathrm{l}_{glass[\mathrm{dB}]} & \text{for LoS} \end{cases} \tag{3.8}$$

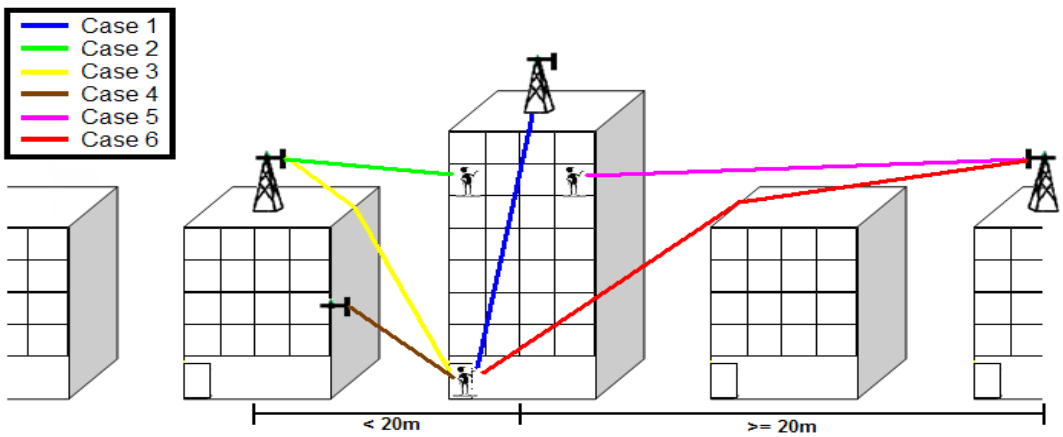

Figure 3.1. Different cases of path loss.

Concerning path loss, there are 5 others situations that can be identified. When the distance between BS and MT is less than 20 m and there is LoS, Figure 3.1, case 2, free space model (2.8) plus MWM in LoS (3.8) are the propagation models used to obtain the total loss. Which the BS is located on the top of an adjacent building, the distance between BS and MT is less than 20 m and BS is in NLoS with MT, the path loss is calculated by free space plus extra attenuation (2.18) added to (3.8) in NLoS, Figure 3.1, case 3. When one BS is in the adjacent building façade the loss is calculated according to

(2.8) if the distance is less than 20 m, and (2.6) if it is more than 20m, plus (3.8) in LoS, Figure 3.1, case 4. When the BS is in LoS and more than 20 m far away to the MT, COST 231 - Walfish-Ikegami (2.6) plus (3.8) in LoS are the models applied, Figure 3.1, case 5. For last situation, Figure 3.1, case 6, when the BS is in NLoS and more than 20 m far away to the MT, the calculation is done according to (2.7) plus (3.8) in NLoS. All these are summarised in Table 3.1.

Table 3.1. Different cases of path loss, its characteristics and propagation models.

Cases of Path Loss	Characteristics		Propagation Models	
	LoS	Description	Description	Equation
1	No	BS on the top of the same building as MT	MWM	(3.7)
2	Yes	Distance between BS and MT is less than 20m	Free Space+MWM	(2.8)+(3.8)
3	No	BS on adjacent building top, distance between BS and MT is less than 20m	Free Space plus extra attenuation+MWM	(2.18)+(3.8)
4	Yes	BS on adjacent building facade, distance between BS and MT is less than 20m	Free Space+MWM	(2.8)+(3.8)
		BS on adjacent building facade, distance between BS and MT is more than 20m	Walfish-Ikegami+MWM	(2.6)+(3.8)
5	Yes	Distance between BS and MT is more than 20m	Walfish-Ikegami+MWM	(2.6)+(3.8)
6	No	Distance between BS and MT is more than 20m	Walfish-Ikegami+MWM	(2.7)+(3.8)

In order to decide if there is LoS between BS and MT, the first Fresnel zone principle criterion is used, [RMSP87], Figure 3.2.

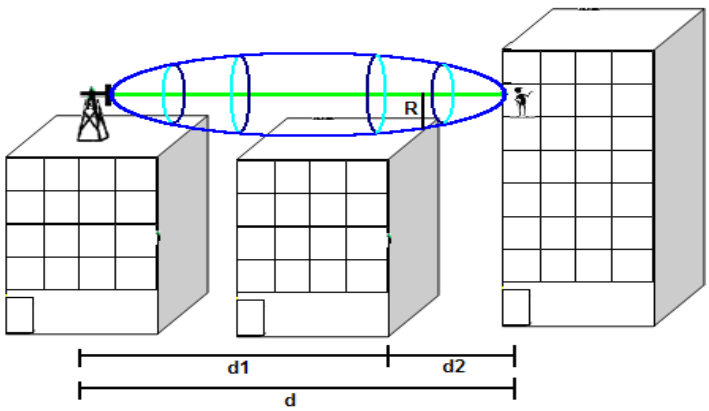

Figure 3.2. First Fresnel zone.

The direct ray between BS and MT is calculated, then, it is verified through (3.9) if the first Fresnel zone is obstructed by the top of the last building before the MT. If it is, the MT is in NLoS, if it is not, the MT is in LoS with BS.

$$R_{[m]}^{Fresnel} = \sqrt{\frac{d_1(d - d_1)}{d} \cdot \lambda} \qquad (3.9)$$

where

- d: distance between BS and MT.
- d_1: distance between BS and building top

The received power is calculated according to its sensitivity plus a margin, (3.10). This power variation is the fading margins sum according to a percentage chosen by the user and this is done to try offsetting the fading losses, (3.11).

$$P_{r[\mathrm{dBm}]} = P_{rx_{\min}[\mathrm{dBm}]} + \Delta P_{[\mathrm{dB}]} \tag{3.10}$$

where:

- P_{rxmin}: sensitivity;
- ΔP: margin, given by

$$\Delta P_{[\mathrm{dB}]} = M_{SF[\mathrm{dB}]}(\%) + M_{FF[\mathrm{dB}]}(\%) \tag{3.11}$$

with

- M_{SF}: slow fading margin;
- M_{FF}: fast fading margin.

In a study like this the BS antenna gain can not be neglected. Therefore, a model to calculate the BS three-dimensional antenna gain. The interpolation method is based on the assumption that both the horizontal and the vertical radiation patterns of the antenna are available, $G_H(\phi)$ and $G_V(\theta)$ [GCFP99], Figure 3.3. As usual, $G_H(\phi)$ is assumed to be known for a range of 2π, with $\phi \in [0,2\pi]$, as is $G_V(\theta)$ for $\theta \in [0,\pi]$. Calculating the directional gain of the BS, $G_{BS}(\theta,\phi)$, in any direction $P(\theta,\phi)$ can then be viewed as an interpolation problem, i.e., one wants to obtain the value of a function at a general point from the knowledge of its value at specific points the interval of which contains the interval for the general point. This is clearly a two-dimensional problem, since one is dealing with two coordinates, θ and ϕ. The basic idea of the method is to obtain the directional gain in any direction $P(\theta,\phi)$ from the values of $G_{\theta 1}$, $G_{\theta 2}$, $G\phi_1$ and $G\phi_2$. This is done by weighting them with the relative angular distances between the direction of interest and the horizontal (θ_2) and vertical (θ_1, ϕ_1, ϕ_2) planes, i.e., the four points on the surface of sphere closest to the point of interest. The weight by which the value of the directional gain on a given radiation plane is taken is inversely proportional to the angular distance. Thus, the closer the direction of interest is to the given radiation plane, the higher the weight. Summarising, the calculation is done according to:

$$G_{BS[\mathrm{dB}]} = \frac{\left[\phi_1 G_{\phi 2} + \phi_2 G_{\phi 1}\right]\dfrac{\theta_1\theta_2}{(\theta_1+\theta_2)^2} + \left[\theta_1 G_{\theta 2} + \theta_2 G_{\theta 1}\right]\dfrac{\phi_1\phi_2}{(\phi_1+\phi_2)^2}}{\left[\phi_1+\phi_2\right]\dfrac{\theta_1\theta_2}{(\theta_1+\theta_2)^2} + \left[\theta_1+\theta_2\right]\dfrac{\phi_1\phi_2}{(\phi_1+\phi_2)^2}} \tag{3.12}$$

In the calculation of antenna gain, the situation of LoS is taken into account, i.e., if the BS is in LoS with the MT, the gain is calculated in the MT direction. If the BS is in NLoS, the gain is calculated in the higher building direction that is in the direct path between MT and BS.

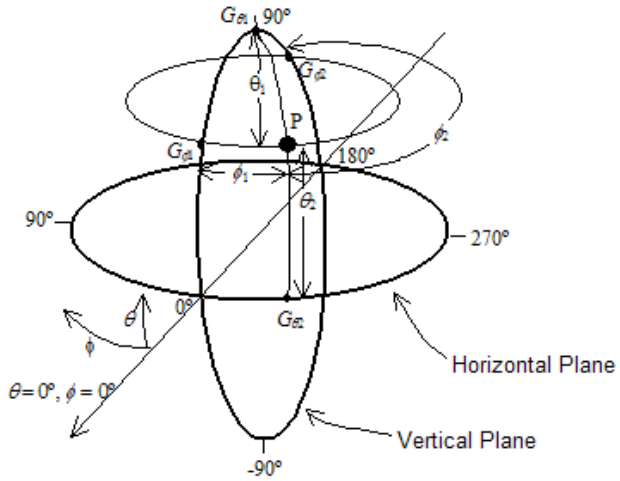

Figure 3.3. Three-dimensional pattern used for the interpolation of the antenna gain (extract from [GCFP99]).

3.2 Simulator Overview

In order to implement the models, an entirely new simulator was made: "*UMInS*". The simulator was developed in C++ using the Borland C++ Builder software [CODE08].

The main objective of this application is to calculate the indoor interference in a UMTS network. It calculates the interference for a user located in the centre building of a scenario. The simulation type adopted for the simulator was the statistical approach (snapshot).

The simulator can be split into three main blocks, Figure 3.4: configuration, simulation and results.

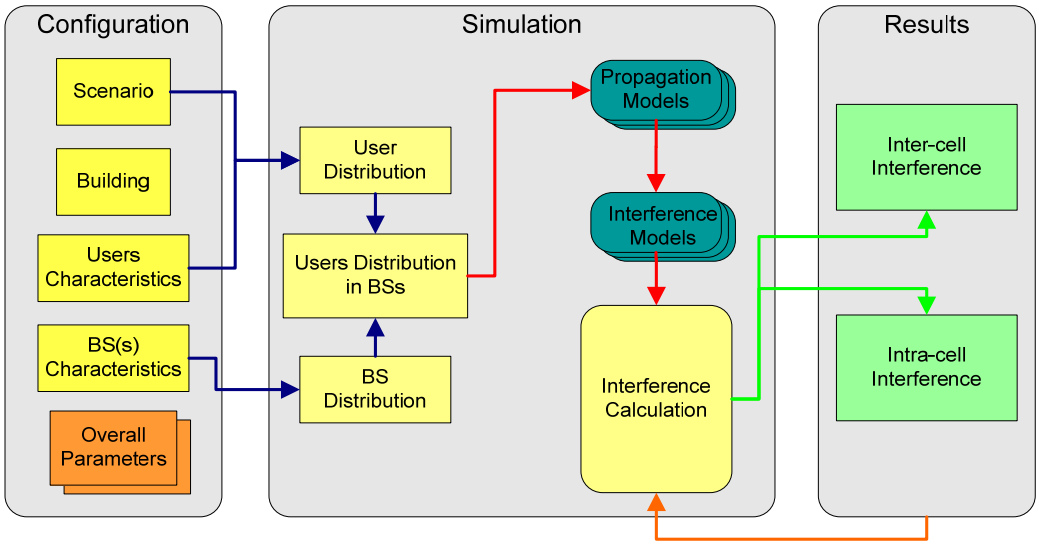

Figure 3.4. Simulator Structure

In the configuration block, all the initial system planning and parameterisation is done. It is in this point that the tool user chooses what kind of scenario he/she wants: dense urban, urban, suburban, or a different scenario created by him/her. One also chooses the characteristics of the centre building (height and number of floors), users (number of users, percentage of voice and data service, percentage of mobility), BSs (number of BSs, position and radiation pattern), and overall parameters, like frequency and standard deviation for fading distributions and BSs antennas tilt.

In the simulation block, BSs are distributed according to their coordinates. Users are distributed uniformly around the scenario. After placing the users, the network is deployed. A first network analysis is performed, the cell radius for a single user is calculated for each service, according to the COST231 – WI NLoS model. All the users within the coverage area are candidates to be served. After knowing the users in the coverage area, they need to go through three phases, in which priority is given to users nearer to the BS. The first test is the load factor that cannot be more than 75% in DL and 50% in UL, (2.1) and (2.2). The second test is the transmitter power sum, which cannot be more than the BS maximum transmitter power, Table 2.2. For the last test, the codes for each service cannot be more than the limit, as shown in Table B.1. The link budget used in this analysis is presented in Annex B. After all the configurations and parameters are filled in, the interference is calculated, the algorithm behind this calculation is explained further in the following section.

In the last block, results, as the name suggests, the results of the simulation, interference values of inter- and intra-cells in DL/UL are saved in files.

3.3 Interference and Path Loss Algorithm

For the calculation of the interference, the algorithm that calculates the inter- and intra-cells interferences in DL and UL was developed separately, as shown in Figure 3.5.

The algorithm starts with the operative mode choice: auto or manual. The difference between both modes is the number of penetrated walls, i.e., in manual mode the user specifies the penetrated situation that the MT will be, while auto mode does the calculation for all cases of penetrated walls (glass, one wall and two walls).

After the choice of calculation mode, the tool user chooses the service that will be analysed. Then, the interference calculation per floor starts, with intra-cell interference in DL and UL followed by the inter-cell interference in DL and UL. In the first step, the received power is calculated according to (3.10), the power control not being used. This calculation is done taking the received power based only on the noise (B.7) plus one set margin (3.11) into account. Afterwards, the recalculation of the interference is performed and power control is activated, i.e., the power received is calculated taking the interference level previously calculated (B.10) into account and the margin is not used. These two steps are repeated in each floor n_{max} times. The MT that started in the bottom floor starts going up in the building, and when it arrives to upper floor the simulation ends.

All interference calculations are done for the same service of the MT in test. As mentioned before, the simulator starts with the intra-cell interference calculation in DL, the algorithm behind the calculation

being shown in Figure 3.6. It starts with the search for the BS that serves the MT under analysis. After

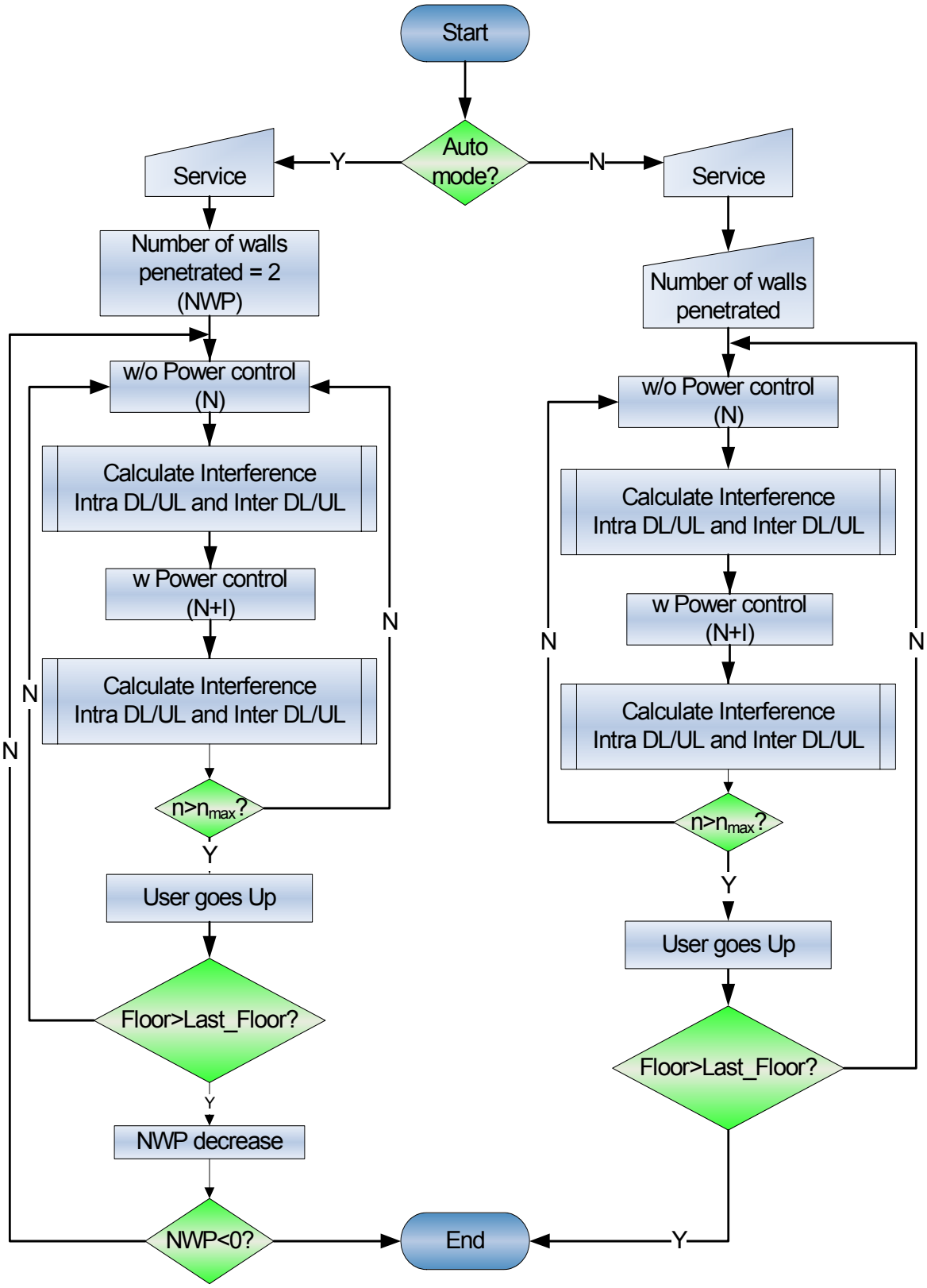

Figure 3.5. Interference Calculation Model

it has found the BS, it chooses the MT sector. If the MT is the only MT in the sector, the interference will be equal to zero, when it is not, it is calculated according to (3.3). When the receiver requires a

transmitter power above the limit, the power receiver decision algorithm reduces the power to the minimum, taking only the sensitivity power into account, ensuring the minimum service, Figure C.1. The algorithm of Figure C.1 also decides if the user is served or not. It starts calculating the transmitter power required for the received power (3.10), and then compares the transmitter power with the maximum power that the BS can supply. If it is above the limit, the margin is removed and the comparison is done again. If this new value is above the limit, the MT is not served, if not, the MT is served with the minimum power. The orthogonality factor is randomly generated according to a uniform distribution, assuming different values for each scenario, 0.05 to 0.2 for indoor, 0.4 to 0.6 for pedestrian and 0.6 to 0.8 for vehicular. It is considered 0 for perfect orthogonal codes. The path loss can assume different models according to different situations.

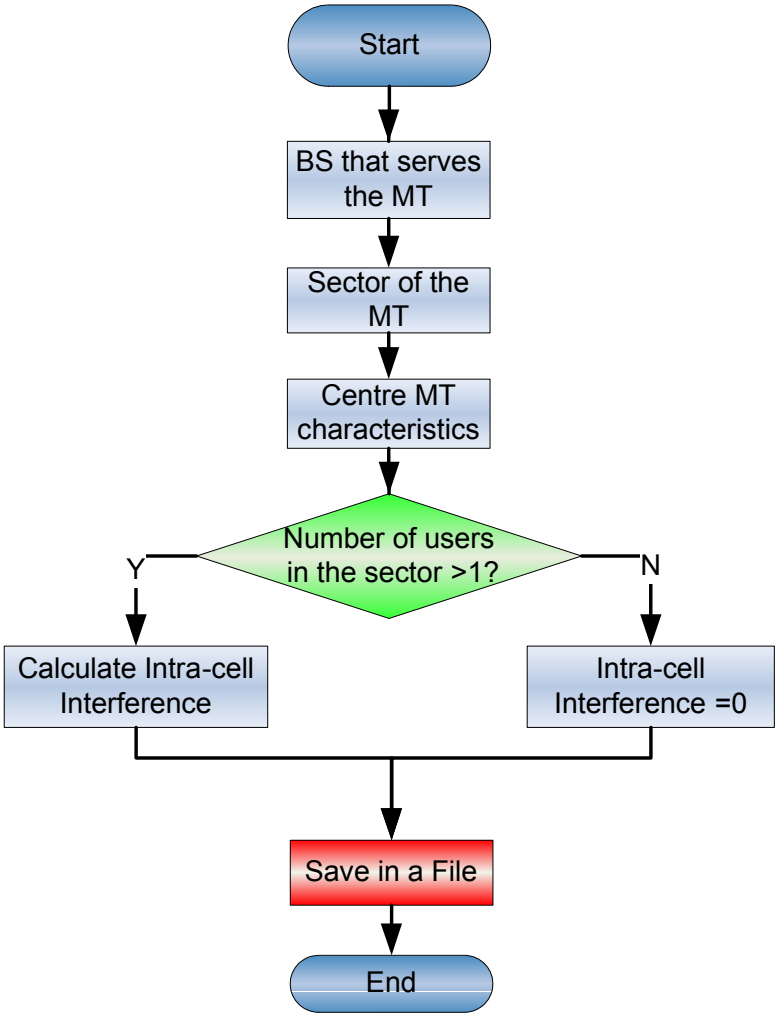

Figure 3.6. Intra-cell interference in DL algorithm

The intra-cell interference in UL is the next interference to be calculated. As in the previous case, the interference is calculated for the same BS and the same sector. The required MT transmitter power is calculated. If this power is higher than the limit, the interference is equal to zero, because the MT is not served. But when it is below the limit, the interference for the MT service is calculated according to

(3.5). The MT transmitter power is calculated according to (B.1). As well as in DL, the UL uses a power receiver decision algorithm. The only difference between these two links is the device maximum power, Figure C.2. The service activity factor assumes 0.5 for voice and 1 for data. The algorithm is represented in detail in Figure 3.7.

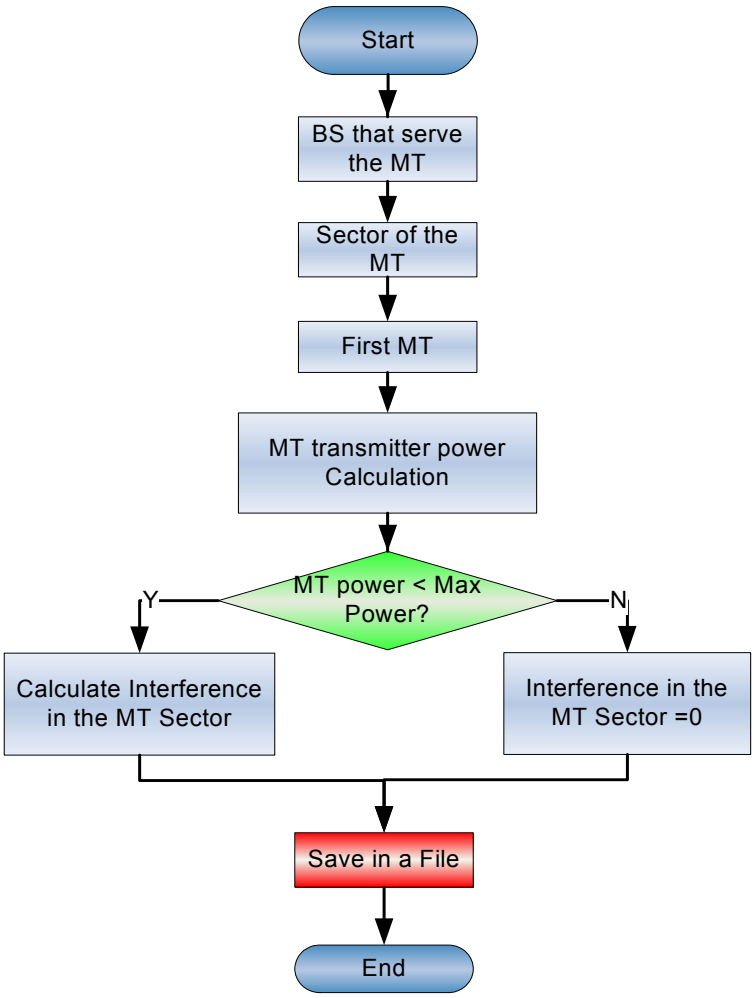

Figure 3.7. Intra-Cell interference in UL algorithm

The next interference to be calculated is the inter-cell interference in DL. Theoretically, in DL, inter-cell interference is the interference caused by all BSs around the BS that is providing service. But according to [EPCC06], based on [Chen03], the BSs in the first and second tiers around the BS of the MT are the only ones considered, because the received power from the BSs outside the second tier is negligible. Thus, if the BSs are more than four times the maximum coverage radius, the BSs will be out of the interference range and are not taken into account. The algorithm begins by picking the MT, and then it starts to run all BSs. If a BS is outside the second tier, it automatically skips to another. This loop runs over and over again, until no more BSs exist. When a BS is found inside the limit, it runs all sectors. If the sector is the same as the MT, the program skips to another sector. However, if the sector is different, the distance between MT and BS is tested. If the distance between MT and BS is less than BS maximum coverage range, the MT is covered by that BS and it will be interfered by it. Therefore the interference is calculated according to (3.6). These values are added when the

interference is being calculated. The inter-cell interference in DL algorithm is represented in Figure 3.8.

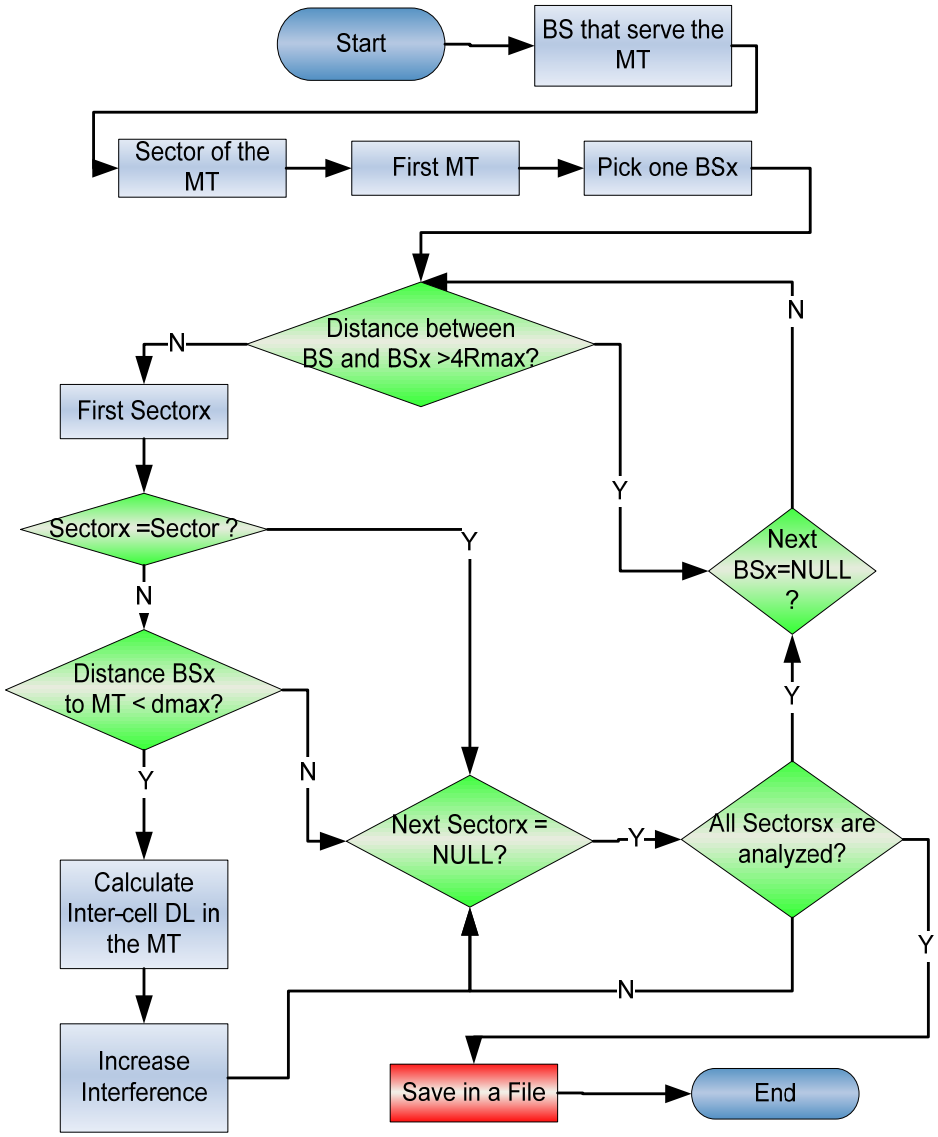

Figure 3.8. Inter-cell interference in DL algorithm

Then the inter-cell interference in UL is calculated,. The algorithm is represented in Figure 3.9. The calculation starts with the search of the BS of the MT, then it picks the sector and after that, as in the DL, it runs all BSs and does the test of the second tier. In case it passes the test, it starts the sector selection. If the sector is the same as the MT, the program skips to another sector. However, if the sector is different, an MTx is chosen. If it is performing the same service as the reference MT and the distance between it and the BS that serves the MT is lower then the UL maximum range, the program goes to the next step, the MTx transmitter power calculation. If the power is within the boundary, the interference is calculated according to (3.5) and added to the other values of interference. This process ends when all MTxs of all sectors of all BSs are analysed. As in the other interferences, the power receiver algorithm is used. In this particular case, the power control is not perfect because the interferering BS does not control the MTs that are connected to another BS.

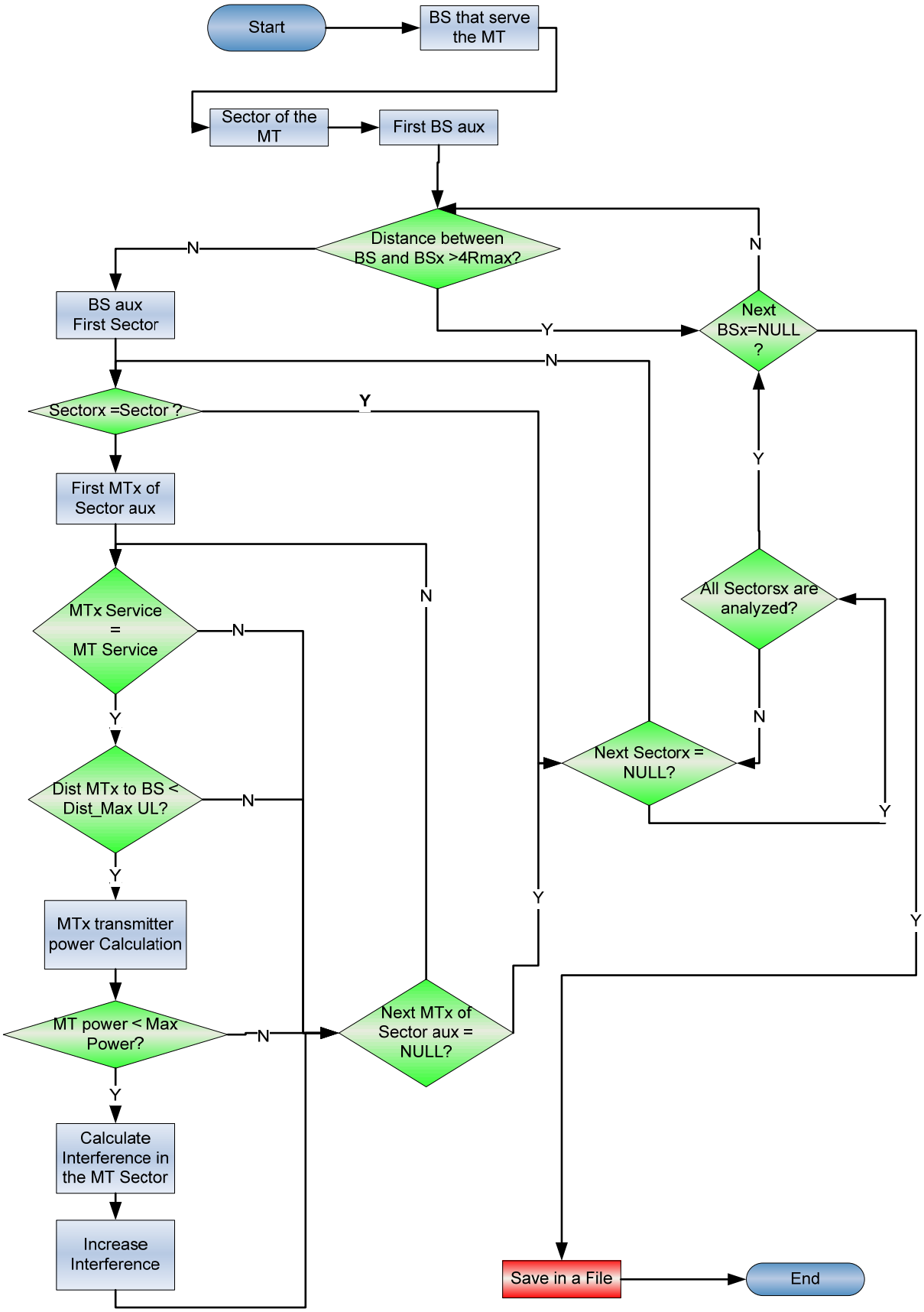

Figure 3.9. Inter-cell interference in UL algorithm

After these interference calculations a second cycle is performed. The difference between first and second steps is the power control activation, the calculation procedure maintains equal. All results obtained through simulations are saved in files on the simulator directory.

The path loss is an important parameter for interference calculation. So, in order to obtain a good interference estimation, an algorithm that combines different propagation models was created, Figure 3.10.

The algorithm starts by verifying the BS and MT location. If they are in the same building the path loss calculation is done according to (3.7). If not, the algorithm begins with the search of the outdoor model that best fulfils the situation. So, in the first step, the distance between BS and MT is calculated. If it is more than 20 m far away from each other, Wasfish-Ikegami is the model applied. Walfish-Ikegami presents two ways, i.e., when they are in LoS the calculation is performed by (2.6), when they are in NLoS the calculation is done according to (2.7). When they are less than 20 m, the BS location is evaluated. If it is not on a building roof, the free space model (2.8) is the one used. If it is, free space (2.8) is applied in case of LoS and free space plus extra attenuation (2.18) in case of NLoS. All LoS conditions are verified through first Fresnel zone principle (3.9).

Once the outdoor model is selected, it is combined with the indoor model MWM (3.8). With this, the total path loss is achieved and the algorithm ends.

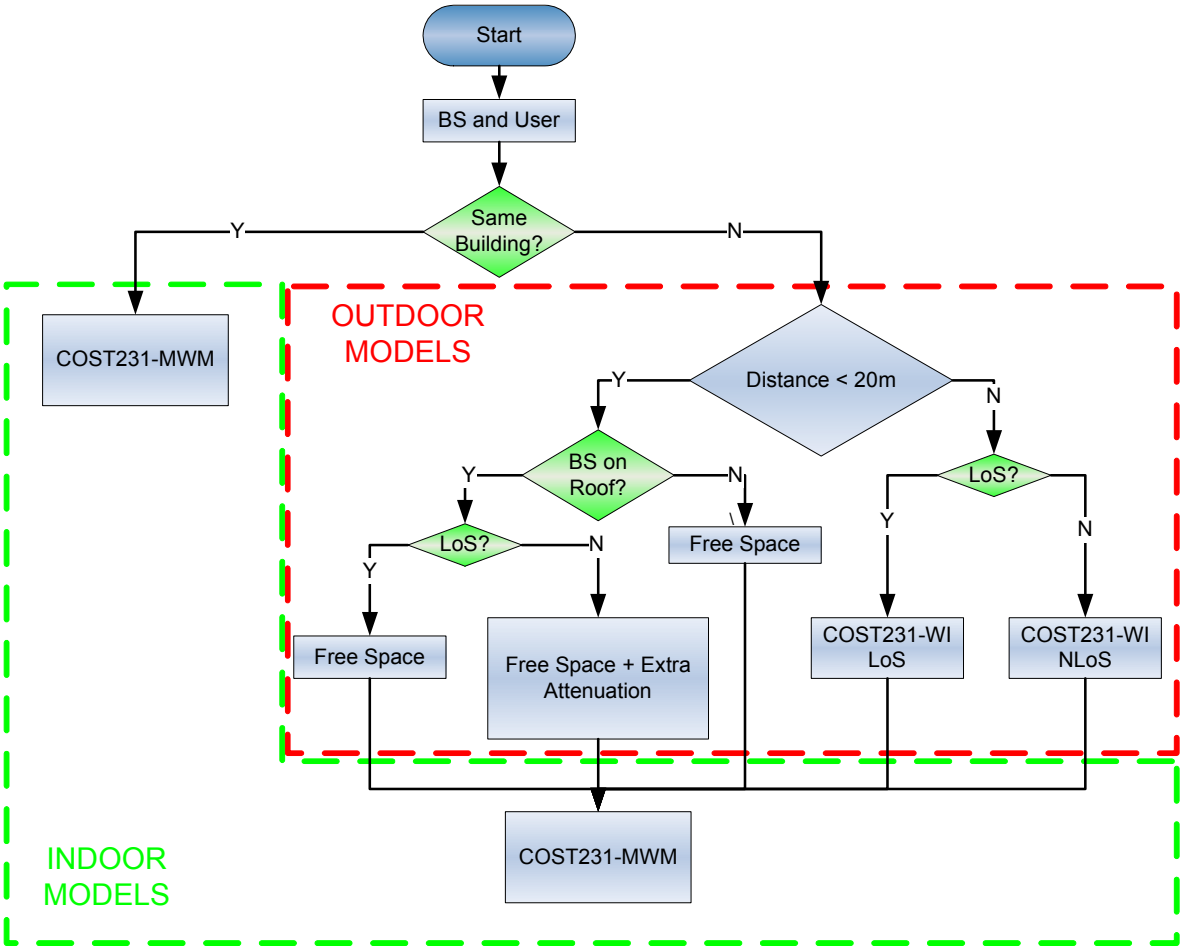

Figure 3.10. Path loss decision algorithm.

3.4 Inputs and Output Files

In order to run the simulator, it is not necessary to insert any input file in the UMInS application. The only file that can be loaded is the radiation pattern. All parameters required for simulation are filled in the program by the tool user. In the user's manual in Annex E, all these are detailed.

In the end of each interference calculation all parameters/results are downloaded for files*.xls that the simulator creates. These files contain all information necessary to perform the analysis. Therefore, the files that are created by the program are the following ones:

- Buildings.xls: this file contains the buildings information as the ID and the centre buildings coordinates *x* and *y*.
- Users.xls: this file gives the user information such as the ID, coordinates *x*, *y*, *z* and the mobility. The mobility parameter assumes three different values 0 for indoor, 1 for pedestrian and 2 for vehicular.
- Bs.xls: this file contains the information about the BS ID and location (*x*, *y* and *z*).
- Bs_u.xls: this file presents the user distribution for each sector of each BS.
- Interf.xls: this file has all simulation results, such as the information of BS and MT that was analysed (IDs and coordination *x*, *y* and *z*); the number of floors where the MT is, the number of penetration walls (0 for penetration through the glass, 1 for penetration through the glass plus one wall and 2 for penetration through the glass plus 2 walls); the service that the MT is doing (1 for voice CS 12.2 kbps, 2 for data CS 64 kbps, 3 for data PS 64 kbps, 4 for data PS 128 kbps and 5 for data PS 384 kbps); the fading margin value, the path loss value; the number of MTs performed service in the MT sector; the MT orthogonality factor; the total noise value; the sensitivity receiver in DL and UL; the interference values, intra-cell in DL and UL, inter-cell in DL and UL; the carrier-noise ratio (*C/N)* values in DL and UL; the carrier-interference ratio (*C/I*) values in DL and UL; the carrier-noise plus interference ratio (*C/(N+I)*) values in DL and UL.
- Interf_new.xls: this file contains the recalculation values. The file structure is equal to the Interf.xls.

3.5 Simulator Assessment

This section addresses the assessment made to validate the simulator results, which allows simulations with a certain degree of confidence. So the interference models, path loss model, antenna gain model, BSs type, fading margins and number of simulations are all different parameters that will be assessed. In the evaluation, all kinds of random parameters are turned off and the MT characteristics are chosen carefully.

For this work, different types of BSs are used, as shown in Table D.1. The maximum power is the only characteristic that distinguishes them. So, for the first test, different types of BS were chosen and then it was checked if its maximum power corresponds to the type. In fact, the simulator passed the test.

For the path loss assessment, six different tests were required to ensure the correct functioning of path loss algorithm, Figure 3.10. These six tests correspond to the six cases of Figure 3.1. In the first case, the BS was put in the top of the MT building, assuring that the model (3.7) is called. For case 2, one BS was placed a little less than 20 m to the MT in LoS, on the top of an adjacent building, to guarantee the model (2.8) usage. The case 3 is similar to case 2 but now the MT is in NLoS, therefore the model to be confirmed is (2.18), free space plus extra attenuation. The case 4 is equal to the case 2, but the BS is in the adjacent building façade, not on the top. In case 5, the BS is more than 20 m away from the MT, on a building top and the MT is in LoS, model to be confirmed WI – LoS. The case 6 is similar to case 2 but now the MT is in NLoS, model to be confirmed WI-NLoS. It is also assuring in each test the correct indoor model functionality. After performing all these tests the conclusion was that all path loss models are working properly.

To ensure the correct calculation of the radiation pattern gain model (3.12), a test was done. Two MTs were fitted strategically, as shown in Figure 3.11. Then, the algorithm gain was run and the gain was calculated manually. After that, the comparison between both values was made and concluded they were equal.

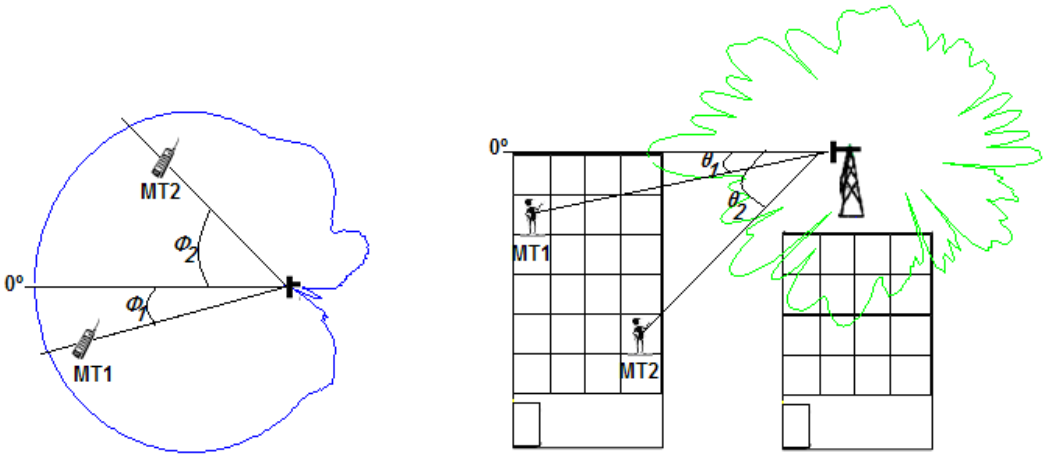

(a) Horizontal Plane (b) Vertical Plane

Figure 3.11. Radiation pattern gain illustration test.

The next assessment study is the interference model. The objective is to check the correct operation of this model. Starting with the intra-cell DL assessment, then intra-cell UL, inter-cell DL and, in the end, inter-cell UL.

For the intra-cell DL interference test, two MTs with different distances and all other equal characteristics were picked, i.e., same frequency, service, mobility, orthogonality factor, number of penetrated walls and radiation pattern gain, as Figure 3.12 shows. After that, the intra-cell DL interference was calculated. The interference in MT1 is higher than in MT2, as expected. This happens because the path loss attenuation gets higher the farther the MTs are, so, consequently

interference decreases.

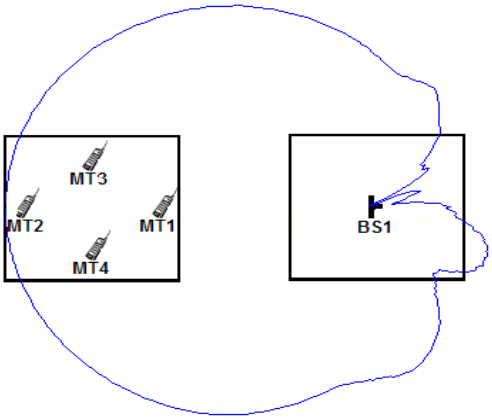

Figure 3.12. Pattern to test the intra-cell interference.

For the intra-cell UL interference test, the procedure was the same as before, only the service was changed. So MT3 and MT4 of Figure 3.12 were picked. They have the same frequency, mobility, number of penetrated walls, radiation pattern gain, orthogonality factor, and distance. The results were the expected. When a MT is performing a data service the interference is higher than when it is doing voice one. Another test that was done in the UL case to confirm the power control. Putting all MTs with the same service, it was concluded that the interference caused by all MTs was equal.

For the inter-cell interference test, two BSs with some MTs within the cells were chosen, Figure 3.13. As previously, MTs have all the same characteristics with one exception. In the case of DL, the position was changed. Analysing the results, it was concluded that the interference in MTs closer to the BS is higher than in the others far away. For example, when MT5 and MT6 were picked, these MTs were interfered by BS1, but MT6 is more interfered because it is closer to BS1 than MT5. For UL, the tests were similar, MTs with different positions and then different services were analysed. MTs closer to BS interfere more than MTs far away. And MTs with data services interfere more than MTs with voice service.

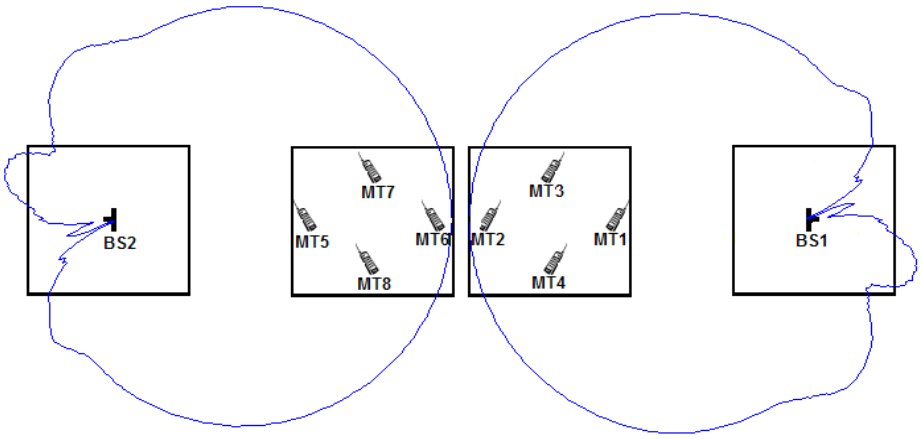

Figure 3.13. Pattern to test the inter-cell interference.

In order to make a good analysis the fading margins were removed, as mentioned before. However, it

is required to guarantee their correct calculation. The theoretical and simulated CDFs for the Rayleigh and Gauss distribution results are very similar, with the average mean error being below 0.8% and 1.1% for the Rayleigh and Gauss distribution, respectively. The error for the Rayleigh distribution is mainly due to computational approximations, while for the Gaussian distribution it also has to do with the numerical approximation that has to be performed for the inverse of the error function. Note that what is really implemented in the simulator is the inverse of the distributions, since what is needed is the value of the distribution and not the probability of occurence. Random generated values, described by a uniform distribution which takes values between 0 and 1, are used as inputs of these inverse distributions.

After all these tests, to ensure the correct interference calculation, several simulations were done to know how many simulations, in each floor, are required to achieve a statistic valid value. The *C/I* (that is obtain through (B.11)), receiver power and interference are the values that have relevance for this work. Therefore, simulations for the extreme cases were performed, i.e., simulations for a far BS and a BS in a building top with the user at the bottom and last floor, Figure 3.1 case 1, 5 and 6. Some parameters were used, namely average, relative mean error and standard deviation, (3.13), (3.14) and (3.15), respectively.

$$\bar{z} = \frac{\sum_{i=1}^{N_s} z_i}{N_s} \tag{3.13}$$

where:

- z_i: sample i;
- N_s: number of samples;

$$\bar{e} = \left| \frac{z_r - z_i}{z_r} \right| \tag{3.14}$$

where:

- z_r: reference value;

$$\sigma = \sqrt{\frac{1}{N_s} \sum_{i=1}^{N_s} (z_i - \bar{z})^2} \tag{3.15}$$

The number of 100 simulations was considered for maximum. In order to get the minimum number of required simulation, the ratio of the standard deviation over average must be evaluated. The results of this ratio are presented in Figure 3.14 for *C/I*, in Figure F.1 for interference and in Figure F.2 for receiver power. These results show a small variation for a number of simulations greater than 30.

First of all, as reference value for the relative mean error, the average of 100 simulations is considered. The relative mean error results of *C/I*, interference and receiver power is presented in Figure 3.15, F.3 and F.4 respectively. The parameter *C/I* has a relative mean error below 5% for simulations equal to or greater than 30. For interference and receiver power in all simulations the relative mean error is below 5%. This means that, increasing the number of simulations would have

minimal impact on the results.

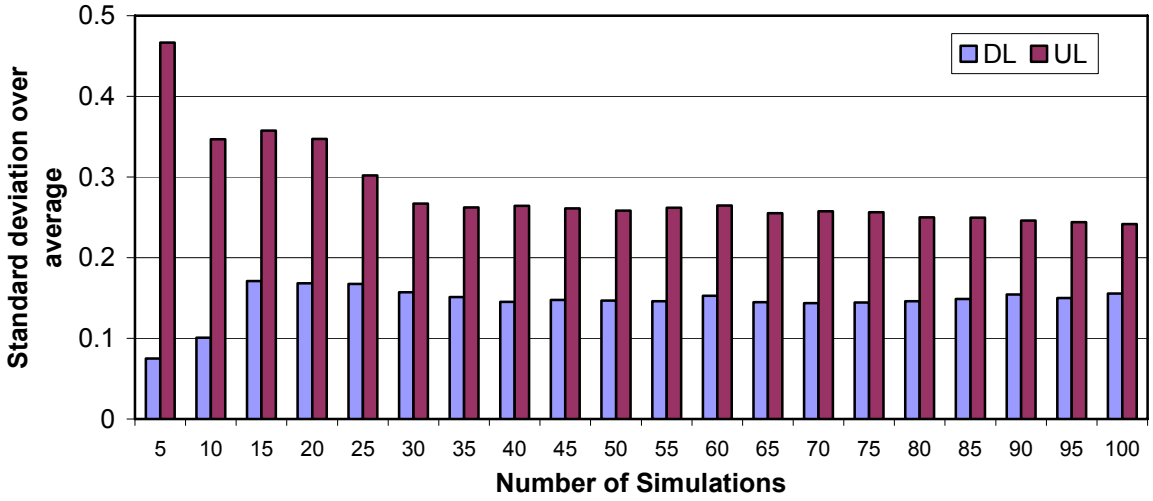

Figure 3.14. C/I standard deviation over average ratio for 100 simulations of case 6.

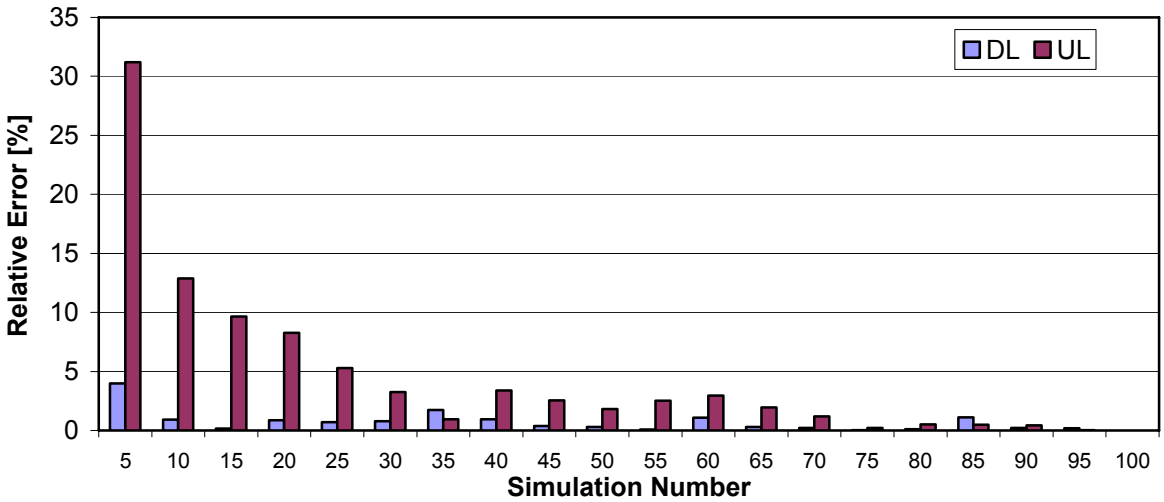

Figure 3.15. C/I Relative mean error evolution for 100 simulations as reference of case 6.

The decision of the number of simulations has as major objective, to minimise the simulation time. Time is a limited resource, which can not be neglected. So, considering all the results, it can be concluded that 30 simulations seem to be the most suitable number, reducing the simulation time to 1h20 on average, and still having statistical relevant results. It should be pointed out that this analysis has been performed for the other considered situations, and the output results have been confirmed by the same parameters. However, these analyses are not presented here, since it seemed unnecessary, though they confirm the results, namely in what regards the most suitable number of simulations.

Once, the minimum number of simulation with statistical relevant results per floor is achieved, the minimum number of simulation for each scenario was assessed. In order to get this number 15 simulation was performed. Than the relative mean error for 5 and 10 simulation were done considering

15 as the maximum number of simulations. Looking for the results of Tables F.1 and F.2, it can be concluded that 5 are enough simulations to obtain valid results with maximum relative mean error of 5%.

Chapter 4

Results Analysis

One important step in this thesis is the data collection to asses the theoretical developed model. Therefore, in this chapter, the results of the measurements done are shown. First, one describes how the data was collected. Then the results assessments and interpretation are done, as well as the simulation results are shown. The comparison between reality and simulation is carried on. With the objective to study the impact in interference behaviour some parameters were changed. At first the reference scenario is simulated, and then, the parameters are changed one by one, and the results of each case are analysed.

4.1 Reference Scenario

In order to obtain a coherent analysis and consistent conclusions, it is important to have a reference scenario, since it is from that scenario that the parameters are changed one by one. All characteristics of reference scenario are summarised in Table 4.1.

Table 4.1. Reference scenario characteristics.

Scenario	Type	Dense Urban	
	Building Heights [m]		21
	(w_{bx}, w_{by}) [m]		(40, 40)
	(w_{sx}, w_{sy}) [m]		(12, 12)
	Number of Buildings in *x*-axis		20
	Number of Buildings in *y*-axis		20
Centre Building	Number of Floors		11
	Building Height [m]		33
Users	Number		100
	Mobility [%]	Indoor	50
		Pedestrian	25
		Vehicular	25
	Service [%]	Voice	70
		Data	30
System	Frequency [MHz]		2000
	σ_{FF} [dB]		7
	σ_{SF} [dB]		7.5
	Margin [%]	BS	40
		MT	40
	Tilt [º]		0
	Radiation Pattern		P7755.00
	P_t^{max} [dBm]	MT	21
		Macro-Cell	41.75
		Micro-Cell	31.75
	Load Factor max [%]	DL	75
		UL	50
MT Characteristics	Service	12.2kbps (cs) Voice	
	Location	Random	

For the reference scenario, the values that fit better the city of Lisbon were taken into account. Therefore, the scenario type is a dense urban with 21 m of buildings height, 40 m of buildings separation and 12 m of streets width. A scenario of 20 by 20 buildings, was taken the minimum distance among BSs in dense urban into account, which is 400 m; this window allows at least 3 BSs, which seemed enough for the thesis purpose. The centre building has 11 floors with 3 m height per floor and 33 m of building height. The environment has 100 users, being 50, 25 and 25 for indoor, pedestrian and vehicular mobility, respectively (the difference between pedestrian and vehicular it is not taken into account). So half users are indoor and the other half are outdoor, with 30% of the users performing data and 70% voice. The service is split this way with the objective of having more voice users than data ones. The standard deviations for the fast and slow fading are 7 and 7.5 dB, respectively, because these are the usually values for these margins. For MTs and BSs, the

probability is 40%, providing a margin of 8.8 dB.

This scenario uses only one BS placed on different locations, always at the buildings top, 3 m above the roof. The antenna is the P7755.00, [POWE08], with 0º of tilt, as it is shown in Figure D.1. The maximum transmitter powers are 41.75 dBm and 31.75 dBm for macro- and micro-cells, respectively, since 25% of the total power is for control and signalling. MT has 21 dBm as maximum transmission power. The system maximum load factors are 75% and 50% to DL and UL, respectively. For the MT in central building (MT in study), voice was the service chosen, and its location is random on each floor.

4.2 Measurements

4.2.1 Overview

At the beginning, the idea was to collect various measures in different scenarios, but unfortunately this was not possible, since it is very difficult to get places to perform indoor measurements. The availability of the measure device was another reason, though the main one was the time issue. So the possible scenario for the measurements was the north tower of Instituto Superior Técnico (Technical University of Lisbon), Figure 4.1. This choice fits in the scenario represented in Figure 3.1 case 5, when the BS is in LoS with the MT, because this building is higher than other neighbour buildings.

(a) Side View (b) Top View

Figure 4.1. North tower of Instituto Superior Técnico view (extract from [MAPS08]).

Figure 4.2 shows all equipment used in the measurements. The measurements set are composed by one MT (Nokia N80), one USB cable, one laptop and a cart. This cart has a vertical variable stick with a basket at the top. To avoid undesired attenuation the basket is in plastic and the stick in wood.

The software used was the NEMO Outdoor V4.24 [ANIT08]. This software is an extremely versatile

and portable engineering tool for measuring and monitoring the air interface of mobile networks. Despite its name, NEMO Outdoor also performs indoor measurements. More information, such as equipment specifications can be found in [ANIT08].

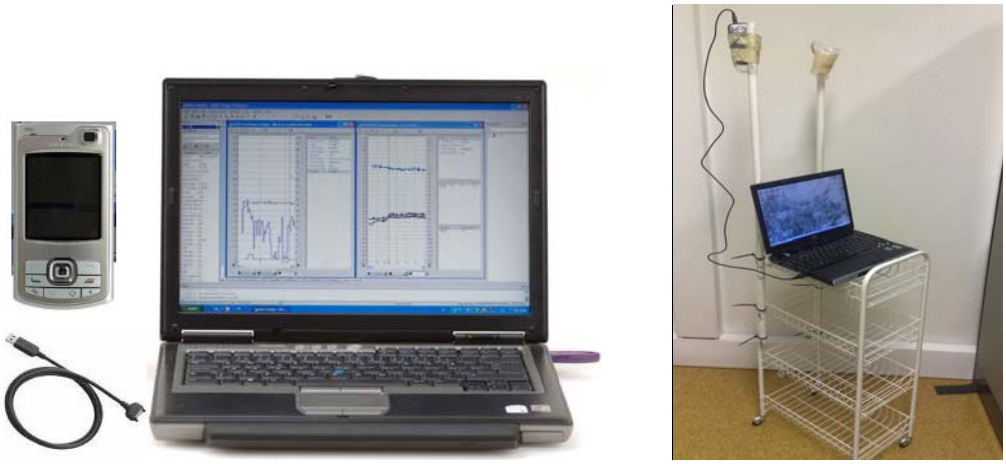

Figure 4.2. Measurements Set.

All measurements made were for the voice service, because the desired results are for this service. The measurements were performed on one of the Portuguese operators.

Some steps were required to perform the measurements. In order to save time in manually configurations, the automatic device detection functionality in NEMO Outdoor was chosen. In each floor, the floor blueprint, to be used as a map, was imported to the NEMO Outdoor. The measurements were taken at all corner rooms, hall, elevator room and male's restroom from the 4º to the 11º floor of the IST north tower. The measurements were done in these places in order to represent the case when the MT is attenuated by only glass (0 walls), glass plus one wall (1wall), and glass plus two walls (2walls). The measurements began with one voice call. In the course of the call, the marker function of the NEMO was selected. Markers were placing on the loaded map performing some kind of cross path in the rooms and a straight path in the hall, like the blue lines that are presented in Figure 4.3. In each marking the results, were saved in a file.

Figure 4.3. Example of one floor blueprint.

The file with the results had an extensive number of parameters, so in order to reduce these parameter numbers, two programs were implemented: the UMInLocation and the UMInFilter, Annex E. UMInLocation has as main objective to filter the necessary information to locate the BSs that are providing service to the MT. The aim of UMInFilter is to filter the information required for this thesis. In spite of the *.xls files created by UMinFilter to have information about all cells, only active set cells are used for the results analysis because the other categories do not fit in the purpose of this work.

4.2.2 Measurements Results

In this section, the measurements results are discussed. Measurement files show that connection was established with 5 BSs, i.e., 15 sectors. But only 3 sectors served the MT in all floors, the sectors with the SC 126, 232 and 217. So, the analysis is focused on these sectors. In Table 4.2, one presents the total point markers uploaded from the measurement files.

Table 4.2. Number of measurements points for each sector.

	Points								
	Sectors								
	126			217			232		
Floor	0walls	1wall	2walls	0walls	1wall	2walls	0walls	1wall	2walls
4	185	62	104	9	3	2	111	48	36
5	320	99	77	220	65	36	278	83	67
6	157	53	54	32	28	16	142	55	50
7	146	74	52	67	26	39	124	37	31
8	185	36	53	75	51	39	98	34	33
9	189	67	39	167	47	56	89	25	24
10	129	58	58	74	29	38	59	26	52
11	188	67	74	93	23	18	52	12	55
Total per position	1499	516	511	737	272	244	953	320	348
Total per Sector	2526			1253			1621		
Total	5400								

To understand the results, it was required to have some additional information about these BSs, such as the location, azimuth of each sector, and antennas tilt and height, Table 4.3. With this information, each BS was drawn on a map on the real position with the real azimuths. Google Earth was used to do this, Figure 4.4. The antennas tilts are -10º, -8º and -6º for sector 126, 232 and 217, respectively. The BS with the sector 126 has a 40 m height, while the BS with sectors 232 and 217 has a 25 m height. Due to the irregularity of the terrain, it was required to know the terrain elevation of the sectors. So, using Google Earth and a map with terrain elevations to confirm the values, the elevations are 85 m for sector 126, 98 m for sectors 232 and 217, and 95 m for the IST north tower.

Sector 126 is at 30 m and sectors 232 and 217 are at 28 m above the IST north tower ground level. With these heights and knowing the tilts of each sector, the distance where the antenna has its maximum vertical gain were calculated. So, sectors 126, 232 and 217 have their maximum vertical gain at 170, 200 and 266 m away. Knowing that sector 126 is at 240 m and sectors 232 and 217 are

Table 4.3. Information of BS sector.

SC	Tilt [º]	Height [m]	Terrain Elevation [m]	Distance to IST North Tower [m]
126	-10	40	85	240
217	-6	25	95	335
232	-8	25	95	335

at 335 m from the IST north tower, it can be concluded that the sectors are radiating the tower with the upper half of their vertical radiation pattern. In what concerns the horizontal pattern, sector 126 is radiating with the main lobe, sector 232 with the front side and sector 217 with the side profile.

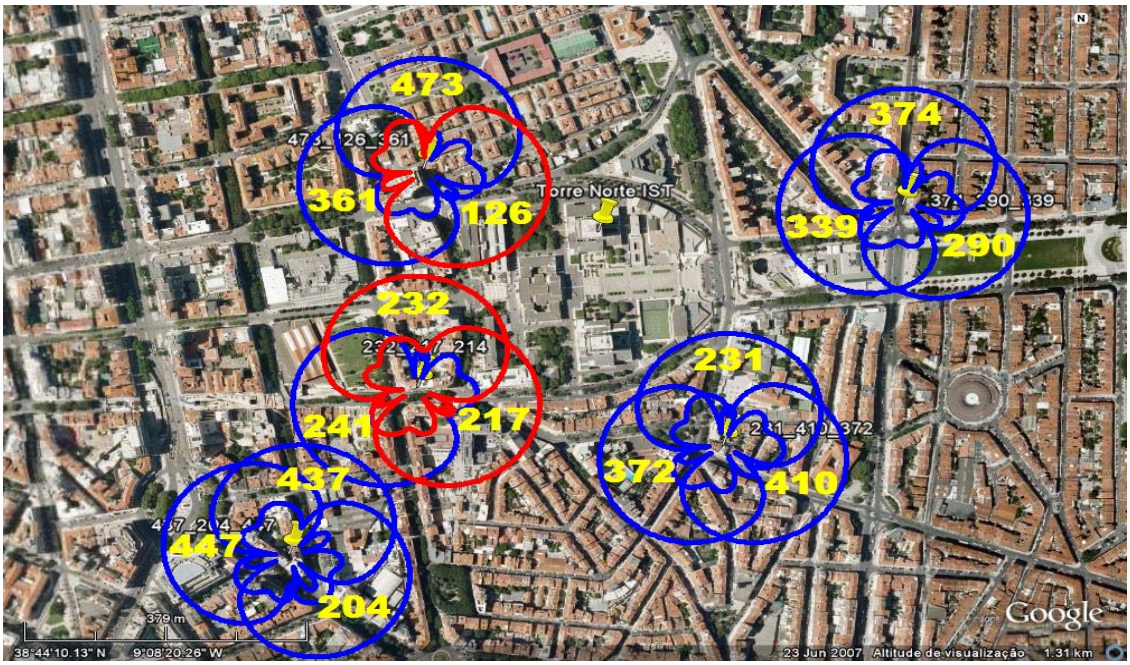

Figure 4.4. Detected BSs with sectors (extract from Google Earth).

After filtering and using Excel, the results were drawn, as shown in Annex G. According to these figures, E_b/N_0 shows a trend to become lower with the MT ascending in the building. Only sector 217 shows a positive slope, but it is so lower that can be said that E_b/N_0 has a constant behaviour around 11 dB. The cause for this can be its azimuth. But more interesting than an individual analysis for each sector is a global view. So, for each case (0, 1 and 2 walls) an average over all sectors results was performed and the standard deviation quadratic mean was calculated. In case of 2 walls the trend line is given by first line of (4.1); for 1 wall by second line of (4.1); and for 0 walls by third line of (4.1). Figure 4.5 shows the trend lines of the measurements results and Table 4.4 the standard deviation.

$$(E_b / N_0)_{[dB]} = \begin{cases} -0.45 \times F_N + 16.08, & 2w \\ -0.23 \times F_N + 14.39, & 1w \\ -0.27 \times F_N + 15.43, & 0w \end{cases} \qquad (4.1)$$

where

- F_N: Number of the floor.

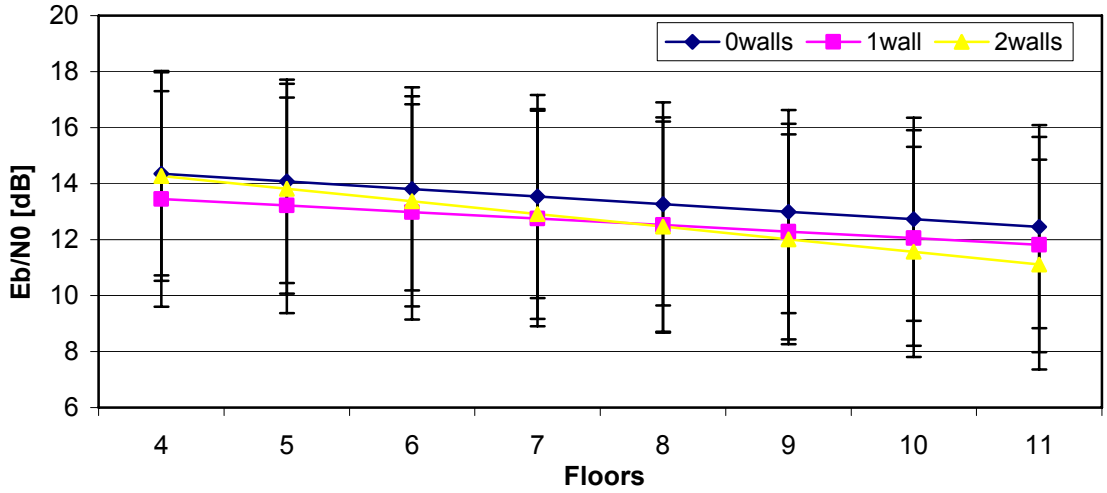

Figure 4.5. Average of the combination of the three sectors measured values trend lines.

Table 4.4. Measurements trend lines standard deviation.

Standard Deviation [dB]		
0 w	1 w	2 w
3.63	3.85	3.75

For 0 and 1 walls the trend is more or less the same, i.e., -0.25 dB per floor with 0.8 dB of difference on average. In the case of 2 walls, measurements reveal -0.45dB per floor. The radiation pattern has an influence in these negatives slopes because the BSs are radiating the tower with their upper half profile. Therefore, as higher the user is, the less gain the antenna has. The lower difference between adjacent floors in the different cases is due to the propagation that is nearly always in LoS. The behaviour for the 2 walls is not the expected one, i.e. the slope is two times the others. This could happen due to the different number of measure markers points took, Table G.2, but it is not the case. The problem could be the measurements gap for this case. In Figure 4.3, it is possible to see the gap, in the two walls case only two sides of the tower are covered while in the other cases all sides are covered.

In conclusion, when the MT is on the upper floor the interference is higher than on the lower floor. This conclusion can be taken because, in R99, E_b/N_0 is proportional to the SINR.

4.3 Measurements vs. Simulation

4.3.1 Overview

In order to evaluate the simulator, a scenario based on the measurements environment was created. All characteristics of this simulated scenario are described in Table 4.5. All parameters that are omitted in this section are the default values of the reference scenario.

Table 4.5. Simulation parameters for real scenario.

Scenario	Type	Dense Urban
	Building Heights [m]	25
	(w_{bx}, w_{by}) [m]	(180, 180)
	(w_{sx}, w_{sy}) [m]	(159.5, 159.5)
	Number of Buildings in *x*-axis	7
	Number of Buildings in *y*-axis	7
Centre Building	Number of Floors	12
	Building Height [m]	36
System	BS1 coordinates (*x*, *y*, *z*) [m]	(-170, 170, 30)
	BS2 coordinates (*x*, *y*, *z*) [m]	(-190, -190, 28)
	Tilt [º]	-10
	Radiation Pattern	K742212
MT Characteristics	Service	12.2kbps (cs) Voice
	Location	Random

The first step is to evaluate how approximated the real scenario is to the simulated environment. One wants a scenario that contains a central building with IST north tower characteristics, 2 BSs with same requirements as BSs with sectors 126, 217 and 232, and an environment with the same characteristics as the reality.

the dense urban was chosen, since this site is located in the Lisbon city, Figure 4.6 (a). The average of buildings height in the neighbourhood is 25 m, 3m per floor and 1 m for the roof. The centre building has 20.5 m of width and 20.5 m of length, and all buildings on simulator have the same length and width. To get w_b and w_s values, the distance in LoS to sector 126 and the buildings dimensions are taken into account. The buildings separation has 180m and the street width has 159.5 m, Figure 4.6 (b), w_b and w_s in *x*-axis has the same length as w_b and w_s in *y*-axis. The simulator window size is a square with 1 km side, so 7 buildings for *x*-axis and *y*-axis are chosen. The central building has 12 floors with 3 m of height each, and the ground floor being also considered.

In Figure 4.6 (b), BS1 represents the BS with sector 126 and BS2 the BS with sectors 217 and 232. IST north tower is in the centre, BS1 is 230 m west and 70 m north, while BS2 is 250 m west and 250m south. On the simulator, these are not the coordinates used, because with these locations the BSs are either in LoS condition or on the roof top. So, BS1 is located on -170 m for *x*, 170 m for *y* and 30 m for *z*. With this location BS1 is on the roof top at 240 m in LoS to the centre building. BS2 is located on -190 m for *x*, -190 m for *y* and 28 m for *z*. Despite the distance in LoS to the IST north tower being less than 335 m, the BS is on the roof top and in situation of LoS with extra attenuation. The antenna used is shown in Figure D.4. The simulator puts all antennas with the same tilt, which is a limitation. So, despite the fact that real antennas have different tilts, for simulation all antennas have 10º of down tilt. The service used by the MT located in the centre building is voice service.

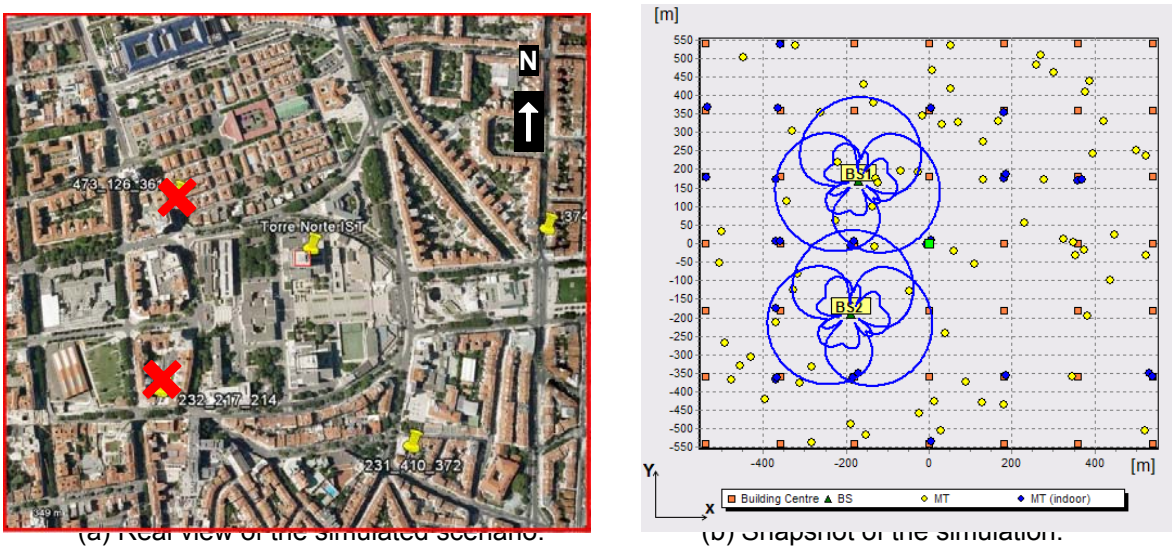

(a) Real view of the simulated scenario. (b) Snapshot of the simulation.

Figure 4.6. Reality vs. Simulation.

4.3.2 Results

In this section, the results of the simulation performed for the real scenario are presented. Since the measurements results obtained are for DL, and the idea is to compare the real scenario with the simulation values, only DL simulation results are shown.

Figure 4.7 shows the trend lines of the simulations results. The trend lines is given by (4.2), i.e., in the case of 0 walls (one glass of attenuation only) is given by first line, for 1 wall by second line, and for 2 walls is given by third line. The standard deviation of these trend lines is presented in Table 4.6.

$$(C/I)_{[dB]} = \begin{cases} -0.11 \times F_N + 12.05, & 0w \\ -0.09 \times F_N + 11.55, & 1w \\ -0.10 \times F_N + 11.03, & 2w \end{cases} \quad (4.2)$$

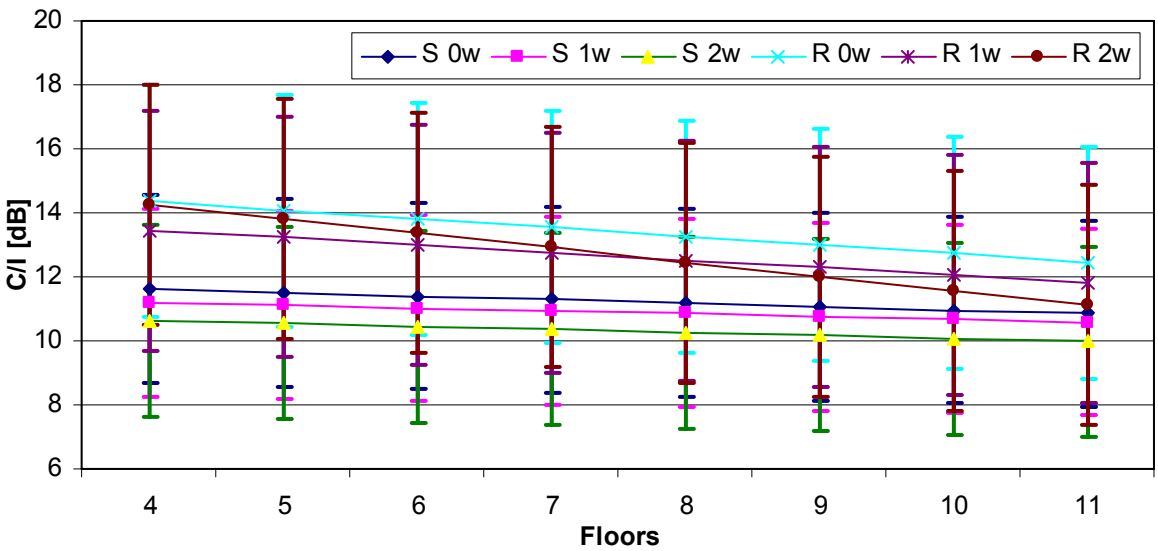

Figure 4.7. Results of reality vs. simulation.

Table 4.6. Trend lines standard deviation for Real case.

Standard Deviation [dB]		
0 w	1 w	2 w
2.92	2.93	2.99

Analysing Figure 4.7, both real and simulated results present the same trend. Despite the different in the inference level for each case, 2 dB on average, they are within the standard deviation limits. In the simulated case, *C/I* has its best values when the MT is only attenuated by 1 glass, followed by 1 wall and then 2 walls. They present a slope that is almost half of the measurements, i.e., it decreases on average 0.1dB per floor and a difference between each case of penetrated walls is 0.5 dB. Simulations show that the measurements results for the 2 walls situation do not have the right behaviour. Although, these results reinforce the idea that the interference is higher as higher the MT is.

The main reason for the difference between real and simulated results is due to the attempt to approximate the virtual scenario to reality; which is an irregular scenario, while in the simulator the environment is regular. Other reasons can be pointed out, like the unknown of total users served, while measurements were performed, and the fact that only two BSs are considered in the simulations, while in reality there are more than two interfering BSs. With this second reason one question can be arisen: if in simulation the number of BSs are less than the real case, *C/I* should be higher? The answer for this is: the power control in the simulator reacts to the interference level in order to compensate it, allowing for the MT to communicate. So, if the interference level is low the power required to compensate is not too much, being the reason for the simulation results to present on average 2 dB of difference, Figure 4.8. Despite all these difference, it can be said that the simulator is a good tool for interference analysis.

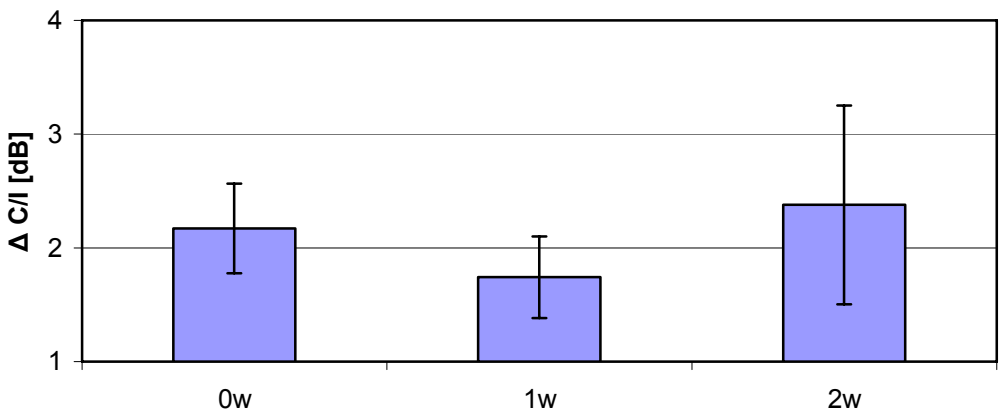

Figure 4.8. Difference between reality and simulation results.

4.4 Simulation Results

After 110 hour of simulations, its results are presented. First, the results of the default scenario, in Section 4.4.1, are examined. Afterwards, simulation results of the parameters variation are studied in

the following subsection.

4.4.1 Reference Scenario

In the reference scenario, a depth analysis is performed, i.e., noise, interference, received power and *C/I* results are shown in order to understand the phenomenon.

Noise, among other parameters, depends on the load factor, (A.9). Figure 4.8 shows that while the MT is going up in the building, for different cases of penetrated walls, noise is approximately constant, Figure H.1 to H.2. Consequently the load factor is also approximately constant too. The load factor is the cause for the higher noise values in DL compared to UL, because the maximum value in DL is 75% and in UL it is only 50%. One can notice a difference between the first and the second cycle values, one more time the load factor is the cause for that. The received power in the second cycle is higher, Figure 4.11 and H.9, so MT/BS require a higher power transmitter, therefore, some users are rejected and others do not have enough power to communicate, consequently the load factor in DL and UL become lower, as well as the noise.

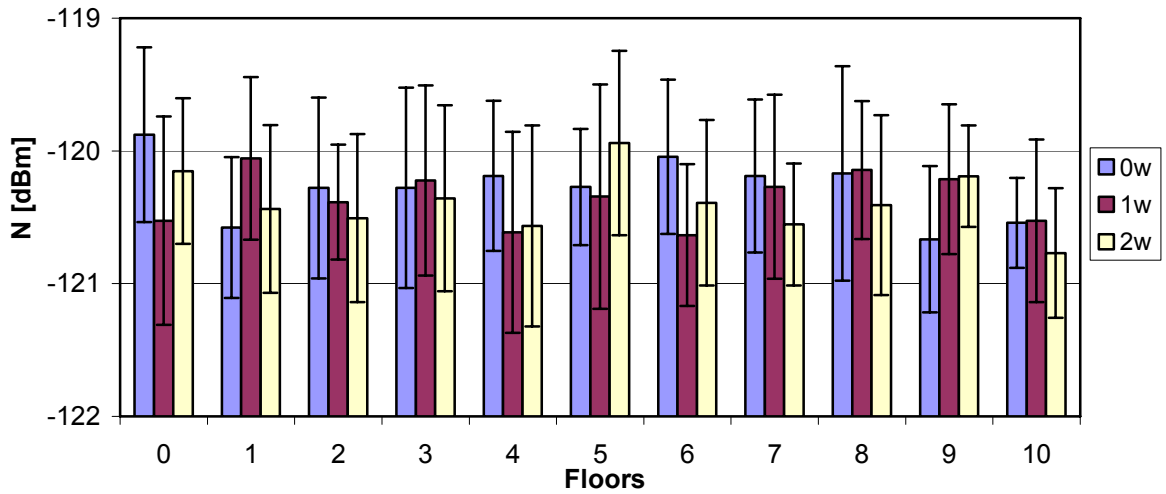

Figure 4.9. Reference scenario noise results in DL for the second cycle.

Analysing Figures 4.10 and H.4 to H.6, interference is almost equal in the two cycles, as expected. This happens because the only difference between them is the power control in the second cycle. The interference in DL is higher than in UL. The main cause is the power transmitted by the BS being higher than the MT one. In DL, interference shows a trend to become higher as higher the MT is, because while the MT is going up in the building the path loss attenuation decreases and the MT becomes visible by the BS. It can be also noticed a bigger step from the 7th floor, which occurs because the model for path loss calculation is changed to a LoS model, free space or WI LoS. The number of penetration walls shows to have an impact on interference, i.e., it becomes 2.9 dB lower when MT goes from the 0 walls situation to the of 1 wall one, and when MT goes to the 2 walls situation it becomes 2.8 dB lower in relation to the 1 wall one. In UL, the interference shows a constant behaviour, independently of the number of penetrated walls, because the number of users is almost equal in all simulations.

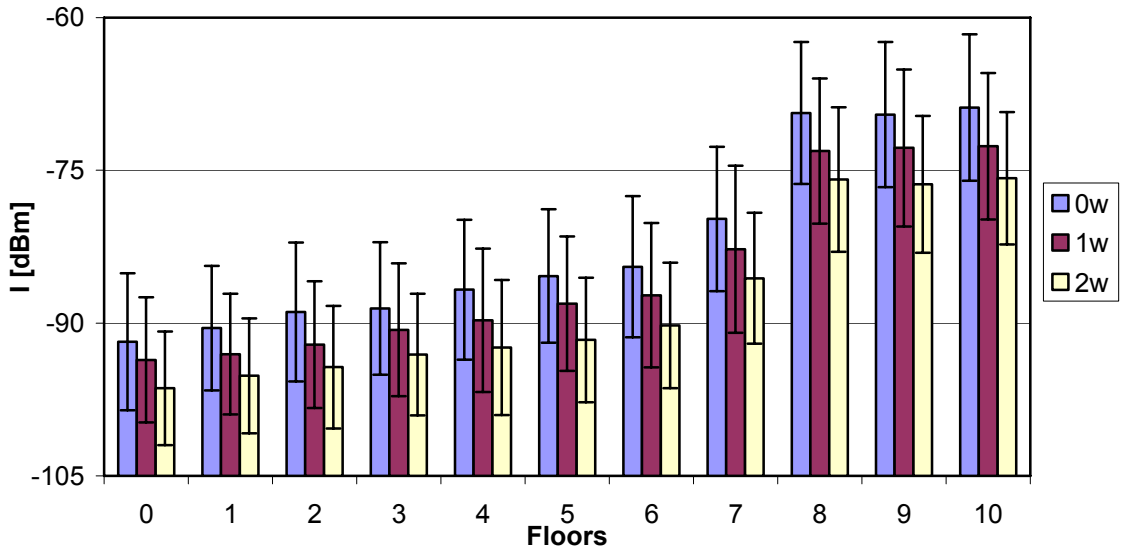

Figure 4.10. Reference scenario Interference results in DL for the second cycle.

The received power has an increase from the first cycle to the second one, Figures 4.11, H.7 to H.9. In the first cycle the received power only depends on noise, (B.7), so, power is approximately constant for different floors and walls scenarios. In the second cycle, power control is activated, i.e., the received power depends on noise plus interference, (B.10), therefore, the received power has a different behaviour.

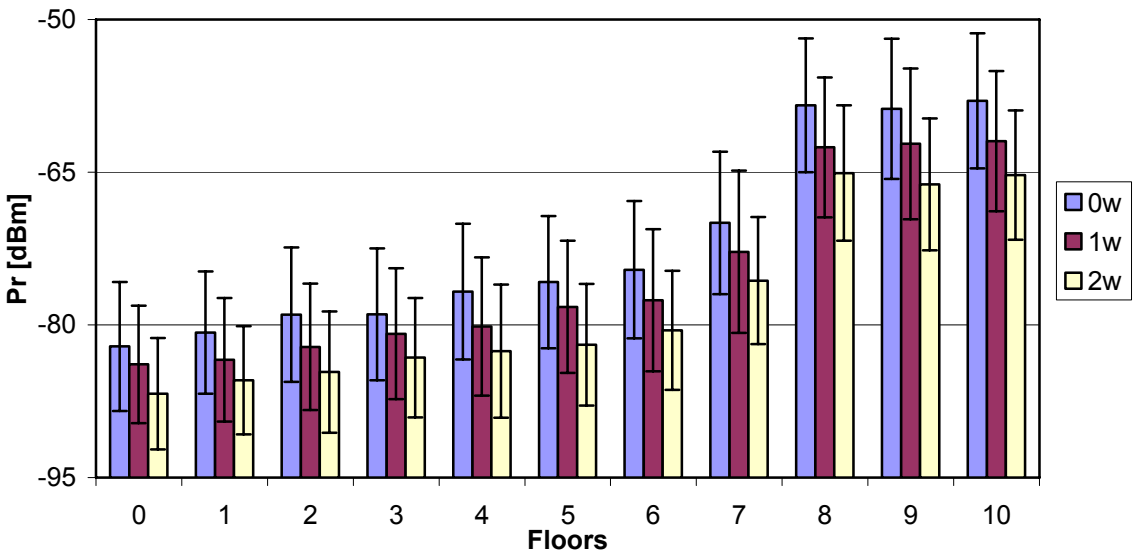

Figure 4.11. Reference scenario received power results in DL for the second cycle.

At the first cycle, the *C/I* that is obtain through (B.11), in DL and UL, tends to become lower as higher the MT is, and it is better as more walls the MT has around, Figures H.10 and H.11, because the received power is more or less constant in the entire building and the interference increases. As known, if *C/I* is less than 0, the MT will not establish connection, therefore, in this point the MT is not enabled to perform the service. So, in the second cycle with power control implementation, the received power leaves the constant trend to become upward, *C/I* becomes positive with an increase trend, allowing the MT to get service, Figures 4.12 and H.12.

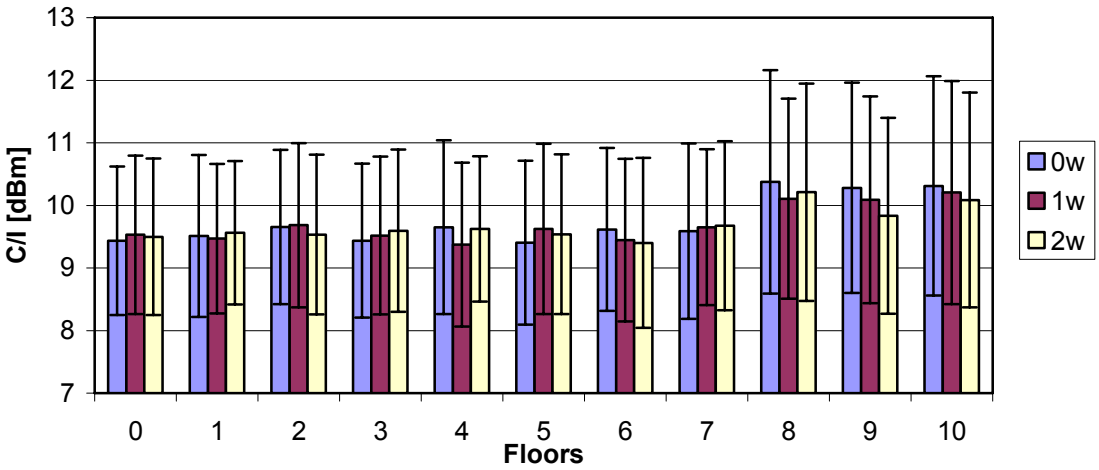

Figure 4.12. Reference scenario C/I results in DL for the second cycle.

4.4.2 Dependence on Distances

The distance between MT and BS was changed in order to verify how the system reacts. Increasing and decreasing the distance between MT and BS has an impact in a major parameter: received power. As near as the BS is to the MT, the higher the MT received power, consequently the interference is higher. So, analysing the Figure 4.13, the trend lines for reference are given by (4.3), in the case of a near BS are given by (4.4), and for far BS are given by (4.5). The standard deviation for each trend line is shown in Table 4.7.

$$I^{REF}_{[dBm]} = \begin{cases} 2.52 \times F_N - 97.29, & \text{DL} \\ -0.09 \times F_N - 111.16, & \text{UL} \end{cases} \tag{4.3}$$

$$I^{Near}_{[dBm]} = \begin{cases} 2.31 \times F_N - 87.82, & \text{DL} \\ -0.06 \times F_N - 110.79, & \text{UL} \end{cases} \tag{4.4}$$

$$I^{Far}_{[dBm]} = \begin{cases} 2.68 \times F_N - 102.77, & \text{DL} \\ -0.07 \times F_N - 111.42, & \text{UL} \end{cases} \tag{4.5}$$

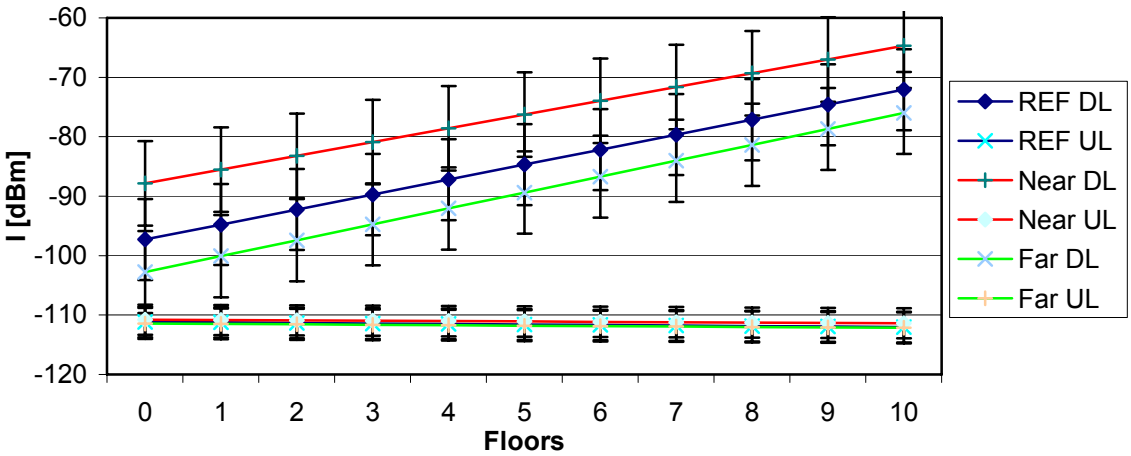

Figure 4.13. Dependence on distance trend lines, in the case of 0 walls.

Table 4.7. Trend lines standard deviation for distance case.

Standard Deviation [dB]					
DL			UL		
REF	Near	Far	REF	Near	Far
6.82	7.11	6.91	2.58	2.54	2.60

Figure 4.13 shows that the behaviour in DL and UL maintains almost equal with the distance variation. However, interference presents variations in DL, the slope of trend lines being 2.5 dB per floor. The interference is approximately 8 dB higher when the BS is near to the MT, and it becomes 5 dB below the reference level when the BS is in a far positions, Figure 4.14. In UL, the interference does not present any relevant variation, because the number of served users is practically equal during the simulation. For the other cases of penetrated walls the behaviour is almost equal, Figures H.13 and H.14. As previously mentioned, received power is higher as closer the BS is to the MT, Figures H.15 and H.16.

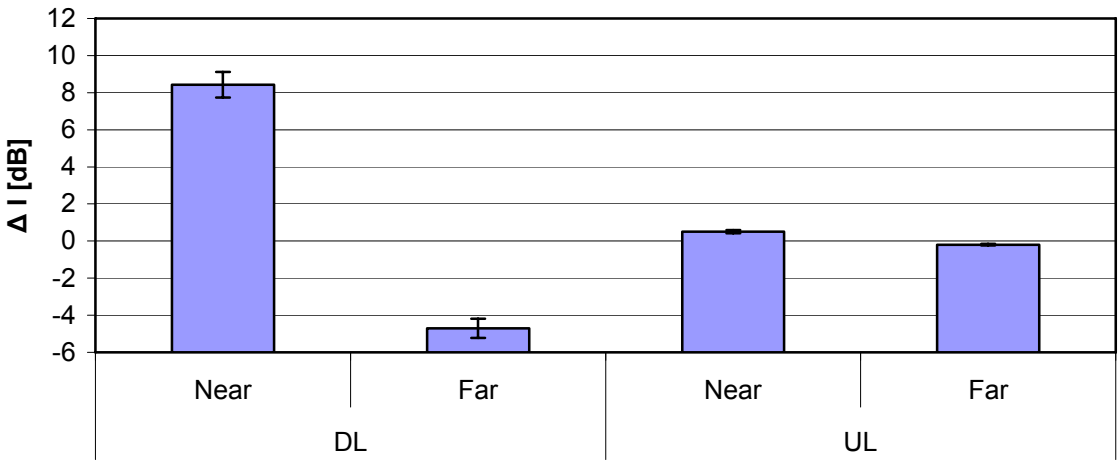

Figure 4.14. Dependence on distance relative to the reference case.

4.4.3 Dependence on Central Building Height

The simulations were performed for different heights of the central building. The higher central building is the reference case with 33m of height; in the case of central building equal to neighbours, it has 21 m of height; when the central building is lower than others, it has 12 m of height. All other

In order to have a better analysis in this case, the interference results were split in two ways, MT in LoS and in NLoS. So, the reference scenario trend line in DL is rewrited for (4.6). In the case of the buildings have all the same height, the interference trend is given by (4.7). The last case, when the central building is lower than other buildings, the interference trend is given by (4.8). The standard deviations are in Table 4.8.

$$I_{DL\ [\mathrm{dBm}]}^{REF} = \begin{cases} 1.23 \times F_N - 93.97, & \mathrm{NLoS} \\ 3.27 \times F_N - 80.05, & \mathrm{LoS} \end{cases} \tag{4.6}$$

$$I^{Equal}_{[dBm]} = \begin{cases} 0.98 \times F_N - 95.38 & , \text{DL} \\ -0.01 \times F_N - 111.15, & \text{UL} \end{cases} \quad (4.7)$$

$$I^{Lower}_{[dBm]} = \begin{cases} 1.38 \times F_N - 95.82 & , \text{DL} \\ -0.01 \times F_N - 111.81, & \text{UL} \end{cases} \quad (4.8)$$

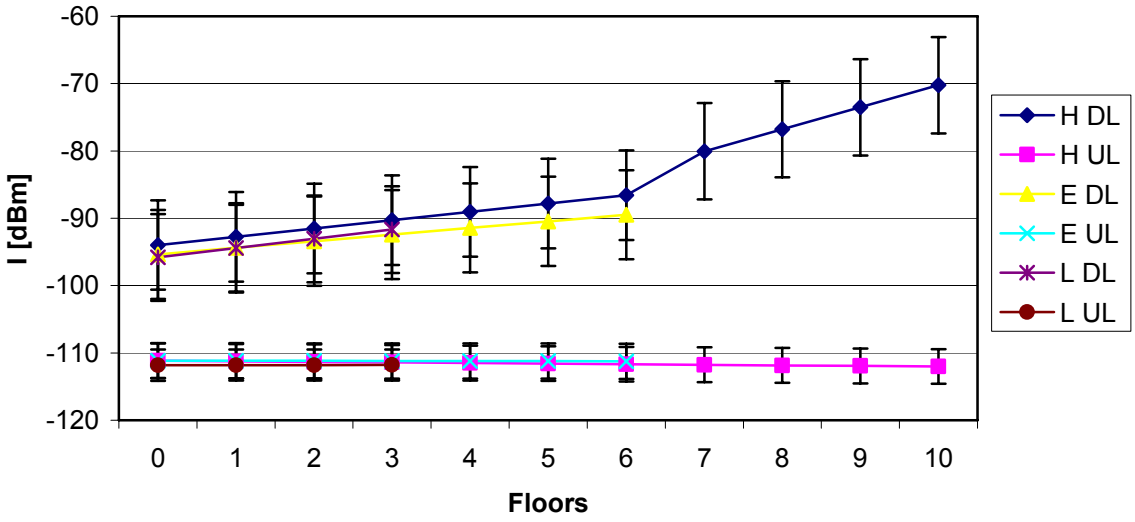

Figure 4.15. Dependence on centre building height trend lines, in the case of 0 walls.

Table 4.8. Trend lines standard deviation for height case.

Standard Deviation [dB]						
DL				UL		
H (NLoS)	H (LoS)	E	L	H	E	L
6.65	7.15	6.62	6.43	2.58	2.61	2.32

The main parameter that changes with the building height variation is the path loss attenuation, i.e., the path loss calculation is performed according to LoS existence. This parameter has a visible impact the interference results, Figure 4.15. When the height of the central building is equal to the others or lower than others, the MT is always in NLoS with the BS, so, as expected, the difference between these two cases does not exist.

In DL, in the reference case, interference has the same performance as the other two cases until the 7th floor, and from there the slope has more 2 dB and the standard deviation gets higher in 0.5 dB. When the MT is between 0 and 6th floors, it is in NLoS, and from the 7th floor it becomes in LoS with BS. When there is LoS between MT and BS, the path loss is lower than in NLoS, consequently the interference is higher in LoS. These are the reasons for the different behaviours.

The LoS does not have a direct influence in UL, i.e., the interference in UL depends on the number of users served. With building height variation, the number of users during the simulation is almost equal, therefore, interference behaviour does not present variations.

4.4.4 Dependence on Street Width

Street widths are increased to the double and decreased to half, i.e., to 24 m and 6 m. The path loss attenuation is the main parameter that suffers impact with these changes. Therefore, the trend lines are one more time split into two, one for NLoS and an other for LoS. In the case of double width, the interference is given by (4.9), and for half width by (4.10). The lines are shown in Figure 4.16, and standard deviations are shown in Table 4.9.

$$I^{2w_s}_{[\mathrm{dBm}]} = \begin{cases} 1.33 \times F_N - 96.07, & \mathrm{DL\ NLoS} \\ 3.79 \times F_N - 80.11, & \mathrm{DL\ LoS} \\ -0.41 \times F_N - 102.91, & \mathrm{UL} \end{cases} \tag{4.9}$$

$$I^{w_s/2}_{[\mathrm{dBm}]} = \begin{cases} 1.23 \times F_N - 90.56, & \mathrm{DL\ NLoS} \\ 2.54 \times F_N - 78.60, & \mathrm{DL\ LoS} \\ -0.09 \times F_N - 109.67, & \mathrm{UL} \end{cases} \tag{4.10}$$

In DL, when the MT is in NLoS, Walfish-Ikegami model is used in the majority of the cases, so, when the streets enlarge its width the attenuation becomes lower, the opposite being also true, i.e., when the street width is reduced the attenuation becomes higher. Interference has an inverse behaviour in relation to the path loss, i.e., when path loss increases the interference decrease.

As Figure 4.16 shows, the NLoS slope is almost equal for different width. Although, the interference level is quite different, i.e. when the width is duplicated the interference increases 2.42 dB and while it is reduced for half, the interference decreases 2.81 dB. The Interference for the LoS case does not suffer impact with these changes because LoS models are independent of the street width, Figure 4.17.

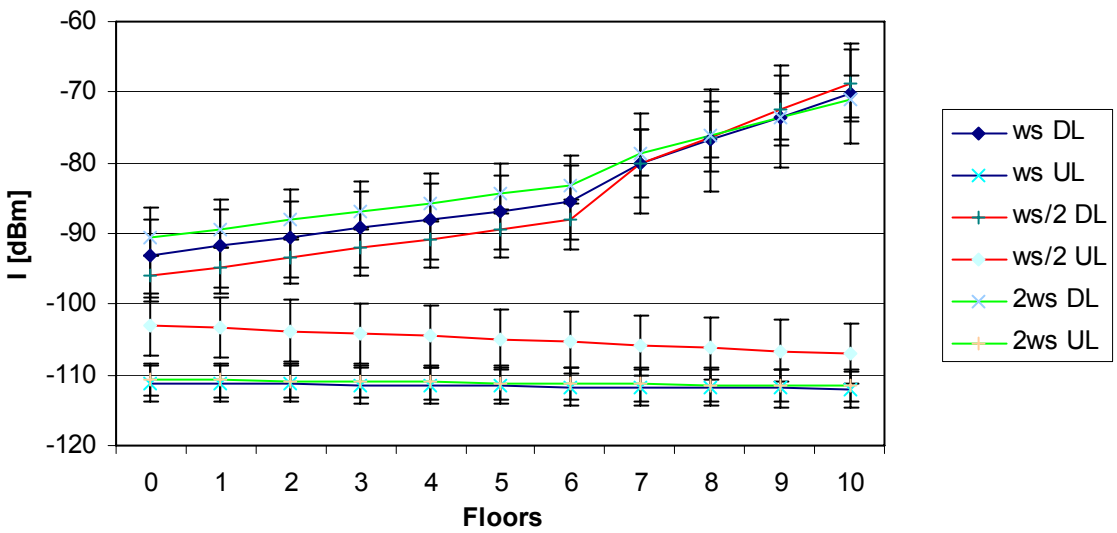

Figure 4.16. Dependence on street width trend lines, in the case of 0 walls.

Table 4.9. Trend lines standard deviations for width case.

	Standard Deviation [dB]		
	DL		UL
	NLoS	LoS	
$w_s/2$	2.86	4.90	4.32
w_s	6.65	7.15	2.58
$2w_s$	2.67	3.28	2.32

In UL, the behaviour is almost equal, though, it can be noticed a higher interference level for $w_s/2$, Figure 4.17. When the streets have half of the width the scenario becomes smaller, so users are nearer the BS, consequently, less transmitted power is required to establish connection, more users are served, and the interference level increases. In the case of $2w_s$, the scenario becomes larger, the difference of interference level with the reference is approximately 0, because the number of users served is almost the same as in w_s, however, the difference is positive. In the case of NLoS, the Walfish-Ikegami model is the reason for this, thus, when w_s increases, path loss decreases and the interference increases. In the case of LoS, models change with the distance, if hence BSs are in the same place the distance will be the same, as well as the interference.

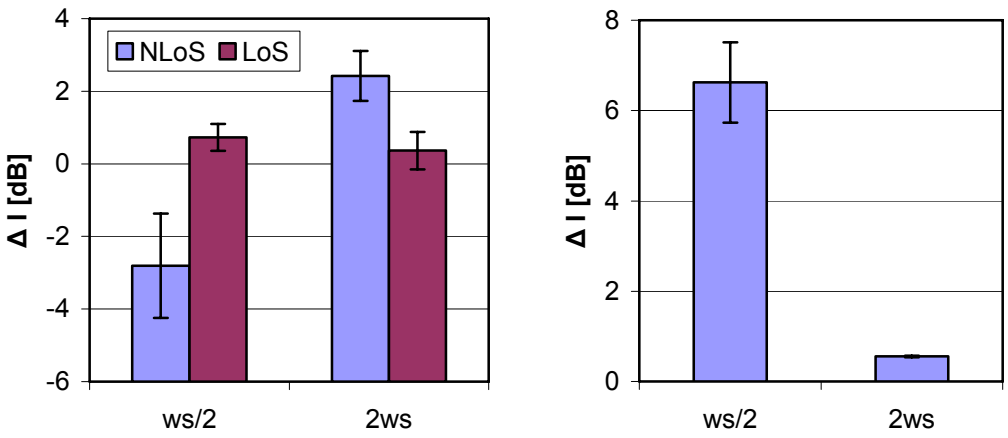

(a) DL. (b) UL.

Figure 4.17. Dependence on street width relative to the reference case, in the case of 0walls.

4.4.5 Dependence on Antenna Tilts

Simulations with 5º and 10º of antenna down tilts were performed. The antenna with 0º of tilt corresponds to the reference. The tilt change has a direct impact on the antenna gain, as it can be seen in Figure H.17.

For 5º of antenna down tilt the interference trend line is given by (4.11), while for 10º it is given by (4.12), Figure 4.18. The standard deviations of these results are depicted in Table 4.10.

$$I^{5^\circ}_{[dBm]} = \begin{cases} 2.53 \times F_N - 101.07, & DL \\ 0.04 \times F_N - 112.35, & UL \end{cases} \quad (4.11)$$

$$I^{10^\circ}_{[dBm]} = \begin{cases} 2.43 \times F_N - 98.92, & DL \\ 0.1071 \times F_N - 109.83, & UL \end{cases} \quad (4.12)$$

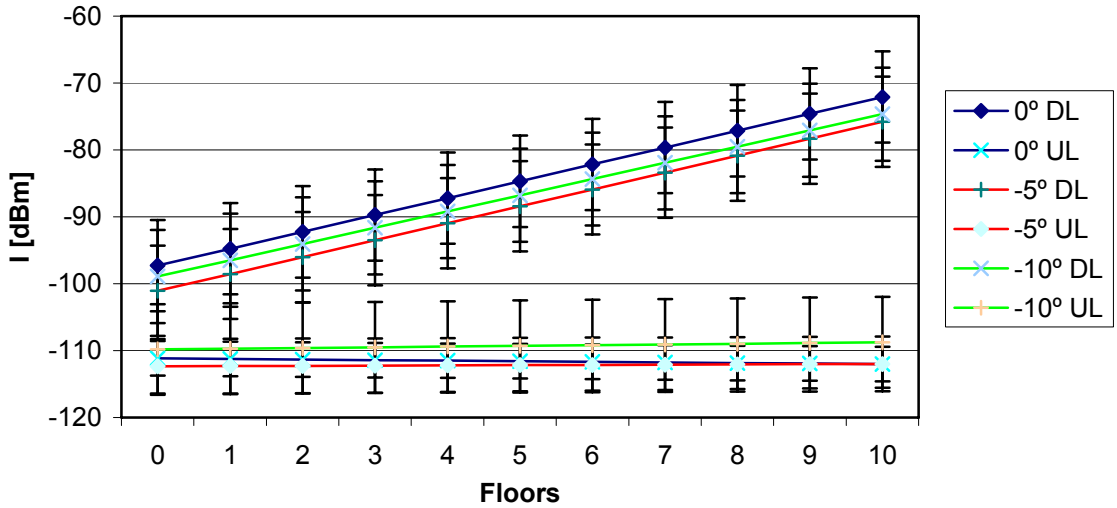

Figure 4.18. Dependence on antenna tilts trend lines, in the case of 0 walls.

Table 4.10. Trend lines standard deviations for tilt case.

	Standard Deviation [dB]		
	Tilt		
	0º	-5º	-10º
DL	6.82	6.74	6.96
UL	2.58	4.08	6.79

For the different tilts, the trend lines have a slope approximately equal, but a different interference level, Figure 4.19.

In DL, the levels of interference for -5º and -10º are better than for 0º. An improvement of 2 dB and 4 dB exists for the cases of -10º and -5º respectively, because with these tilts BSs improve the transmitter power, i.e., for the same received power and path loss, higher gain results in a lower transmitter power, consequently lower interference. Between -5º and -10º there is a difference of 1.65 dB, Figure 4.19. The interference values for -5º are lower than for -10º, because the antenna beam width is 6 dB resulting in a better performance.

In UL, the difference between 0º and -5º is almost 0, and between 0º and -10º is around 2 dB. A higher interference level reveals a higher number of served users, despite the interference level increase, more users are served.

The antenna tilts shows to have a key rule in the interference, i.e., with the tilt changing the interference can be improved in one way (DL/UL) and in the other way it gets worse. So, this parameter should be changed very carefully.

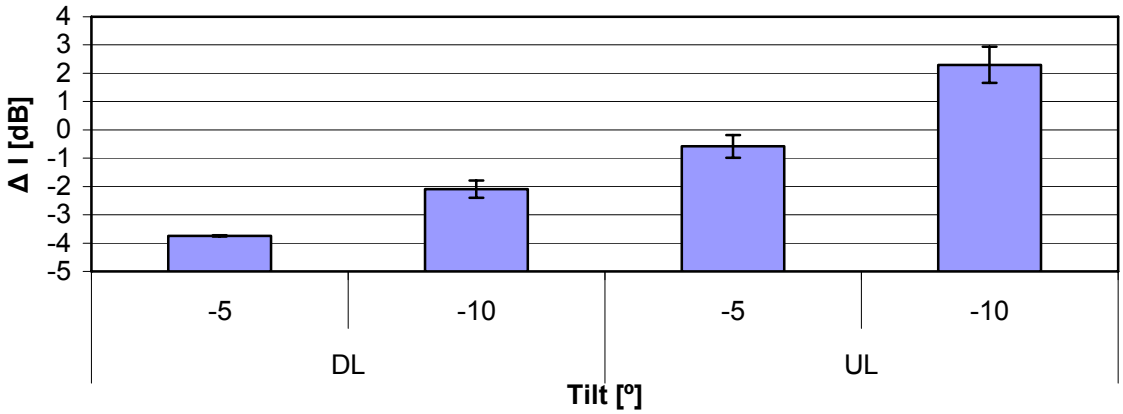

Figure 4.19. Dependence on antenna tilt in relation to the reference case.

4.4.6 Dependence on the Number of BSs

The increase of the BSs number is the last and the more interesting test. Simulations for 2, 3 and 4 BSs were performed. All BSs have the same characteristics as the reference one.

The interference trend lines for all studied BSs situation in DL and UL were drawn. So, in the case of 2 BSs, the interference is given by (4.13), for 3 BSs, it is given by (4.14), and for 4 BSs, by (4.15). The standard deviations of these results are in Table 4.11.

$$I^{2BS}_{[dBm]} = \begin{cases} 2.14 \times F_N - 90.36, & DL \\ 0.10 \times F_N - 111.66, & UL \end{cases} \tag{4.13}$$

$$I^{3BS}_{[dBm]} = \begin{cases} 2.22 \times F_N - 87.79, & DL \\ 0.02 \times F_N - 112.11, & UL \end{cases} \tag{4.14}$$

$$I^{4BS}_{[dBm]} = \begin{cases} 2.14 \times F_N - 82.93, & DL \\ -0.01 \times F_N - 113.25, & UL \end{cases} \tag{4.15}$$

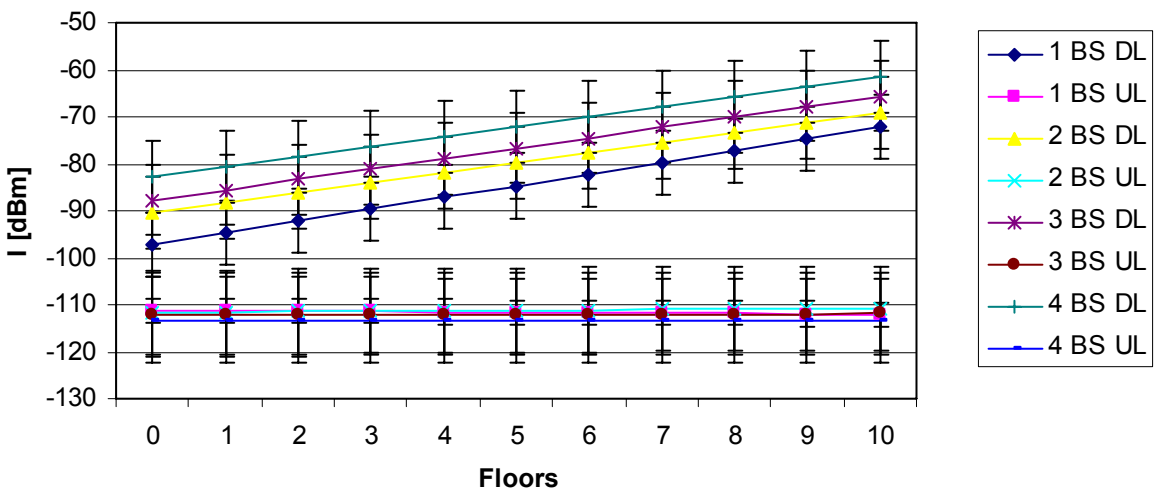

Figure 4.20. Dependence on number of BSs, in the case of 0 walls.

Table 4.11. Trend lines standard deviations for BSs number case.

Standard Deviation [dB]							
DL				UL			
1BS	2BS	3BS	4BS	1BS	2BS	3BS	4BS
6.82	7.68	7.48	7.66	2.58	8.96	8.79	9.04

For the number of BSs variation, the slopes are approximately equal for all different cases, as Figure 4.20 shows. However, as in the previously study cases, it is the interference level that changes. In DL, an increase in the BSs number results in an increase of the interference level, because there are more BSs causing interference in the MT. In the case of 2 BSs, the interference grows 5 dB, Figure 4.21. When one more BS is employed, this difference increases 3 dB, i.e., it becomes 8 dB higher. In the case of 4 BSs the interference has more 12 dB. The standard deviations suffer an increase with the number of BSs rising.

In UL, the interference level becomes lower with the increase of the BSs number. Though, the difference between each other is not as high as in DL, because with more BSs, MTs have more options to spread in the network, decreasing the interference.

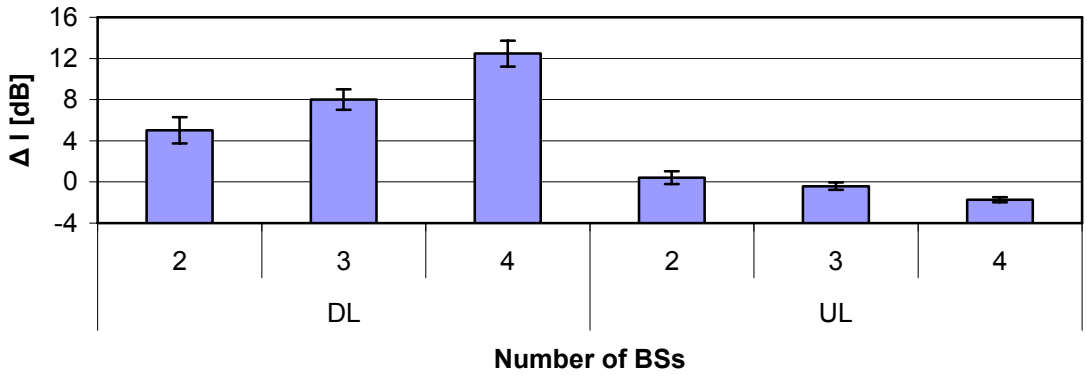

Figure 4.21. Dependence on number of BSs in relation to the reference case.

In conclusion, the variation of this parameter has more impact in DL way than in UL. In DL, for each BS that is employed on the scenario the interference become approximately 4 dB higher.

Chapter 5

Conclusions

In this chapter, the main conclusions of this thesis are pointed out, as well as some future work suggestions.

The main objectives of this thesis were to study and analyse the interference behaviour with the building height in UMTS-FDD. These goals were accomplished through the development of interference models and implementing them in a simulator written in C++. The simulator, named UMInS, was entirely developed for this work. To assess the simulations results, measurement were performed.

Interference in each link is obtained through inter- and intra-cell interferences combination, thus, for interference calculation four models were used. For intra-cell in DL, the model described in [Nguy05] was used, which takes the BS transmitted power, number of users within the cell, orthogonality factor, and the path loss between BS and MT into account. For intra-cell in UL, [Nguy05] was the model chosen, which takes into account the MT transmitted power, path loss, number of users doing the same service as MT, and MT service activity factor. For inter-cell in DL, [EPCC06] was the model used, depending on the total transmitted power of adjacent BSs, orthogonality factor and path loss between MT and other BSs. For inter-cell in UL the model described in [EPCC06] was the choice, takes all users of other BSs, their transmitter power, path loss, service activity factor and one distance relation between the BS that is serving that MT and the interfered BS into account. The path loss in these models is calculated according to an algorithm developed for this thesis, which combines some propagation models as free space, Walfisch-Bertoni and COST-231 Walfisch-Ikegami.

In Chapter 4, the analyses of all measurements and simulations results were shown. The north tower of Instituto Superior Técnico, in the city of Lisbon, was the place where the measurements were performed. This scenario fulfils the case when the MT is in LoS with the BS. The measurements were done for the voice service from the 4th to 11th floor in all corner rooms, halls, elevator rooms and men's rooms, in order to represent when the MT is attenuated for only a glass (0 walls), a glass plus one wall (1 wall) and a glass plus two walls (2 walls). In all measurements, an approximately cross path was followed, trying to cover a maximum area. After data filtering, it was concluded that a connection was established with five BSs, fifteen sectors, however, only three sectors served the MT in all floors. For 0 walls and 1 wall situation, E_b/N_0 falls 0.25 dB per floor, while for 2walls it drops 0.45dB and between each situation there is a difference of 0.8 dB on average. In the case of 2 walls the relation drops faster, probably because in other cases the measurements covered all tower sides while in this particular case they only cover two tower sides. With these results, it can be concluded that the higher the MT is in the building, the higher the interference is.

Once known the E_b/N_0 behaviour, simulations with the real characteristics were performed with the aim to assess the simulator. Simulations results show a decrease trend with a drop of 0.1dB per floor and a difference of 0.5 dB between each penetrated wall. The values slope is almost half of the measurements results, as well as the difference between the situations of penetrated walls. However, the results of the measurements are higher than the simulated ones, with a difference near 2dB. With the simulation, it is proved that the measurements results for 2 walls do not have the correct behaviour. No matter how much it was tried to approximate the simulation scenario to reality, the simulator works with regular scenarios and reality is irregular. Despite all these differences, it can be concluded that the simulator is a good tool for interference study.

In order to verify the interference behaviour, simulations were made by changing some parameters, such as the distance between MT and BS, centre building height, street widths, antennas tilts, and number of BSs, with the purpose to analyse how interference behaves.

First of all, a reference scenario was defined, with one BS, 100 users, voice at 12.2 kbps and a centre building higher than others. In DL, interference has its higher values when the MT is in the 0 walls situation that is near -97 dBm. It has an increase trend of 2.5 dB per floor and a difference of 2.8 dB between each penetrated wall situation. Interference shows this behaviour because the higher the MT is, the more exposed to other sectors it is, and that increases the interference. This trend can be split in two ways, when the MT is in NLoS and LoS: in the former interference rises 1.23 dB per floor and in the latter 3.27 dB. In UL, the interference has an approximately constant behaviour rounding -111 dBm, because the number of users that interferes is more or less equal when the MT goes up. In conclusion, the higher the MT is, the higher the interference in DL is, and it is 2 dB higher when the MT is in LoS than when the MT is in NLoS. In UL the interference has a constant behaviour.

Parameters were changed one by one, the distance being the first one. In DL, the interference does not show changes in its slope, i.e., the interference keeps its increase of 2.5dB per floor. However, the interference level is changed. The nearer the BS is, the higher the MT interference is. For UL, no relevant changes are registered.

When the height of the central building is changed, the analysis is split in LoS and NLoS. When the building has the same height as others, and it is lower than the neighbours, the MT is in NLoS with the BS, so the interference behaviour is equal in both cases. When the building is above the others, and the MT is on the upper floors, it is in LoS, so the slope increases almost two times faster, because the path loss attenuation is higher in NLoS than in LoS. Once more, in UL no relevant changes are registered.

With the street width changing, the path loss attenuation is the main parameter that suffers impact. For DL, while MT is in NLoS the interference slope is almost equal for different widths. Still, the interference level is quite different, i.e., when the width is duplicated, interference increases and when it is reduced to half, interference decreases. Interference in LoS does not suffer impact with these changes. The interference shows this behaviour because NLoS models depend on the street width and LoS models are independent of it. In UL, when the street is reduced to half, the interference level is higher than in other cases. The behaviour could be explained with the number of users served, i.e., with street width reduce to half of its reference value, the scenario gets smaller and users become nearly the BS, so less transmitted power is required to establish connection, consequently more users are served causing more interference.

Antennas tilt is a parameter that shows to have an important role in interference behaviour. This parameter has 0º as default and it was changed to -5º and -10º. In DL, for different tilts the interference slopes maintain equal, although its level is changed. For downtilts of 5º and 10º the interference level is reduced in 3.75 dB and 2.09 dB, respectively, because with this tilts the BS improves its transmitter power, i.e., for the some received power and path loss, higher gain results in a lower transmitter power, consequently lower interference. In UL, only the downtilt of 10º presents a

higher interference level. A higher interference level reveals a higher number of serviced users. In conclusion, in general 5º of downtilt presents a better interference level. However, with little difference, 10º of downtilt served more users.

Then Number of BSs was the last parameter to be changed. With this variation, the interference slope does not suffer important changes, although interference level gets different. In DL, when the number of BS is increased to 2, 3 and 4 the interference level rises 5, 8 and 12 dB, respectively. As expected, an increase in the number of BS results in an increase on the interference level, because the MT is interfered by more BSs. In UL, despite lower, the interference level shows a trend to become lower with the increase of the BSs number. With more BSs, MTs are more spread in the network, resulting in an interference decrease.

Summarising, the higher the MT is in the building, the higher the interference is. This increasing trend has a global rise of 2.5dB per floor and a difference of 2.8dB between each penetrated wall situation. This slope is different if the analysis is split, in NLoS and LoS. When the MT is in LoS the slope increases almost two times faster than when it is in NLoS. With the parameters variation, the interference level is changed but it is maintain its behaviour, the antenna tilts and number of BSs being the parameters that have a big impact on that.

The simulator proves to be a powerful tool in the interference study, but it has its limitations. The BSs have the sectors oriented in the same way, i.e., the sector azimuth can not be changed. The antenna tilt is equal for all antennas, i.e., it is not possible to have antennas with different tilts. There is not other simulator to compare and to assess the values. The measurements were only performed for the case of LoS between MT and BS. The time of each simulation is 80 minutes on average in Intel Pentium 4 3GHz, that enables performing more simulations. For this thesis, 110 hour in simulations were spent.

For future work, it is suggested an improvement of the simulator in its limitations, previously described, implementation of the 3GPP propagation model as complementation of Walfish-Ikegami model, exploration of other points of view using the Gaussian Approach, which is described in this work but not used. With all new technology rising, it would be interesting to perform the same study for HSPA+ and UMTS900.

Annex A - Gaussian Approach Model

This annex describes in detail how the extrapolation of the Gaussian model for GSM1800 to the UMTS band is performed.

According to [Corr07] this model for the GSM1800 band has the following values:

- Average (μ): 10.20 dB;
- Standard deviation (σ): 13.8 dB.

The frequency band of GSM 1800 is:

- UL: [1710, 1785] MHz
- DL: [1805, 1880] MHz

The frequency band of UMTS FDD is:

- UL: [1920, 1980] MHz
- DL: [2110, 2170] MHz

The standard deviation of UMTS can be the same of the GSM1800. The average of the additional loss can be approximated by

$$\mu'_{[\mathrm{dB}]} = 20\log\left(\frac{f_{c[\mathrm{MHz}]}^{UMTS}}{f_{c[\mathrm{MHz}]}^{GSM1800}}\right) \tag{A.1}$$

where:

- f_c^{UMTS}: Central Frequency of UMTS;
- $f_c^{GSM1800}$: Central Frequency of GSM1800.

  with

$$f_{c[\mathrm{MHz}]}^{UMTS} = \frac{2170+1920}{2} = 2045 \tag{A.2}$$

$$f_{c[\mathrm{MHz}]}^{GSM1800} = \frac{1880+1710}{2} = 1795 \tag{A.3}$$

So the extrapolated average for the UMTS band can be given by

$$\begin{aligned}\mu_{[\mathrm{dB}]}^{UMTS} &= \mu_{[\mathrm{dB}]}^{GSM1800} + \mu'_{[\mathrm{dB}]} \\ &= 10.20 + 1.13 \\ &= 11.33\end{aligned} \tag{A.4}$$

The central frequency can be calculated by (A.2) and (A.3) because the main problem of this thesis is the interference, so it is not necessary refer a specific channel of UL or DL band, and the additional average loss is lower than standard deviation.

Concluding, the Gaussian Approach parameters for UMTS band are:

- Average (μ): 11.33 dB;
- Standard deviation (σ): 13.8 dB.

Annex B - Link Budget

In this annex, all calculations concerning the link budget for UMTS R99 used in this thesis are shown.

The path loss in (2.4) can be rewritten by

$$L_{p[\mathrm{dB}]} = EIRP_{[\mathrm{dBm}]} - P_{r[\mathrm{dBm}]} + G_{r[\mathrm{dBi}]} \tag{B.1}$$

where:

- *EIRP*: equivalent isotropic radiated power.

The G_r in (B.1) when diversity is used is substituted by

$$G_{rdiv[\mathrm{dB}]} = G_{r[\mathrm{dB}]} + G_{div[\mathrm{dB}]} \tag{B.2}$$

Where:

- G_{div}: diversity gain.

The diversity considered is the one for UL, since there is no space in the MT for spatial diversity and polarisation diversity requires doubling the transmit equipment at the MT [Sant04].

The power balance in UL and DL are different because EIRP changes. There are differences between MTs and BSs that need to be taken into account [Corr07]. Therefore, EIRP for DL and UL can be estimated by (B.1) and (B.2), respectively.

$$EIRP^{DL}{}_{[\mathrm{dBm}]} = P_{Tx[\mathrm{dBm}]} - L_{cable[\mathrm{dB}]} + G_{t[\mathrm{dBi}]} \tag{B.3}$$

$$EIRP^{UL}{}_{[\mathrm{dBm}]} = P_{Tx[\mathrm{dBm}]} - L_{u[\mathrm{dB}]} + G_{t[\mathrm{dBi}]} \tag{B.4}$$

where:

- P_{Tx}: transmitted power, Table 2.2 shows the common values.
- L_{cable}: cable losses between emitter and antenna;
- L_u: body losses, normally assume values for voice between [3, 10] dB, and for data [0, 3] dB

The received power depends on the link and on the system. Thus it may be calculated by (B.5) and (B.6), for DL and UL respectively.

$$P^{DL}_{Rx[\mathrm{dBm}]} = P_{r[\mathrm{dBm}]} - L_{u[\mathrm{dB}]} \tag{B.5}$$

$$P^{UL}_{Rx[\mathrm{dBm}]} = P_{r[\mathrm{dBm}]} - L_{c[\mathrm{dB}]} \tag{B.6}$$

where:

- P_{Rx}: received power at receiver input.

In UMTS the receiver sensitivity, $P_{Rx\,\min}$, depends on the average noise power and the Signal-to-Noise

Ratio, so it is approximately:

$$P_{Rx\min[\mathrm{dBm}]} = N_{[\mathrm{dBm}]} + \left(\frac{E_b}{N_0}\right)_{[\mathrm{dB}]} \tag{B.7}$$

where:

- N: total noise power;
- G_p: processing gain.

$$G_{p[\mathrm{dB}]} = 10\log(R_c / R_b) \tag{B.8}$$

$$N_{[\mathrm{dBm}]} = -174 + 10 \cdot \log(\Delta f_{[\mathrm{Hz}]}) + F_{[\mathrm{dB}]} + M_{I[\mathrm{dB}]} - G_{P[\mathrm{dB}]} \tag{B.9}$$

where:

- Δf: signal bandwidth, in UMTS it is equal to R_c=3.84Mc/s;
- F: receiver's noise figure.

The receiver sensitivity could be given by (B.10) when knows the interference.

$$P_{Rx\min[\mathrm{dBm}]} = (N + I)_{[\mathrm{dBm}]} + \left(\frac{E_b}{N_0}\right)_{[\mathrm{dB}]} \tag{B.10}$$

The E_b/N_0 values for the different services are presented in Table B.2. The C/I relation is gave by

$$\left(C/I\right)_{[\mathrm{dB}]} = \frac{P_{R[\mathrm{dBm}]}}{\left(I_{intra} + I_{inter}\right)_{[\mathrm{dBm}]}} \tag{B.11}$$

However, many margins should be taken into account, to adjust additional losses due to radio propagation:

$$M_{p[\mathrm{dB}]} = M_{SF[\mathrm{dB}]} + M_{FF[\mathrm{dB}]} + L_{p\ ind[\mathrm{dB}]} - G_{SHO[\mathrm{dB}]} \tag{B.12}$$

Where:

- M_{SF}: slow fading margin;
- M_{FF}: fast fading margin;
- G_{SHO}: soft handover gain.

Finally, the total path loss can be calculated by:

$$L_{p\ total[\mathrm{dB}]} = L_{p[\mathrm{dB}]} + M_{p[\mathrm{dB}]} \tag{B.13}$$

Table B.1. Number of codes for UMTS R99 (extract from [Corr07])

Service [kbps]	SF	#codes (256)
12.2	128	2
64	32	8
128	16	16
384	4	64

Table B.2. Values of E_b/N_0 relation for the R99 services considered (source: Celfinet).

Application Data Rate [kbps]		E_b/N_0 [dB]
12.2 (CS)	UL	6.6
	DL	9.5
64 (CS)	UL	4.3
	DL	7.3
64 (PS)	UL	3.2
	DL	6.3
128 (PS)	UL	2.7
	DL	5.6
384 (PS)	UL	2.5
	DL	6.0

Annex C - Flowcharts

In this annex, the process behind the received power decision algorithm is shown with its flowcharts.

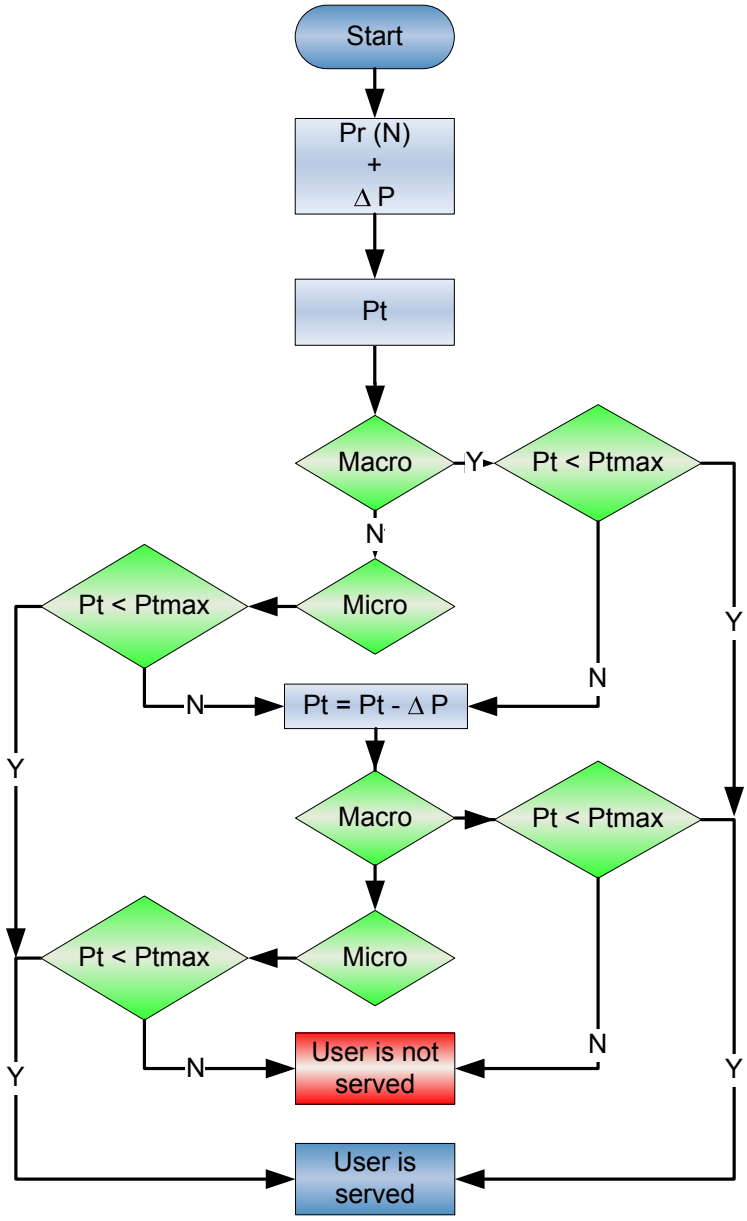

Figure C.1. DL received power decision algorithm.

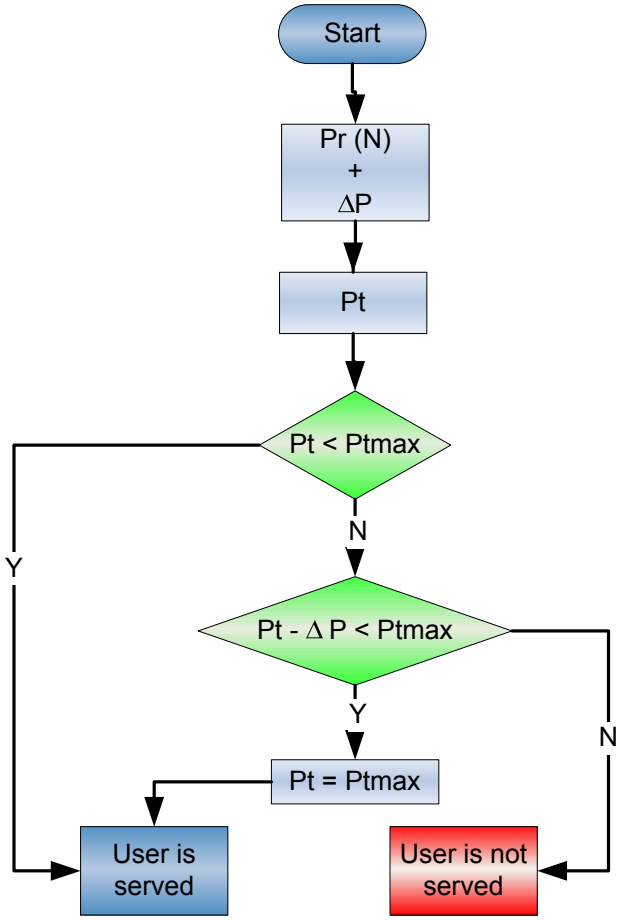

Figure C.2. UL received power decision algorithm.

Annex D - Antennas Properties

This annex shows the antennas characteristics. For all types of antennas the radiation pattern used in this thesis is all the same, Figure D.1 (a).

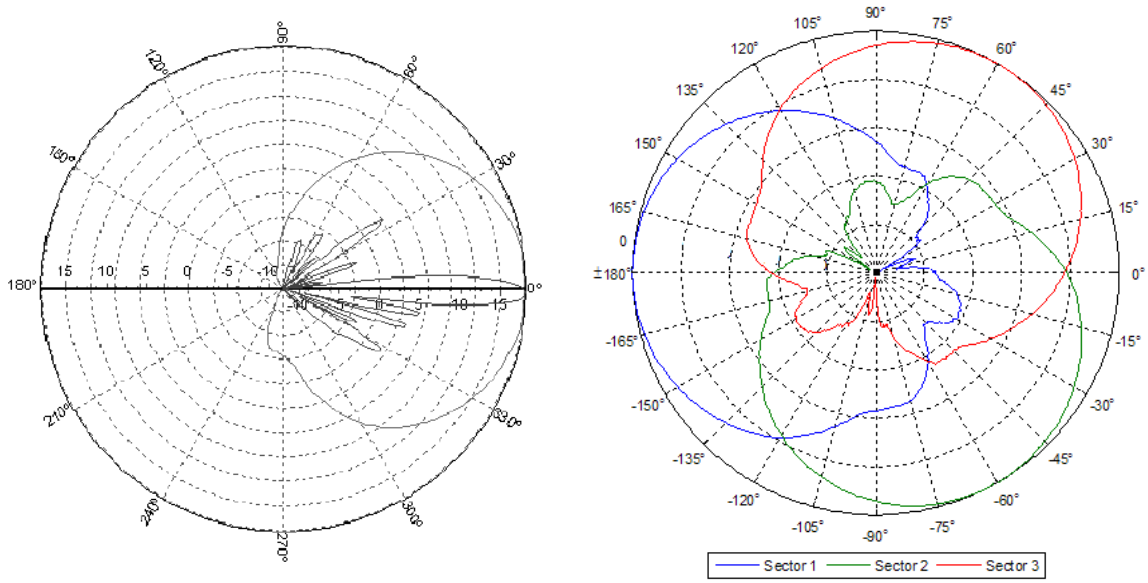

(a) Horizontal and vertical radiation pattern (b) Horizontal radiation pattern with three sectors

Figure D.1 Characteristics of the antenna used in this thesis, P7755.00 (from [POWE08]).

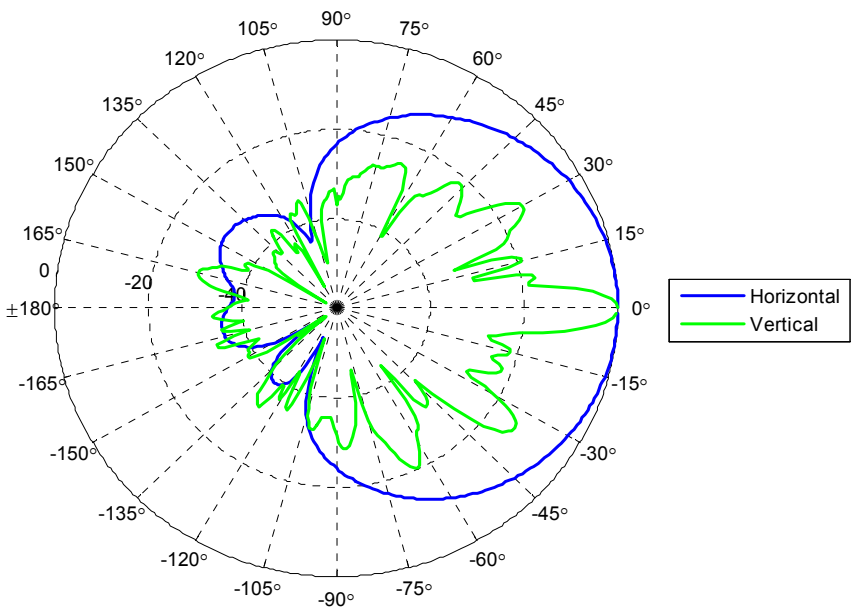

Figure D.2. K742212 Radiation pattern (from [KATH08]).

Table D.1. Different types of antennas (extract from [OFRC05]).

Denomination	Cell Type	Environment	Installation Type
Rtower	Macro-cell	Rural, Suburban	Tower, Mast, Water sump, “Tree”
Uroof	Micro/Macro-cell	Urban	Roof-top
Utower			Tower
Ufacade	Micro-cel		Building façade
Upole			Light pole or other

Annex E - User's Manual

This annex includes the simulator and the measurements filters programs user's manuals.

E.1. UMInS

The simulator platform was developed to be the most self explanatory as possible, by means of presenting a user friendly interface.

The first window that appears when running the simulator is the one corresponding to the main window, where the simulator user has access to several menus that execute different options of the software. These menus are: *File*, Scenario, *Building*, *Network* and *Run*. In the beginning, only *File* and *Scenario* menus are available, Figure E.1. The options can be selected by clicking on the menus or using their specific shortcut.

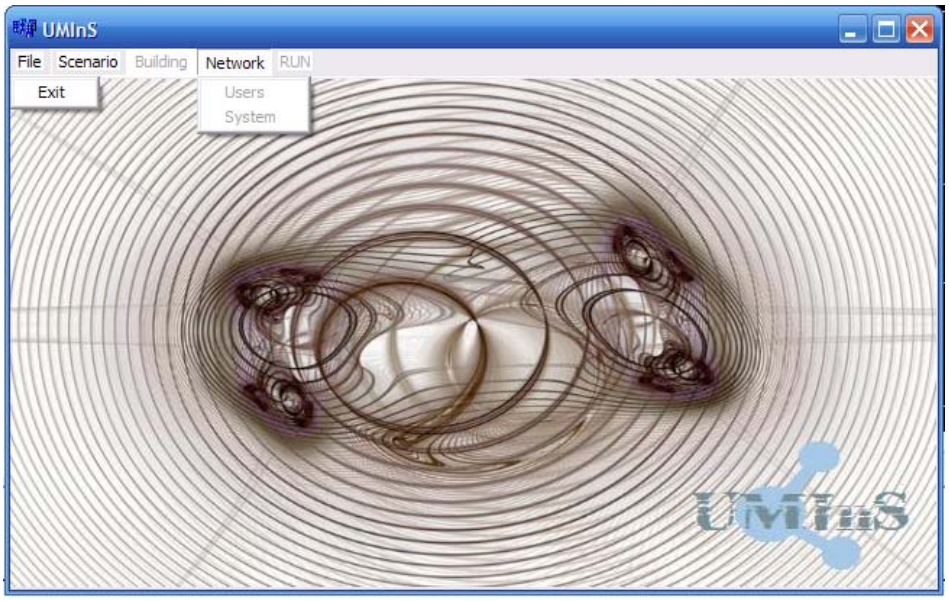

Figure E.1. Main window of the UMInS simulator.

On the *File* menu, one can exit the program (File->Exit). On the Scenario menu, one can define the scenario characteristics, such as w_s, w_b, number of buildings in x- and y-axis and buildings height, Figure E.2. For the values could be used the default ones or define by user. After all values fill in, click in *OK* button to save the information. When the characteristics are defined, the *Building* menu is enabled.

On *Building* menu, one can define the height and number of floors of the centre building, Figure E.3. When the building characteristics are defined, the *Users* and *System* options on *Network* menu is enabled.

On *Network* menu, one can define the users characteristics (*Network->Users*), Figure E.4, and all system options (*Network->System*), Figure E.5. On *Users* option, one can change the number of user

on the simulation, its percentage of mobility (indoor, pedestrian and vehicular) and service (data and voice).

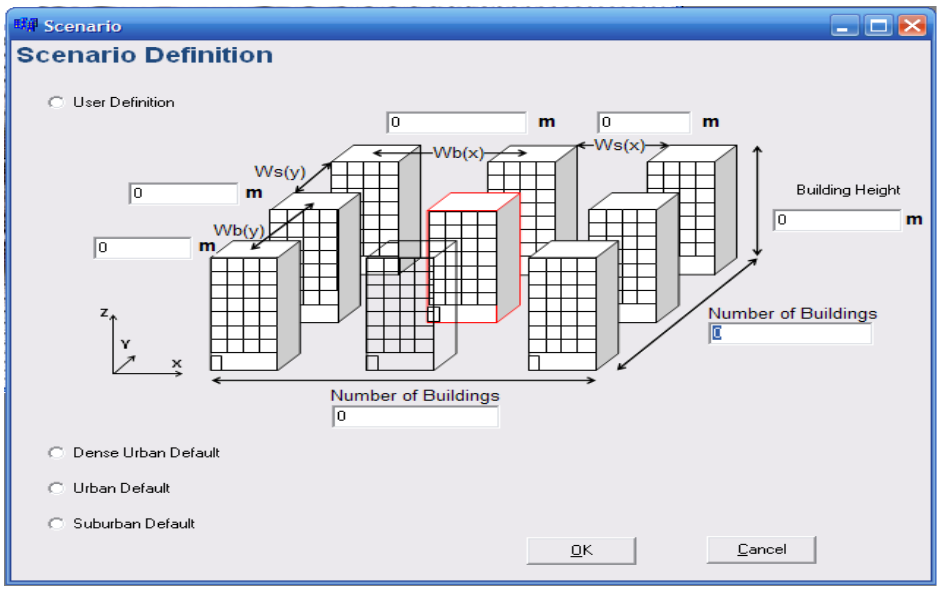

Figure E.2. Scenario window.

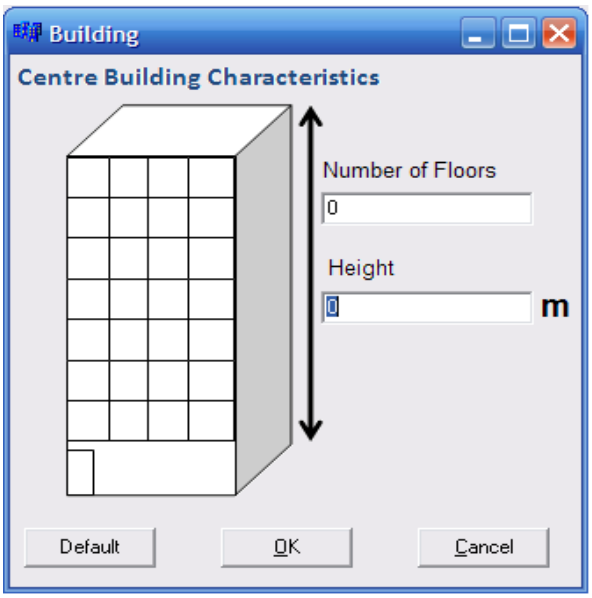

Figure E.3. Building window.

On *System* option, one can define the environment characteristics, such as the standard deviation of the fading distributions, the percentage of set margin to BS and MT, Frequency and the BSs tilt. It is also in this menu that is chosen the BSs location, it can be random or define by user. When is chosen the random option, it is required specify how many he wants generated. For other hand, when it is chosen the *user definition* option, the user needs to fill in the BS coordinates and the antenna type. If the tool user wants other antenna, he/she can by choosing the *other type* entry, Figure E.6. The BSs can be removed, clicking in the *Remove* option. When it is done a new window appears, the *Remove* window, Figure E.7. First search for the BS ID, and then the BS is removed by clicking *Remove* button.

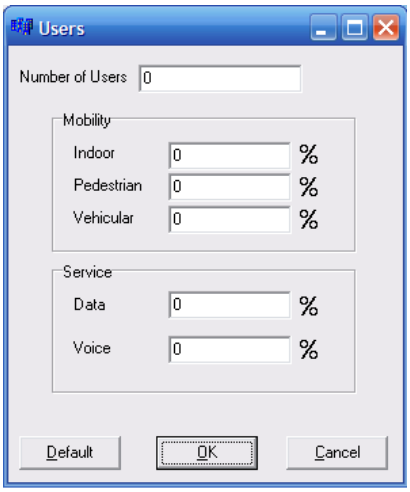

Figure E.4. Users window.

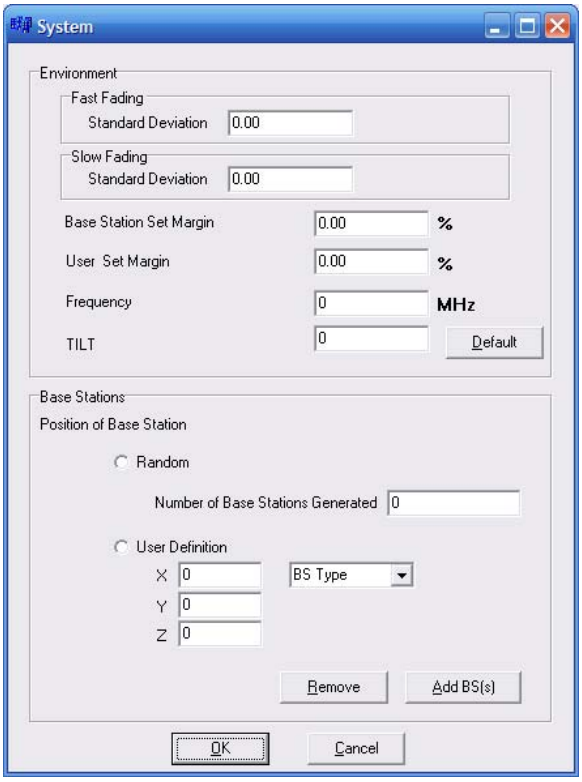

Figure E.5. System window.

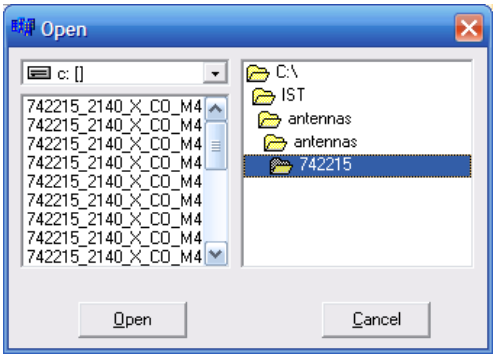

Figure E.6. Other antenna window.

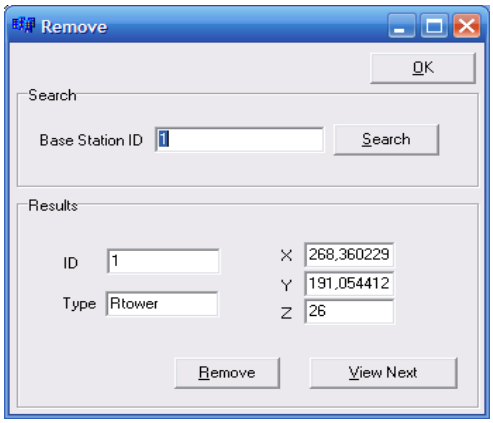

Figure E.7. Remove window.

When the network characteristics are defined, the *Run* menu is enabled. On *Run* menu, one can fill in the finals options to perform the simulation, such as the type of operation mode (auto or manual), the service of the MT in analysis and the type of wall loss when the manual option is chosen, Figure E.8. When all options are chosen the *Calculate Interference* button is enabled, and pressing this button the simulation starts.

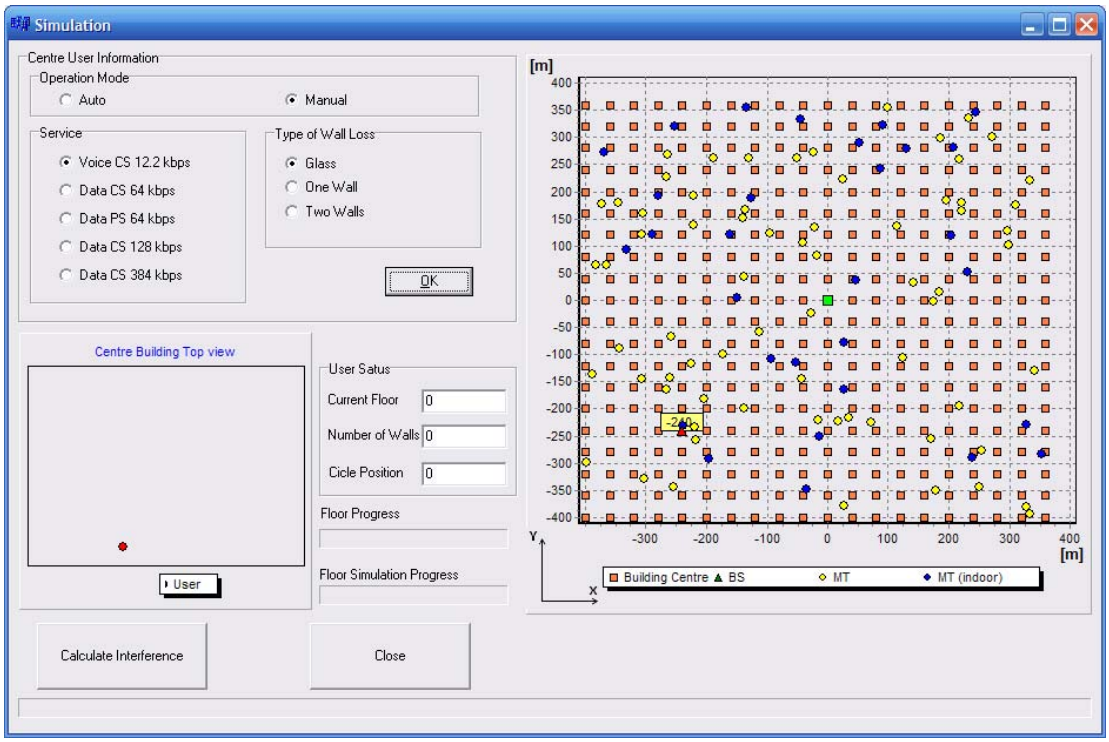

Figure E.8. Simulation window.

Finally, when the bottom progress bar is completed the simulation ends and all simulation information is save in a files *.xls, that are described in Section 3.4.

E.2. UMInLocation and UMInFilter

UMInLocation has only one window, Figure E.9. In this window the tool user selects the directory of

the NEMO logs, and then the file *.dt1 that he want creates the *.xls file. After that, clicking on *MakeFile* button the program creates a file *.xls with the following information: Channel Number (CHN), Cell Identification (CI) and Location Area Code (LAC).

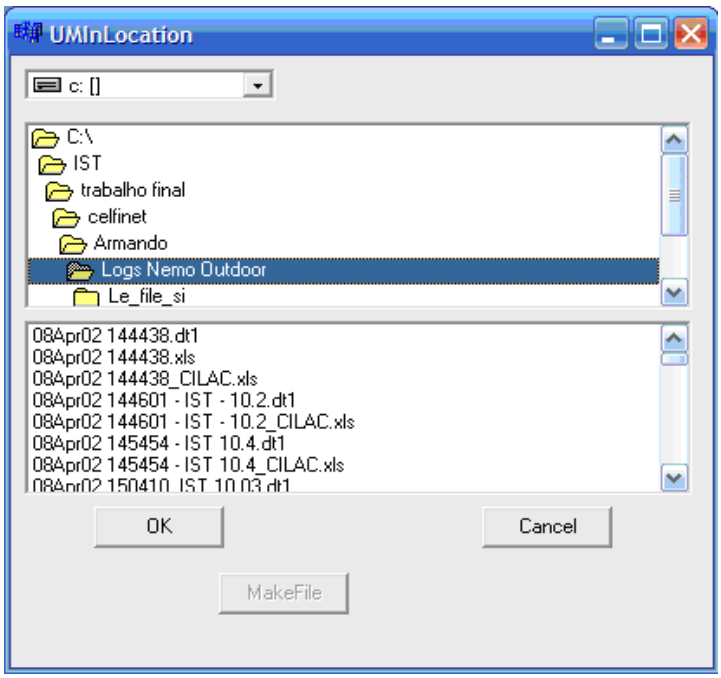

Figure E.9. UMInLocation window.

As previously program, UMInFilter has only one window too, Figure E.10. In this window the tool user selects the directory of the NEMO logs, and then the file *.dt1 that he want creates the *.xls file. Afterwards, clicking on *MakeFile* button, the program creates a file *.xls with the following information: CHN and the respectively carrier Received Signal Strength Indication (RSSI); the CHN, Scrambling Code (SC), E_c/N_0, and the Received Signal Code Power (RSCP) for the active, monitored and detected set cells.

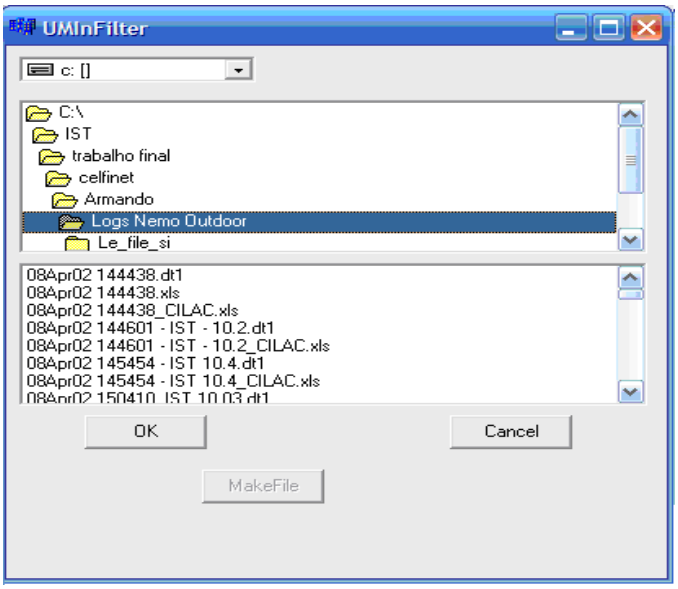

Figure E.10. UMInFilter window.

Annex F - Simulations Assessment

This annexes shows all the simulations graphics done to get the number of simulations. For these analyses, the values taken into account are the standard deviation over average values and the relative mean error. In Figure F.1, one presents the interference standard deviation over average evolution for the case 6 of Figure 3.1. The Figure F.2 is the same as Figure F.1 but for received power.

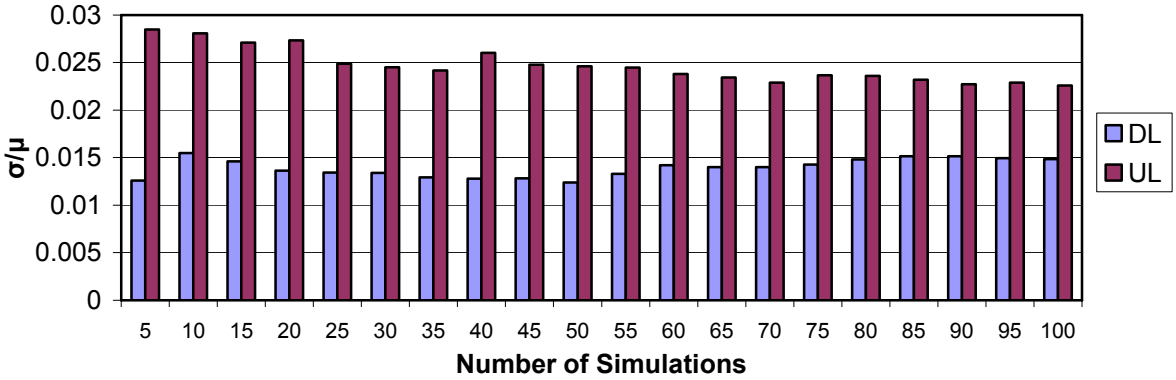

Figure F.1. Interference standard deviation over average values for case 6.

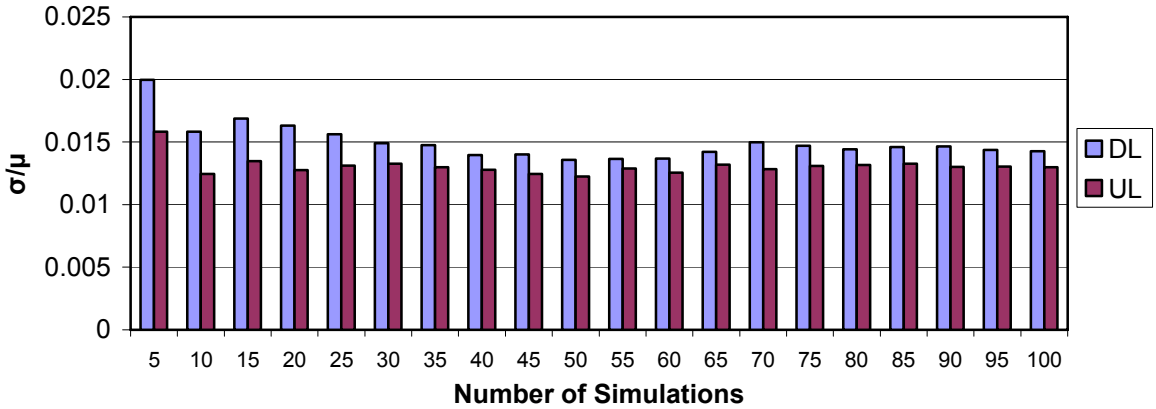

Figure F.2. Received power standard deviation over average values for case 6.

The relative mean error is the other parameter taken into account in the decision of the number of simulations. So the next figures are the relative error for each case.

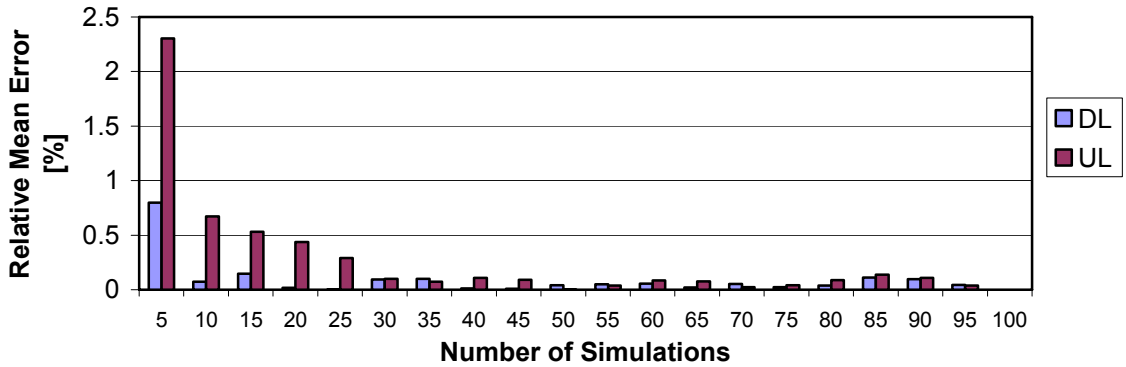

Figure F.3. Interference relative mean error evolution for 100 simulations as reference of case 6.

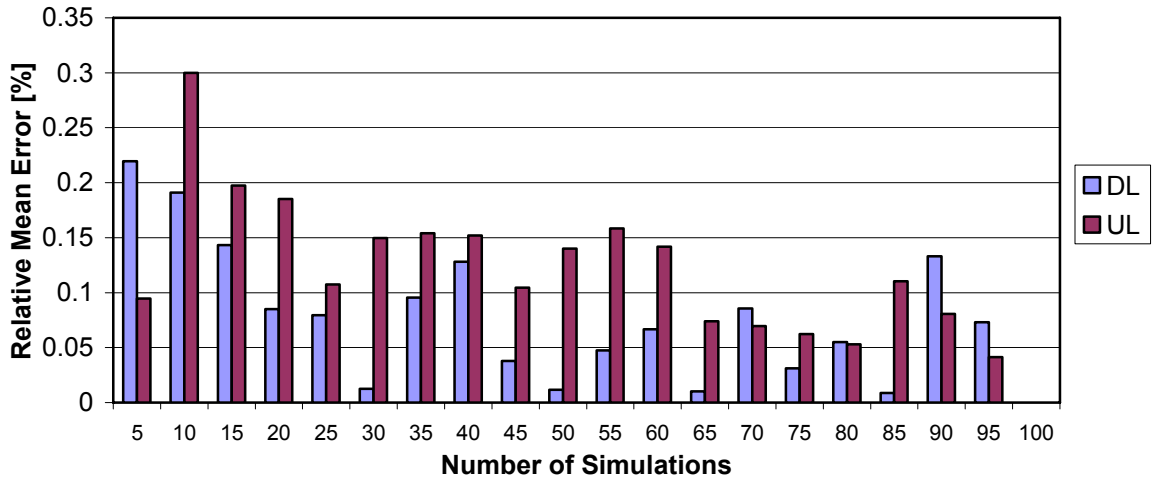

Figure F.4. Received power relative mean error evolution for 100 simulations as reference of case 6.

In Table F.1 and F.2, the relative mean errors in relation to 15 simulations are presented, for each floor and case of penetrated wall.

Table F.1. Relative mean error for 5 simulations.

			Relative Mean Error per Floor [%]										
			0	1	2	3	4	5	6	7	8	9	10
P_r	DL	0w	1.92	1.62	1.25	1.05	1.96	2.14	1.60	5.04	2.51	2.13	2.05
		1w	1.41	1.55	1.96	1.17	2.73	1.48	1.60	3.95	3.37	2.00	2.34
		2w	1.70	1.10	1.90	1.63	1.40	1.45	0.90	2.64	1.97	3.03	2.50
	UL	0w	0.17	0.00	0.11	0.01	0.00	0.06	0.09	0.10	0.03	0.19	0.15
		1w	0.05	0.04	0.03	0.04	0.20	0.11	0.09	0.21	0.18	0.07	0.09
		2w	0.25	0.12	0.06	0.12	0.01	0.16	0.17	0.03	0.13	0.09	0.03
I	DL	0w	1.64	1.27	1.02	0.72	1.73	1.67	1.40	3.94	2.11	1.60	1.46
		1w	1.10	1.02	1.55	0.96	2.01	1.17	1.41	3.30	2.27	1.47	1.85
		2w	1.04	0.75	1.48	1.23	1.38	1.19	0.93	2.11	2.10	2.27	1.88
	UL	0w	0.26	0.20	0.08	0.12	0.22	0.05	0.20	0.26	0.26	0.18	0.10
		1w	0.12	0.03	0.06	0.16	0.10	0.06	0.22	0.17	0.53	0.17	0.27
		2w	0.27	0.20	0.00	0.03	0.05	0.23	0.47	0.38	0.26	0.46	0.34
C/I	DL	0w	0.39	1.45	1.02	1.71	0.62	1.83	0.12	2.82	0.29	1.03	1.39
		1w	1.48	3.12	2.11	0.67	3.48	1.33	0.57	0.76	3.09	1.79	0.96
		2w	3.87	1.53	1.83	2.05	0.83	0.72	0.25	1.50	1.65	1.35	1.50
	UL	0w	1.94	3.57	0.86	2.20	4.16	2.09	0.65	1.51	3.60	0.17	0.68
		1w	0.66	0.36	0.97	1.54	2.11	3.11	4.16	3.65	4.23	3.39	2.76
		2w	0.25	0.72	0.66	1.96	1.37	1.58	4.75	4.09	1.84	3.39	2.05

Table F.2. Relative mean error for 10 simulations.

			Relative Mean Error per Floor [%]										
			0	1	2	3	4	5	6	7	8	9	10
Pr	DL	0w	0.68	0.92	1.26	0.50	1.06	0.93	1.01	2.27	0.54	0.72	0.20
		1w	0.78	1.19	1.06	0.85	1.07	1.14	1.12	2.65	0.18	0.55	0.93
		2w	0.40	0.72	0.82	0.75	1.18	0.84	1.13	3.38	0.73	0.04	0.26
	UL	0w	0.02	0.00	0.06	0.10	0.09	0.08	0.07	0.07	0.07	0.16	0.10
		1w	0.00	0.06	0.00	0.05	0.04	0.06	0.07	0.00	0.07	0.08	0.03
		2w	0.00	0.05	0.07	0.04	0.05	0.05	0.02	0.05	0.14	0.09	0.15
I	DL	0w	0.57	0.83	1.11	0.45	0.81	0.78	0.78	1.87	0.53	0.75	0.36
		1w	0.69	0.97	0.86	0.70	0.99	0.93	0.97	2.25	0.24	0.54	0.75
		2w	0.38	0.68	0.66	0.63	0.93	0.71	0.91	2.82	0.53	0.14	0.16
	UL	0w	0.02	0.00	0.06	0.05	0.18	0.06	0.02	0.07	0.01	0.12	0.07
		1w	0.01	0.03	0.04	0.11	0.03	0.06	0.03	0.04	0.06	0.01	0.11
		2w	0.00	0.06	0.03	0.01	0.07	0.09	0.01	0.03	0.06	0.00	0.01
C/I	DL	0w	0.10	0.04	0.09	0.03	0.82	0.13	0.68	0.42	0.36	0.38	1.00
		1w	0.12	0.73	0.59	0.21	0.55	0.44	0.03	0.40	0.39	0.28	0.45
		2w	0.05	0.29	0.66	0.12	1.02	0.45	0.53	0.91	0.23	0.97	0.66
	UL	0w	0.13	0.24	0.08	0.81	1.73	0.34	1.22	0.04	1.13	0.30	2.33
		1w	0.32	0.41	0.46	1.07	0.02	0.10	0.70	0.55	1.87	1.19	1.91
		2w	0.23	0.17	0.36	0.58	0.26	0.93	0.23	1.41	1.13	1.22	1.80

Annex G - Measurements Results

This annex shows the results of the measurements done in the IST north tower with their trend lines and standard deviation quadratic mean calculated by (G.1). It is also shown the total of measurement maker points, Table G.2.

$$\sigma = \sqrt{\frac{1}{N}\sum_{n=1}^{N}\sigma_n^2} \qquad \text{(G.1)}$$

For the 126 sector the trend lines are given by (G.2). The standard deviation is in Table G.1.

$$\left(E_b / N_0\right)_{[\mathrm{dB}]} = \begin{cases} -\,0.41 \times F_N + 17.52 \;, & 2\mathrm{w} \\ -\,0.17 \times F_N + 14.80 \;, & 1\mathrm{w} \\ -\,0.13 \times F_N + 15.55 \;, & 0\mathrm{w} \end{cases} \qquad \text{(G.2)}$$

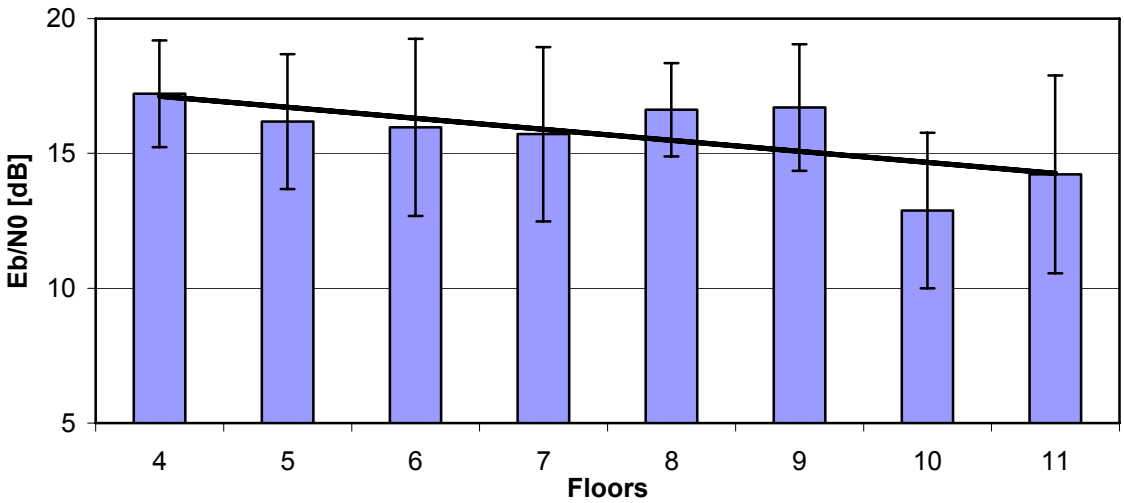

Figure G.1. Sector 126 in the two walls plus one glass situation.

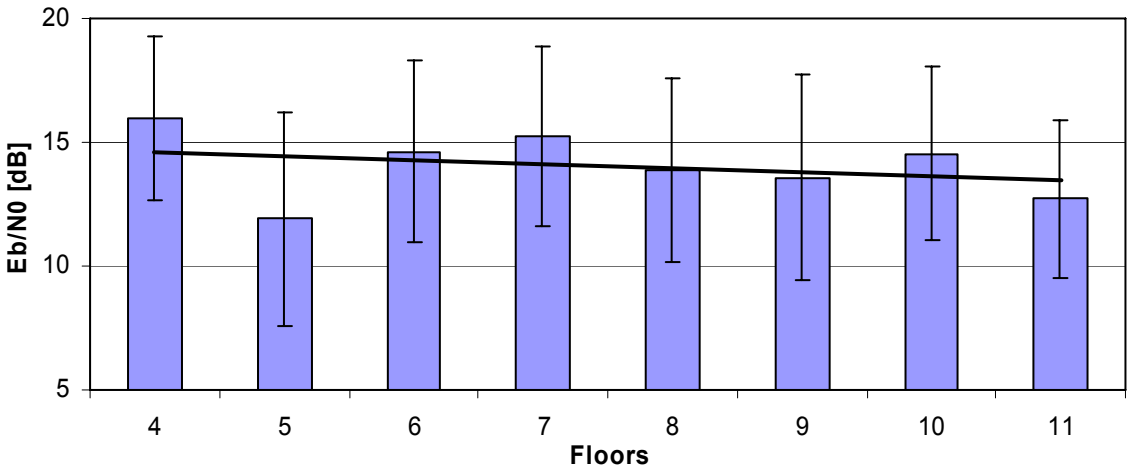

Figure G.2. Sector 126 in the one wall plus one glass situation.

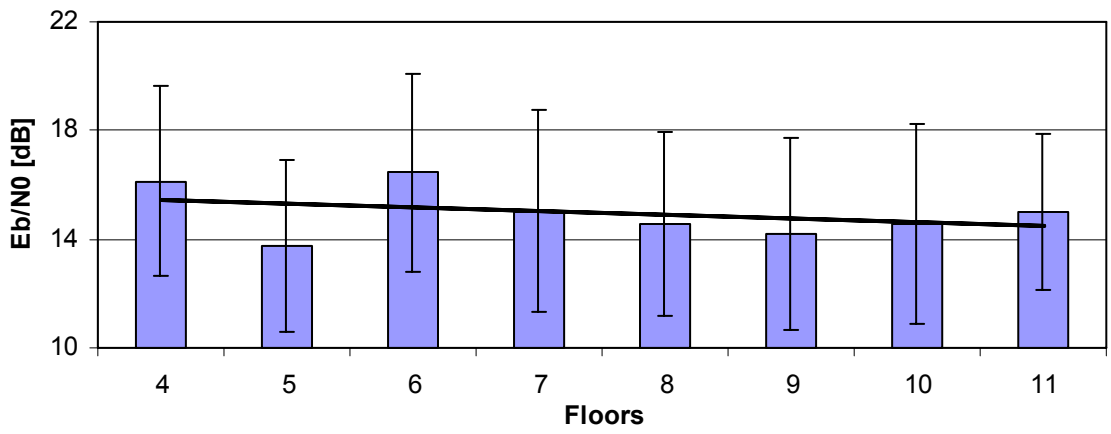

Figure G.3. Sector 126 in the one glass situation.

For the 232 sector the trend lines are given by (G.3). The standard deviation is in Table G.1.

$$\left(E_b / N_0\right)_{[\mathrm{dB}]} = \begin{cases} -\ 0.45 \times F_N\ +\ 13.72\ , & 2\mathrm{w} \\ -\ 0.63 \times F_N\ +\ 14.66\ , & 1\mathrm{w} \\ -\ 0.79 \times F_N\ +\ 16.23\ , & 0\mathrm{w} \end{cases} \qquad \text{(G.3)}$$

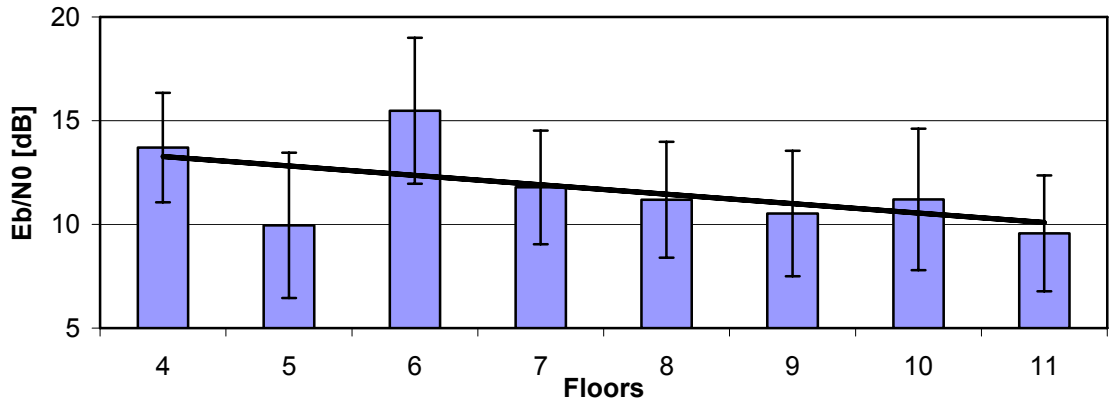

Figure G.4. Sector 232 in the two walls plus one glass situation.

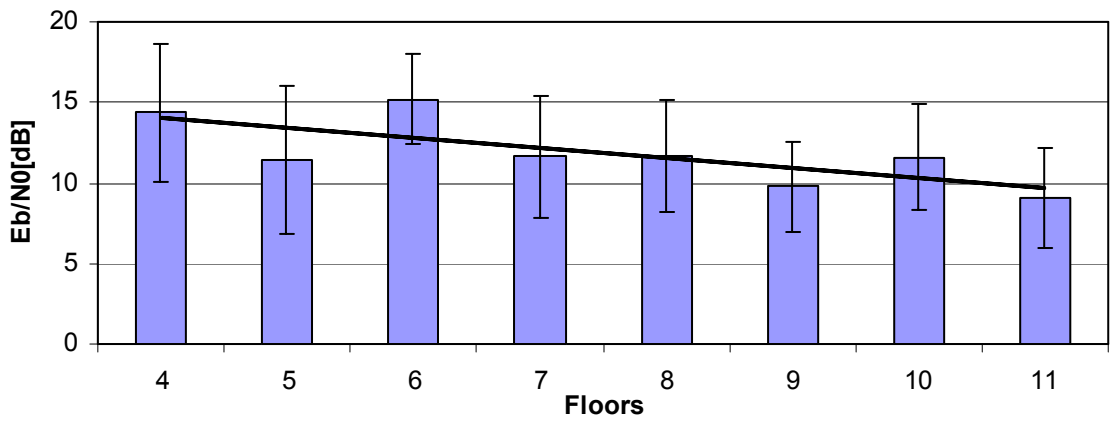

Figure G.5. Sector 232 in the one wall plus one glass situation.

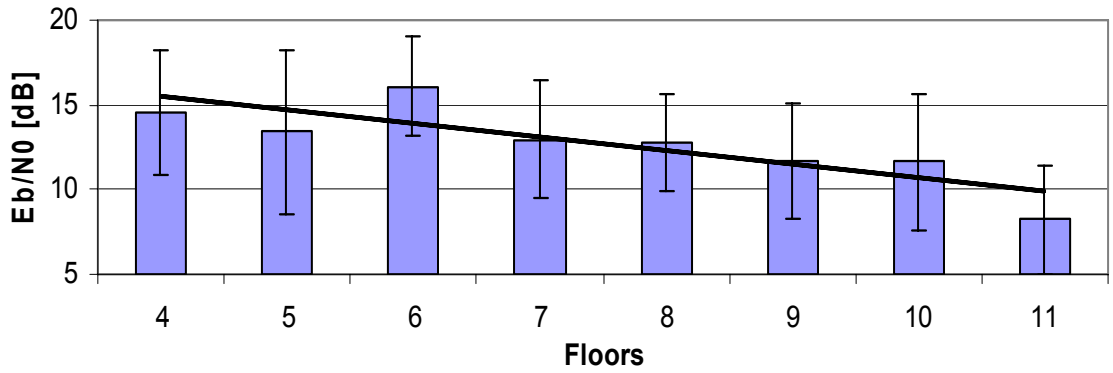

Figure G.6. Sector 232 in the one glass situation.

For the 217 sector two walls case the trend line is given by (G.4). The standard deviation is in Table G.1.

$$(E_b / N_0)_{[dB]} = \begin{cases} 0.18 \times F_N + 9.99 \ , & 2w \\ 0.02 \times F_N + 11.33 \ , & 1w \\ 0.03 \times F_N + 11.35 \ , & 0w \end{cases} \qquad \text{(G.4)}$$

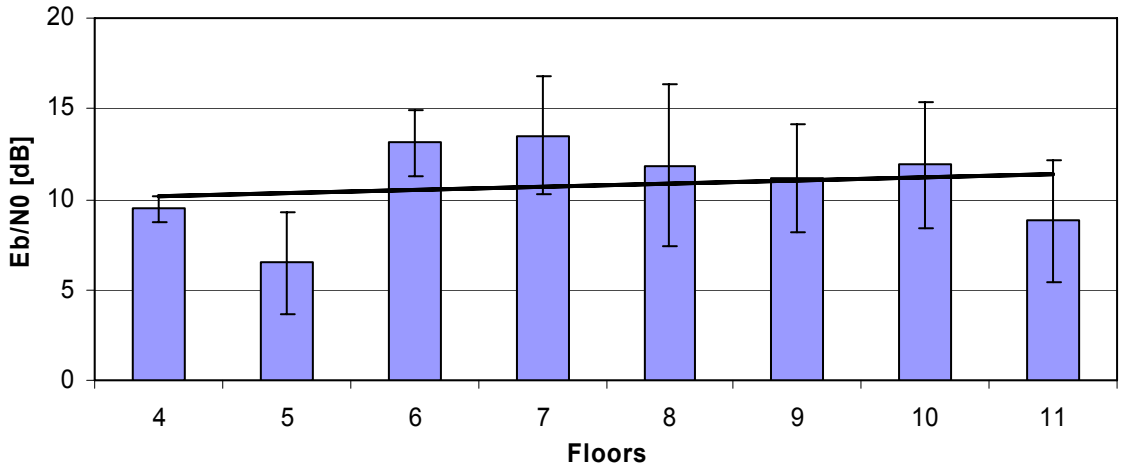

Figure G.7. Sector 217 in the two walls plus one glass situation.

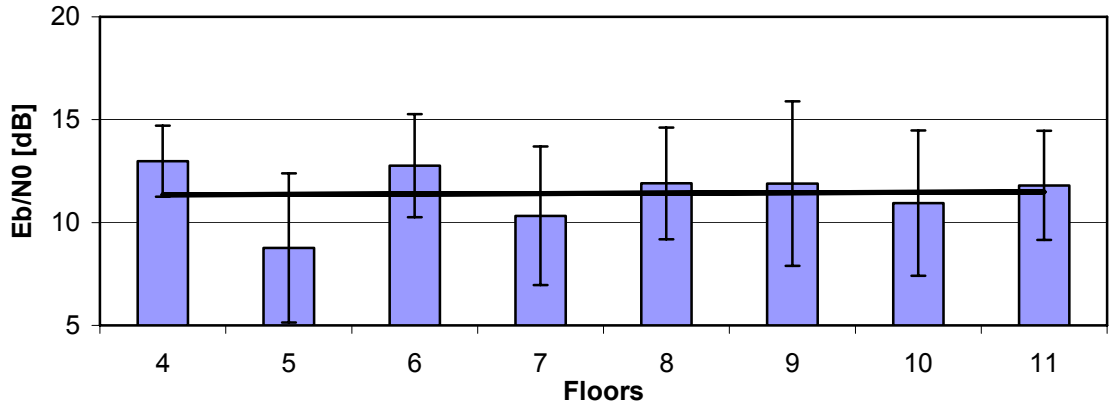

Figure G.8. Sector 217 in the one walls plus one glass situation.

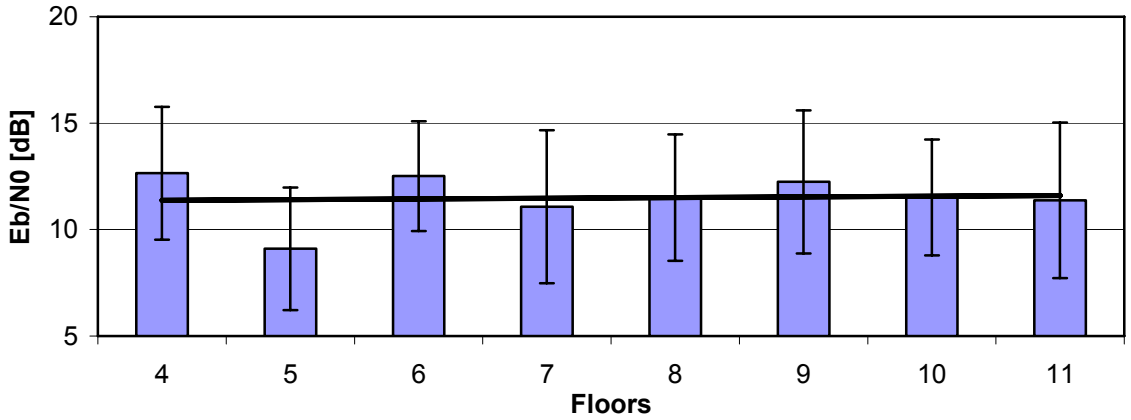

Figure G.9. Sector 217 in the one glass situation.

Table G.1. Standard deviation quadratic mean of measurements.

Standard Deviation [dB]								
126			232			217		
2walls	1wall	0walls	2walls	1wall	0walls	2walls	1wall	0walls
2.78	3.71	3.45	3.07	3.56	3.61	3.06	3.09	3.13

Annex H - Simulations Results

This annex shows additional simulations results. First of all the results for the reference scenario and then the parameters variation results are presented.

Figures H.1 to H.3 represent noise results, Figures H.4 to H.6 represent interference results, Figures H.7 to H.9 represent received power results, and Figures H.10 to H.12 represent C/I results, all for reference scenario.

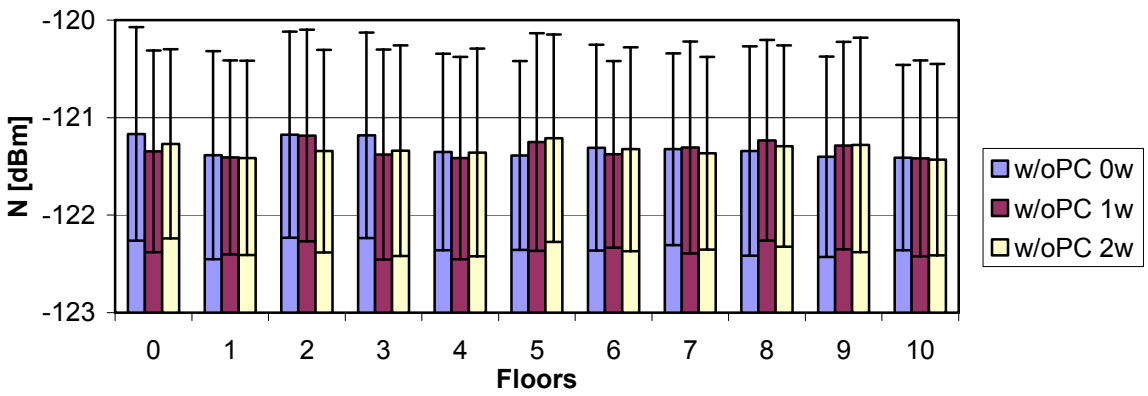

Figure H.1. Reference scenario noise results in DL for first cycle.

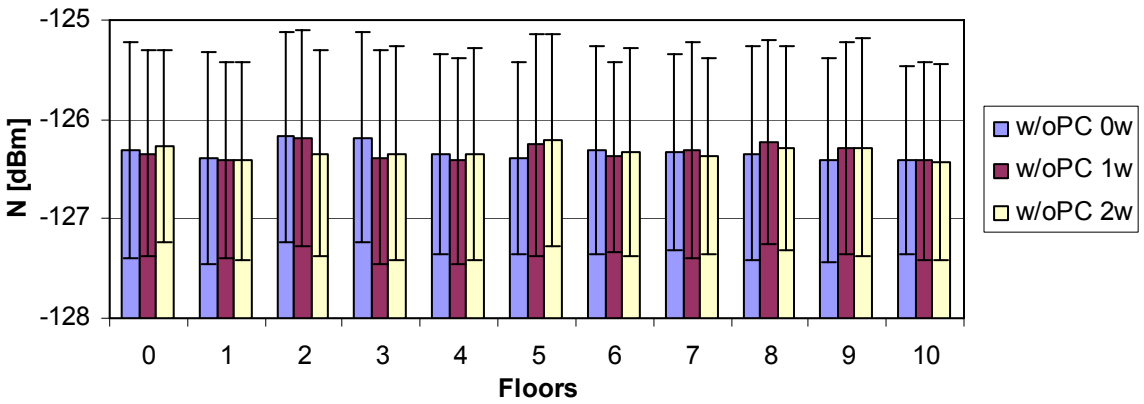

Figure H.2. Reference scenario noise results in UL for first cycle.

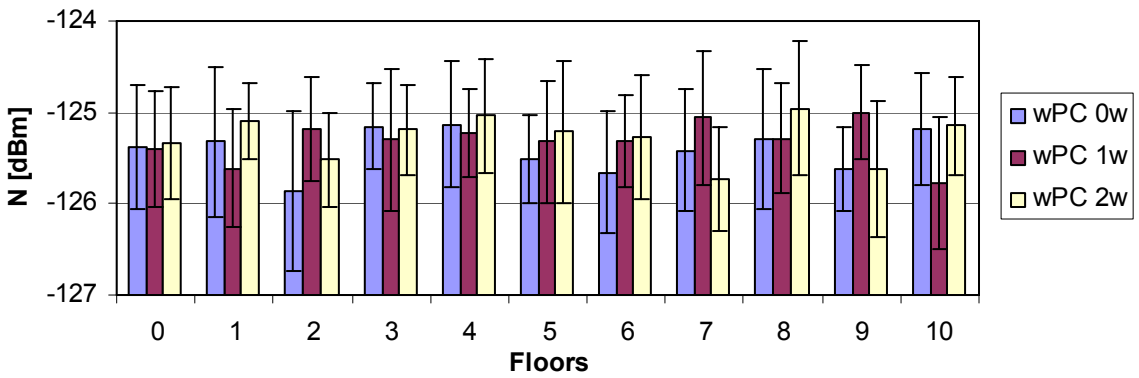

Figure H.3. Reference scenario noise results in UL for second cycle.

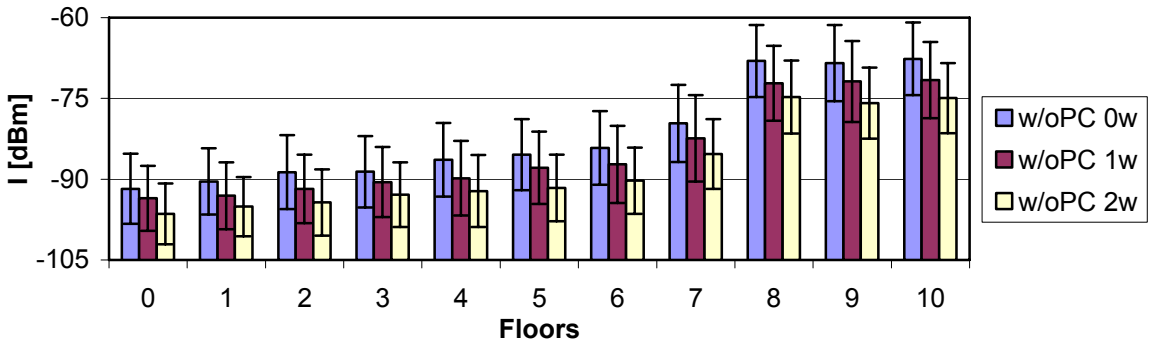

Figure H.4. Reference scenario Interference results in DL for first cycle.

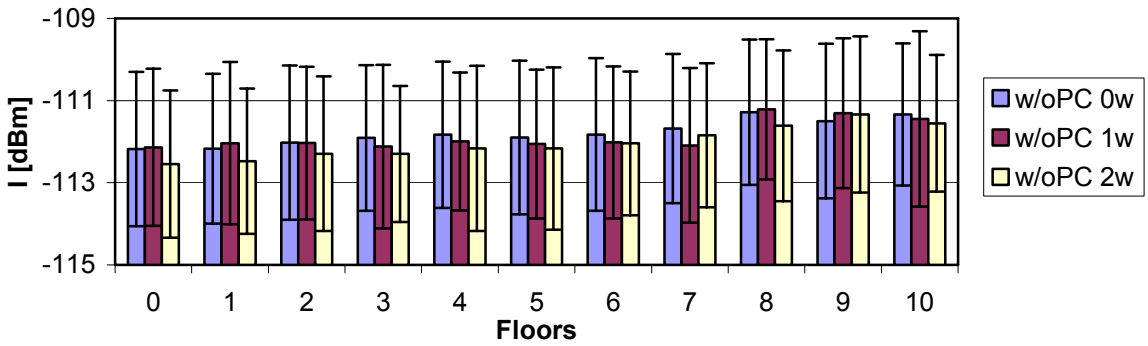

Figure H.5. Reference scenario Interference results in UL for first cycle.

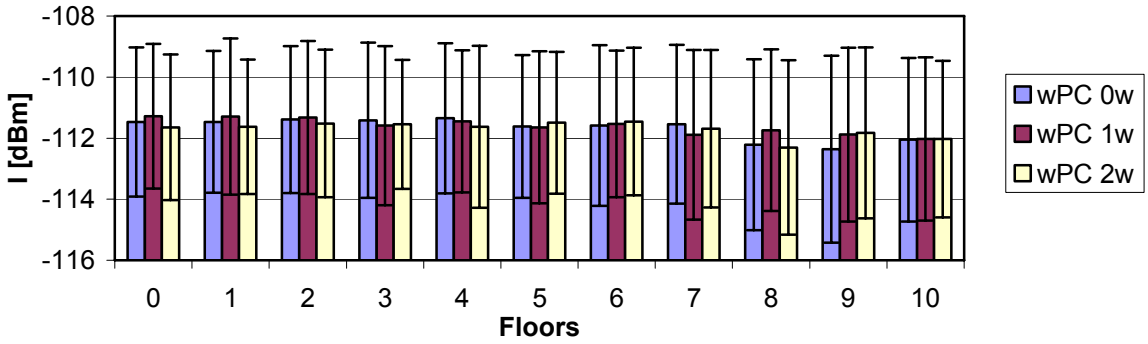

Figure H.6. Reference scenario interference results in UL for second cycle.

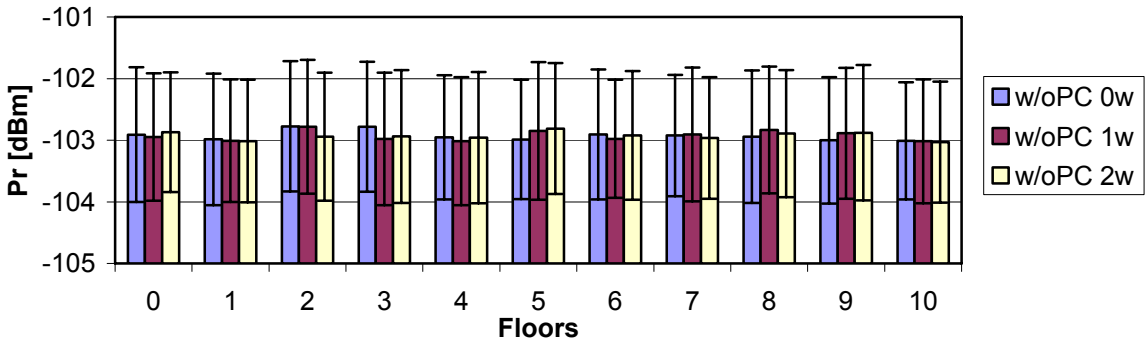

Figure H.7. Reference scenario received power results in DL for first cycle.

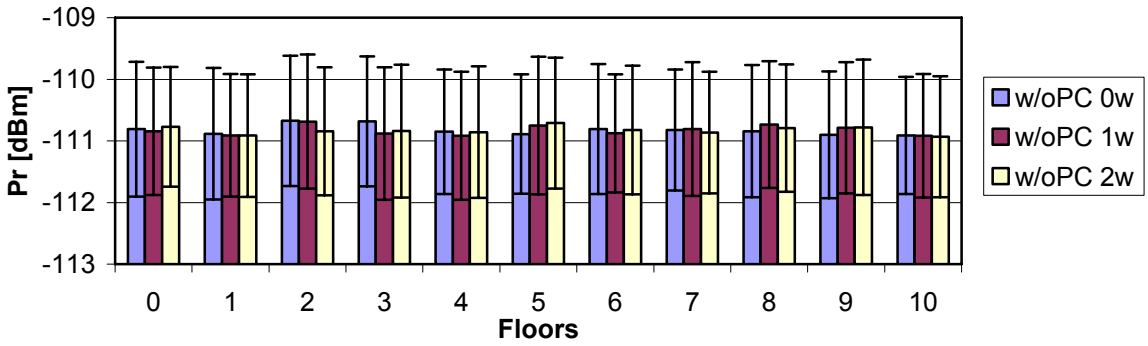

Figure H.8. Reference scenario received power results in UL for first cycle.

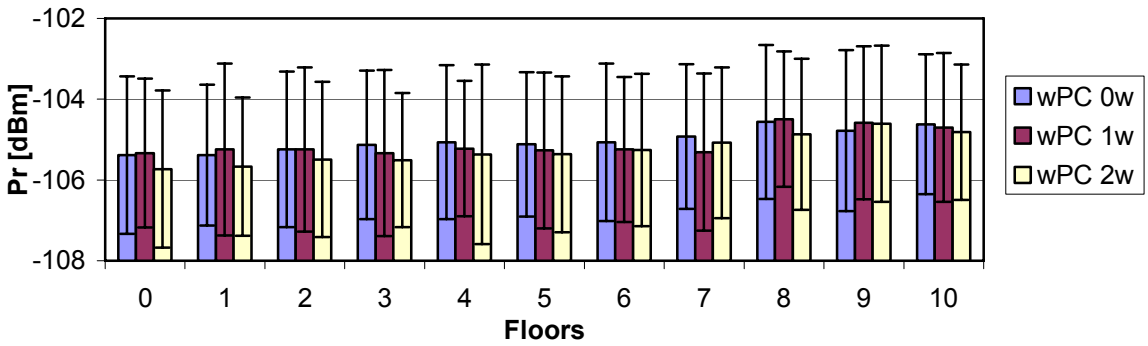

Figure H.9. Reference scenario received power results in UL for second cycle.

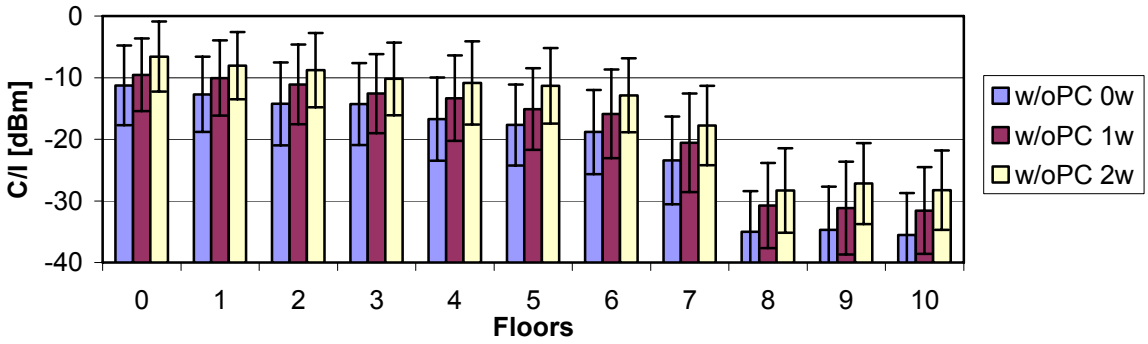

Figure H.10. Reference scenario C/I results in DL for first cycle.

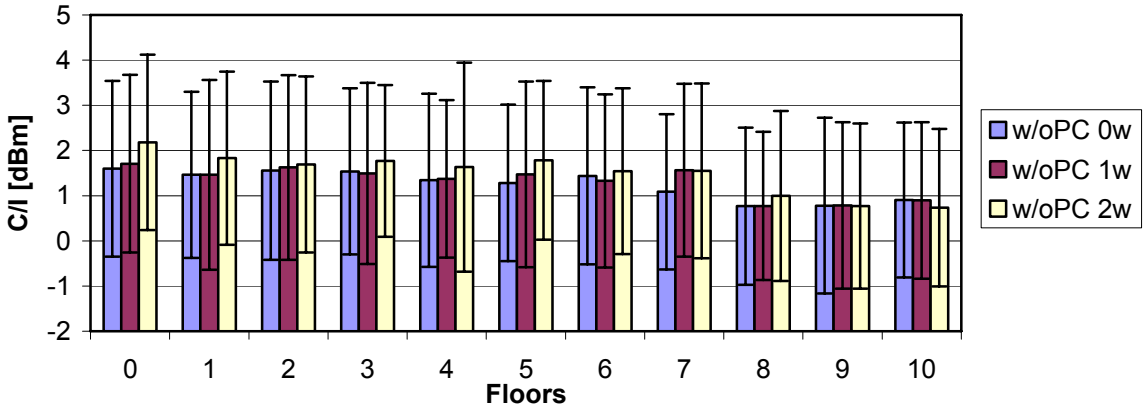

Figure H.11. Reference scenario C/I results in UL for first cycle.

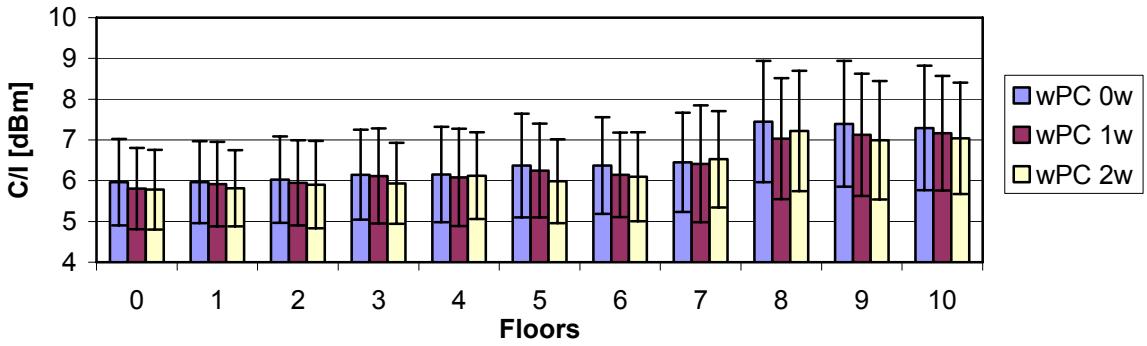

Figure H.12. Reference scenario C/I results in UL for second cycle.

Figure H.13 and H.14 represent the interference trend lines for different distances. For 1 wall case the trend lines for reference is given by (H.1), for near BS by (H.2), and for far BS by (H.3). The standard deviation is in Tables H.1 to H.3.

$$I^{REF}_{[dBm]} = \begin{cases} 2.37 \times F_N - 99.32, & DL \\ -0.07 \times F_N - 111.17, & UL \end{cases} \quad (H.1)$$

$$I^{Near}_{[dBm]} = \begin{cases} 2.21 \times F_N - 90.13, & DL \\ -0.06 \times F_N - 110.79, & UL \end{cases} \quad (H.2)$$

$$I^{Far}_{[dBm]} = \begin{cases} 2.53 \times F_N - 104.88, & DL \\ -0.04 \times F_N - 111.58, & UL \end{cases} \quad (H.3)$$

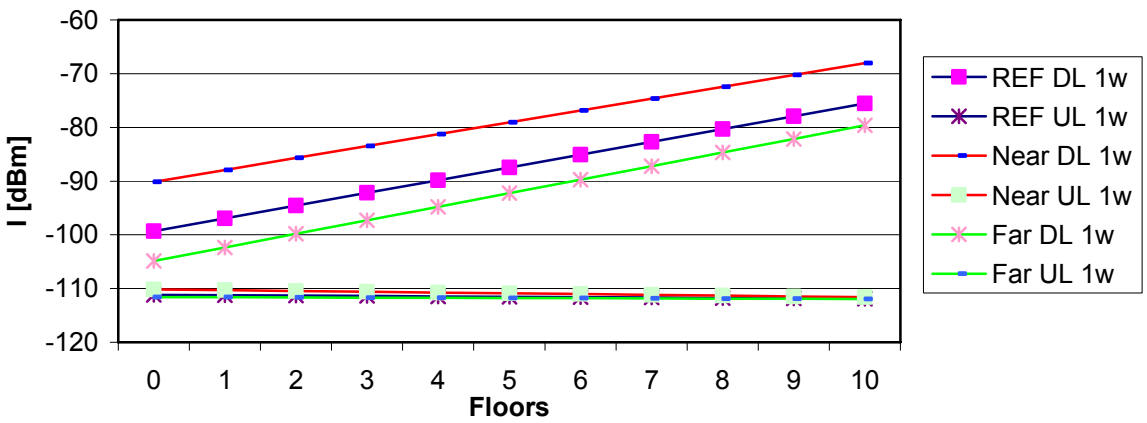

Figure H.13. Interference results for different distance in UL with one penetrated wall.

For 2 walls the trend lines for reference is given by (H.4), for near BS by (H.5), and for far BS by (H.6). The standard deviation is in Tables H.1 to H.3.

$$I^{REF}_{[dBm]} = \begin{cases} 2.28 \times F_N - 101.58, & DL \\ -0.05 \times F_N - 111.42, & UL \end{cases} \quad (H.4)$$

$$I^{Near}_{[dBm]} = \begin{cases} 2.24 \times F_N - 93.59, & DL \\ -0.15 \times F_N - 110.16, & UL \end{cases} \quad (H.5)$$

$$I^{Far}_{[dBm]} = \begin{cases} 2.40 \times F_N - 106.70, & DL \\ 0.02 \times F_N - 112.10, & UL \end{cases} \quad (H.6)$$

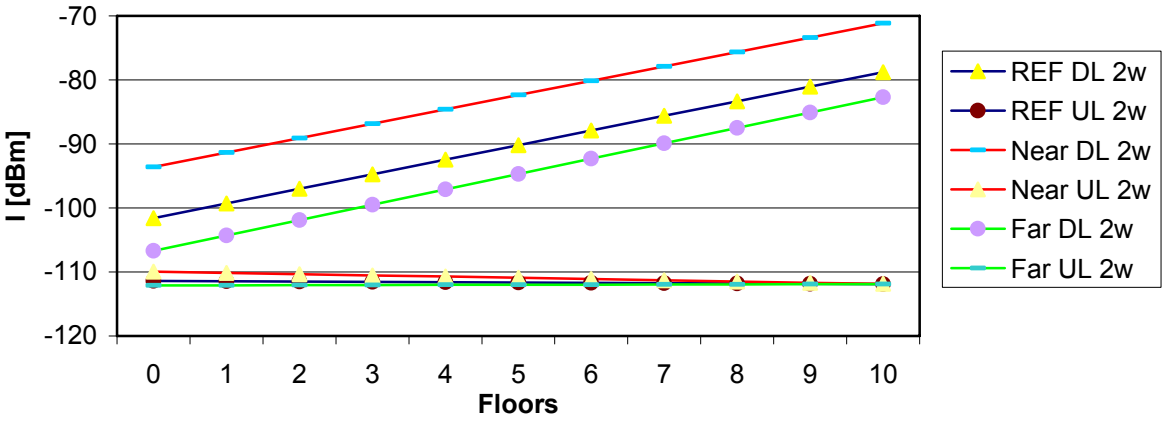

Figure H.14. Interference results for different distance in UL with two penetrated wall.

Table H.1. Reference trend lines Standard deviation.

Reference [dB]					
DL			UL		
Standard Deviation			Standard Deviation		
0w	1w	2w	0w	1w	2w
6.82	6.92	6.28	2.58	2.57	2.49

Table H.2. Near BS trend lines Standard deviation.

Near [dB]					
DL			UL		
Standard Deviation			Standard Deviation		
0w	1w	2w	0w	1w	2w
7.11	7.41	6.79	2.54	2.46	2.47

Table H.3. Far BS trend lines Standard deviation.

Far [dB]					
DL			UL		
Standard Deviation			Standard Deviation		
0w	1w	2w	0w	1w	2w
6.91	6.58	6.18	2.60	2.54	2.47

The received power is an important parameter to take into account for different distance analysis so one presents in Figure H.15 the near BS results and in Figure H.16 the far BS results. Only the results with power control are presented, because these are the final values.

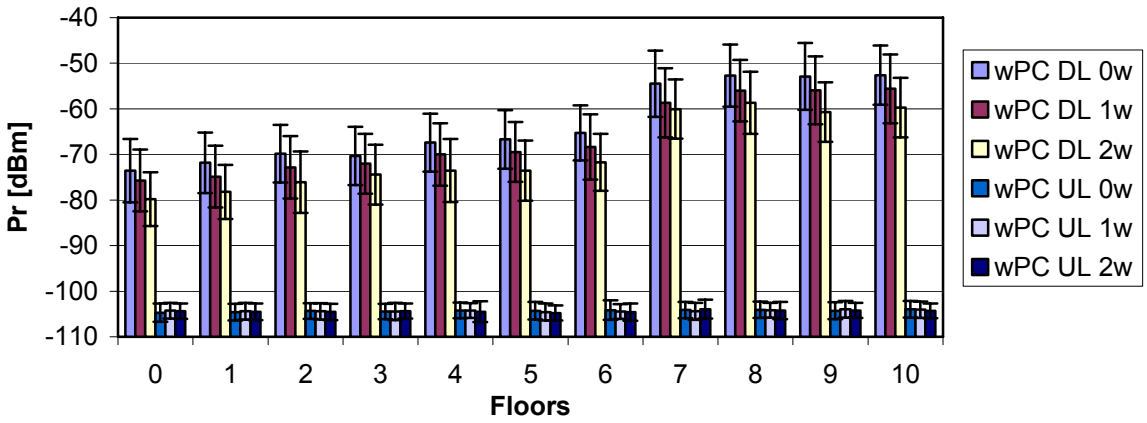

Figure H.15. Near BS received power.

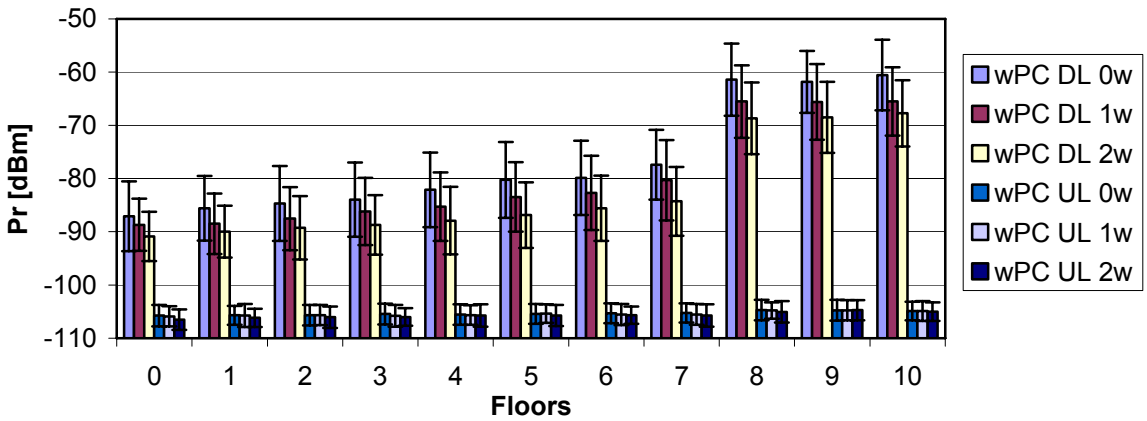

Figure H.16. Far BS received power.

For different tilts simulations is required to know how it is the vertical radiation pattern behaviour. So, in Figure H.17 the vertical pattern for the different tilts is presented.

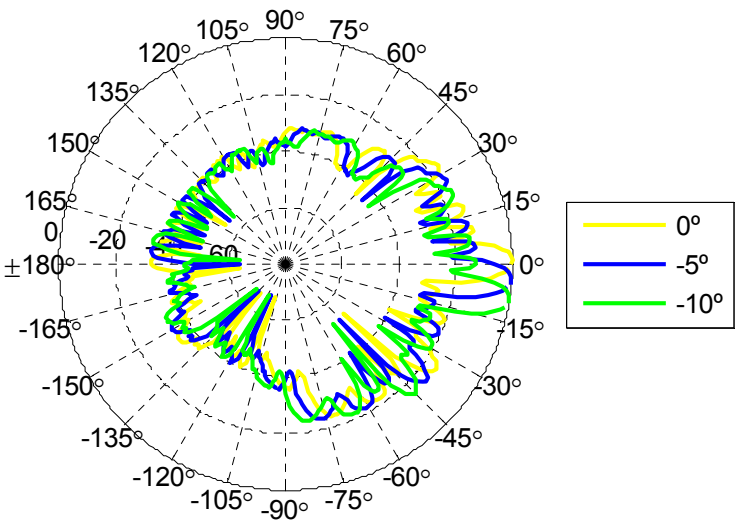

Figure H.17. Vertical radiation pattern with different tilts.

References

[3GPP98] 3GPP, *Selection Procedures for the Choice of Radio Transmission Technologies of the UMTS*, Technical Report, No.30.03U version 3.2.0, Apr.1998. (http://www.3gpp.org/).

[AkPN06] Akl,R., Parvez,A. and Nguyen,S., *Effects of Interference on Capacity in Multi-Cell CDMA Networks*, *Journal of* Systemics, Cybernetics and Informatics, Vol. 3, No. 1, 2006, pp. 94 -100. (http://www.cs.unt.edu/~rakl/APN06.pdf)

[ANIT08] http://www.anite.com/nemo, May 2008.

[Bodi03] Bodic,G., *Mobile Messaging Technologies and Services SMS, EMS and MMS*, John Wiley & Sons, Chichester, UK, 2003.

[Cast01] Castro,J.P., *The UMTS Network and Radio Access Technology: Air Interface Techniques for Future Mobile Systems*, John Wiley John Wiley & Sons, Chichester, UK, 2001.

[Chen03] Chen,Y., "Soft Handover Issues in Radio Resource Management for 3G WCDMA Networks", Ph. D. Thesis, Queen Mary College, University of London, London, UK, Sep. 2003. (http://www.elec.qmul.ac.uk/research/thesis/YueChen2003.pdf)

[CODE08] http://www.codegear.com/, Jan. 2008.

[Cola06] Costa,P. and Ladeira,D., *Planning of UMTS Cellular Networks for Data Services Based on HSDPA (in Portuguese)*, Graduation Project, Instituto Superior Técnico, Lisbon, Portugal, Jun. 2006.

[Corr07] Correia,L.M., *Lecture Notes of Mobile Communications Systems*, Instituto Superior Técnico, Lisbon, Portugal, March 2007.

[DaCo99] Damosso,E. and Correia,L.M., *Digital Mobile Radio Towards Future Generation Systems (COST 231 Final Report)*, COST Telecom Secretariat, European Comission, Brussels, Belgium, 1999.

[EPCC06] Esteves,H., Perreira,M., Correia,L.M., Caseiro,C., *Impact of Intra- and Inter-Cell Interference on UMTS-FDD (in Portuguese)*, Graduation Project, Instituto Superior Técnico, Lisbon, Portugal, Jun. 2006.

[FKRC06] Ferreira,L.S., Kuipers,B.W.M., Rodrigues,C. and Correia,L.M., "Characterisation of signal penetration into buildings for GSM and UMTS", in *Proc. of ISWCS'2006 – 3rd International Symposium on Wireless Communication Systems,* Valencia, Spain, Sep. 2006.

[GCFP99] Gil,F., Claro,A.R., Ferreira,J.M., Pardelinha,C. and Correia,L.M., *A 3-D Extrapolation*

Model for Base Station Antennas Radiation Patterns, Proceedings of VTC'99 Fall – IEEE 50th Vehicular Technology Conference, Amsterdam, the Netherlands, Sep. 1999.

[Hata80] Hata,M., *Empirical Formula for Propagation Loss in Land Mobile Radio Services*, IEEE Trans. on Vehicular Technology, Vol. 29, No.3, Aug. 1980, pp. 317-325.

[HoTo04] Holma,H. and Toskala,A., *WCDMA for UMTS – Radio Access For Third Generation Mobile Communications*, John Wiley & Sons, Chichester, UK, 2004, Third Edition.

[HoTo06] Holma,H. and Toskala,A., *HSDPA/HSUPA for UMTS - High Speed Radio Access for Mobile Communications*, John Wiley & Sons, Chichester, UK, 2006.

[IkYo84] Ikegami,F., Yoshida,S., Takeuchi,T. And Umehira,M., *Propagation Factors Controlling Mean Field Strength on Urban Streets*, IEEE Trans. on Antennas and Propagation, Vol. AP-32, No. 8, Aug. 1984, pp. 882-889.

[KATH08] http://www.kathrein.de/, May 2008.

[LaWN06] Laiho,J., Wacker,J. and Novosad,T., *Radio Network Planning and Optimisation for UMTS*, John Wiley & Sons, Chichester, UK, 2006.

[MAPS08] http://maps.live.com/, Jun. 2008.

[MäSt03] Mäder,A. and Staehle,D., *An Analytic Approximation of the Uplink Capacity in a UMTS Network with Heterogeneous Traffic,* Research Report No.310, Research Report Series, Institute of Computer Science, University of Wurzburg, Wurzburg, Belgium, May 2003. (http://www3.informatik.uni-wuerzburg.de/ TR/tr310.pdf)

[MäSt04] Mäder,A. and Staehle,D., *Uplink Blocking Probabilities is Heterogeneous WCDMA Networks Considering Other-Cell Interference*, Research Report No.333, Research Report Series, Institute of Computer Science, University of Wurzburg, Wurzburg, Belgium, Aug. 2004.

[Moli05] Molisch,A.F., *Wireless Communications*, John Willey & Sons, Chichester, UK, 2005.

[NaSh03] Navaie,K. and Sharafat,A., *A framework for UMTS air interface analysis*, Can. J. Elect. Comput. Eng., Vol.28, No. 3, July/Oct. 2003, pp 113-129. (http://www.ieee.org)

[Nguy05] Nguyen,S., *Capacity and Throughput Optimization in Multi-Cell 3G WCDMA Networks*, Master Thesis, University of North Texas, TX, USA, Aug. 2005.

[NTTD08] http://www.nttdocomo.com/, Aug. 2008.

[OFRC05] Oliveira,C., Fernandes,C.C., Reis,C., Carpinteiro,G., Ferreira,L., Correia,L.M., Sebastião,D., *Definition of Exclusion Zones around typical Installations of Base Station Antennas*, Monit Project Report, Lisbon, Portugal, Feb. 2005.

[OkOh68] Okumura,Y., Ohmori,E. and Kawano,T., *Field Strength and Its Variability in VHF and UHF Land-Mobile Service*, Review of the Electrical Communication Laboratory, Vol. 16, no 9-10, 1968, pp. 825-873.

[OlCa02] Oliveira, C. and Carpinteiro, G., *Impacto da Localização de Antenas de Estação de Base de GSM e UMTS na Exposição Humana à Radiação Electromagnética (com a colaboração da Optimus)* (in Portuguese), Dipl. Thesis, IST-TUL, Lisbon, Portugal, 2002.

[POWE08] http://www.powerwave.com/, May2008

[RMSP87] Rao,D.N., Murthy,M.J.K., Sarkar,S.K., Pasricha,P.K., Dutta,H.N. and Reddy,B.M., *Hilly Terrain LOS Fadeouts and Fresnel Zone Considerations from Ray Tracing Techniques*, IEEE Trans. on Antennas and Propagation, Vol. AP-35, No. 11, Nov. 1987, pp. 1330-1333.

[Sant04] Santo,L., *UMTS Performance in Multi-Service Non-Uniform Traffic Networks*, M.Sc. Thesis, Instituto Superior Técnico, Lisbon, Portugal, Dec. 2004.

[Shan02] Shankar,P.M., *Introdution to Wireless Systems*, John Wiley, New York, NY, USA, 2002.

[SKYM03] Sugano,M., Kou,L., Yamamoto,T. and Murata,M., *Impact of Soft Handoff on TCP Throughput over CDMA Wireless Cellular Networks*, in Proc. of VTC 2003 Fall – IEEE Vehicular Technology Conference, Orlando, FL, USA, Oct. 2003.

[TaTr95] Tam,W.K., Tran,V.N., *Propagation Modelling for Indoor Wireless Communication*, Electronics & Communication Engineering Journal, Vol. 7, Issue 5, Oct. 1995, pp. 221-228.

[TöBe93] Törnevik,C., Berg,J.E., Lotse,F, *"900 MHz propagation measurements and path loss models for different indoor environments"*, Proceedings IEEE Vehicular Technology Conference 1993, New Jersey, U.S.A., 1993.

[UMTS07] http://www.umtsworld.com/, October 2007.

[WaAC03] Wang,L., Aghvami,A. and Chambers,W., *On the Capacity of a Wideband Multi-Rate CDMA System with Multi-Service in the Presence of Fading and Power Control Error*, in IEE Proceedings on Communications, Vol.150, No.1, Feb.2003, pp.59-63. (http://www.kcl.ac.uk/content/1/c4/15/79/IEEFPublish.pdf)

[WaBe88] Walfish,J. And Bertoni,H., *A Theoretical Model of UHF Propagation in Urban Environments*, IEEE Trans. on Antennas and Propagation, Vol. 36, No. 12, Dec. 1988, pp. 1788-1796.

[XiBe94] Xia,H.H., Bertoni,H.L., Marciel,L.R., Stewart,A.L., Rowe,R., *Microcellular Propagation Characteristics for Personal Communications in Urban and Suburban Environment*, IEEE Trans. on Antennas and Propagation, Vol. 43, No.3, Aug. 1984, pp. 743-752.

[Yaco93] Yacoub,M.D., *Foundations of Mobile Radio Engineering*, CRC Press, Boca Raton, FL, USA, 1993.

[YYZM03] Yu,J., Yao,Y., Zang,J. and Molish,A., *Reverse Link Capacity of Power-Controlled CDMA Systems With Antenna Arrays in a Multipath Fading Environment*, Technical Report 2003-78, Mitsubishi Electric Research Laboratories, Cambridge, MA, USA., Aug.2003.

(http://www.merl.com/reports/docs/TR2003-078.pdf)

[ZhLi00] Zhuge,L. and Li,V., *Interference Estimation for Admission Control in Multi-Services DS-CDMA Cellular Systems*, *in* Proc. of GLOBECOM'00 - IEEE Global Telecommunications Conference, San Francisco, CA, USA, Nov.2000.